

POLITECNICO DI TORINO

Collegio di Ingegneria Civile

Master's Degree in Civil Engineering

A.a. 2024/2025

Behaviour of existing reinforced concrete slabs: tests vs. structural analysis

Irina Kim

Supervisors: Candidate:

Prof. Alessandro Pasquale Fantilli Prof. Bernardino Chiaia

Abstract

Reinforced concrete slabs are versatile structural elements used in most types of structures. This work focuses on comparing analytical models with actual structural behaviour.

Four segments of a road tunnel deck, composed of prefabricated and cast-in-situ elements, were extracted for laboratory testing. Each segment was subjected to force-controlled loading, and results were recorded in the form of force-deflection curves. The segments were examined to determine geometry, reinforcement layout in both longitudinal and transverse directions, and material properties of concrete and steel.

A finite element model was developed in ANSYS Workbench to simulate the same loading conditions. The results show variability in structural response: one sample demonstrated full continuity of the deck, one exhibited medium continuity, and two showed low continuity. These findings suggest that the joints between prefabricated and cast-in-situ elements have variable effectiveness, potentially due to localized damage, construction imperfections or transient loads during extraction and transportation. Further investigation is necessary to improve the accuracy of numerical models and experimental analysis.

Table of Contents

Abstract	3
List of Figures	6
List of Tables	9
List of Equations	10
1. Introduction	11
2. Assessment of existing structures	13
2.1. New European Technical Rules for the assessment and retrofitting of existing structur	es13
2.1.1. Generic procedure	15
2.1.2. Preliminary assessment	16
2.1.3. Detailed assessment	16
2.1.4. Material properties	17
2.1.4.1. Non-destructive tests	17
2.1.4.2. Destructive tests	18
2.1.5. Geometrical properties	18
2.1.6. Structural model	19
2.1.7. Structural analysis and verifications	19
2.1.7.1 Verifications based on partial factors	20
2.1.7.2 Verifications based on global resistance	20
2.1.7.2 Verifications based on probabilistic format	21
2.1.8. Interventions	21
2.2. Guidelines for the classification and risk management, safety assessment, and monitor of existing bridges	_
2.2.1. Multilevel Approach	22
2.2.2. Level 4. Accurate safety verification	25
2.2.2.1. Fundamental concepts and strategies for safety assessment	25
2.2.2.2. Structural Characterization of the bridge.	27
2.2.2.3. Safety assessment and verifications.	28
3. Tests on existing RC slabs	33
3.1. Load tests	33
3.1.1. General information	33
3.1.2. Description of slots	34
3.1.3. Tests setup	. 35

3.1.4. Instrumentation and loading history	38
3.1.5. Results	41
3.1.5.1. Sample 1	42
3.1.5.2. Sample 2	46
3.1.5.3. Sample 3	50
3.1.5.4. Sample 4	54
3.2. Surveys and Material tests	57
3.2.1. General information	57
3.2.2. Geometric survey	58
3.2.2.1. Transverse survey of the samples	58
3.2.2.2. Longitudinal survey of the sample C4	66
3.2.2.3. General observations following the demolitions	73
3.2.3. Georadar Scanning	76
3.2.3.1. Sample C1	76
3.2.3.2. Sample C2	
3.2.3.3. Sample C3	80
3.2.3.4. Sample C4	81
3.2.4. Material Tests	83
3.2.4.1. Concrete	83
3.2.4.2. Steel reinforcement	87
4. Finite Element Model	90
4.1. Material models for non-linear analysis	90
4.1.1. Concrete model	90
4.1.2. Steel reinforcement model	92
4.2. Geometry modelling	93
4.3. Model setup	96
5. Results comparison and model updating	98
5.1. Sample C1	98
5.2. Sample C2	101
5.3. Sample C3	103
5.4. Sample C4	105
6. Conclusions	108
7. Bibliography	109

List of Figures

Figure 1: Main components of assessment	
Figure 2:Generic procedure of assessment and retrofitting of existing structure	15
Figure 3: Multilevel approach and relationships between levels of analysis	. 23
Figure 4: Logical flow for determining the attention class	. 24
Figure 5: Characteristic cross-section of the deck	
Figure 6: Load schemes 2 and 3, as reported in the 2018 NTC	
Figure 7: Summary of geometric dimensions.	. 35
Figure 8: Loading scheme 2	_
Figure 9: Loading scheme 3	_
Figure 10: Images of supports	_
Figure 11: Test setup for scheme 2	
Figure 12: General view of the test setup for scheme 2 and load cell detail	
Figure 13: Test setup for scheme 3	_
Figure 14: General view for test scheme 3	
Figure 15: Distribution of sensors in scheme 2	-
Figure 16: Distribution of sensors in scheme 3	-
Figure 17: Sensors positioned to monitor the failure of the internal supports	
Figure 18: Sensors positioned to monitor settlement at load application points	-
Figure 19: View of tested spans 1 and 2 respectively	-
Figure 20: Left - view of span 3. Right: Crack pattern on span 1	
Figure 21: Left - saline efflorescences on span 1. Right: Crack pattern on span 3	
Figure 22: Force-displacement curve of span1	
Figure 23: Force-displacement curve of span 2	
Figure 24: Deformations in the transverse direction	
Figure 25: Deformations in the longitudinal direction of span 1	
Figure 26: Deformations in the longitudinal direction of span 2	
Figure 27: Left: View of span 3. Right: Construction joint between span 2 and 3	
Figure 28: Left: Small demolition in span 3. Right: View of not loaded span 1	
Figure 29: Left: Construction joint between span 2 and span 1. Right: Efflorescence in span 1	
Figure 30:Left: Small demolitions near loading point of span 2. Right: Crack pattern at span	
Figure 31: Force-displacement curve of span 2	_
Figure 32: Force-displacement curve of span 3	
Figure 33: Deformations in the transverse direction	
Figure 34: Deformations in the longitudinal direction of span 2	
Figure 35: Deformations in the longitudinal direction of span 3	_
Figure 36: View of span 1 and 2 respectively	_
Figure 37: Restoration on span 1	
Figure 38: Left: Black spots on span 1. Right: Saline efflorescence on span 2	
Figure 39: Force-displacement curve of span 1	. 52
Figure 40: Deformations in the transverse direction	
Figure 41: Deformations in the longitudinal direction of span 1	
Figure 42: Span 3 and support detail	
Figure 43: Significant crack pattern on the front of the slab	
Figure 44: View of small demolition	
Figure 45: Force-displacement curve of span 3	. 55

Figure 46: Deformations in the transverse direction	56
Figure 47: Deformations in the longitudinal direction of span 3	
Figure 48: Approximate location of concrete core samples	
Figure 49: Location of longitudinal cuts (red in cast-in situ part, yellow- in precast parts)	57
Figure 50: Front and back views of sample C1	58
Figure 51: Front and back views of sample C2	58
Figure 52: Front and back views of sample C3	
Figure 53: Orthophoto of slab C4	58
Figure 54: Sample C1 (lateral precast parts-oblique lines, central precast part-vertical lines,	
casting joint-rhombus)	59
Figure 55: Sample C2 (lateral precast parts-oblique lines, central precast part-vertical lines,	
	59
Figure 56: Sample C3 (lateral precast parts-oblique lines, central precast part-vertical lines,	
casting joint- rhombus)	59
Figure 57: Sample C4 (lateral precast parts-oblique lines, central precast part-vertical lines,	
casting joint- rhombus)	60
Figure 58: Details of lateral prefabricated segments in sample C1	60
Figure 59: Details of lateral prefabricated segments in sample C2	61
Figure 60: Details of lateral prefabricated segments in sample C3	61
Figure 61: Details of lateral prefabricated segments in sample C4	61
Figure 62: Details of cast-in-situ joints in sample C1	62
Figure 63: Details of cast-in-situ joints in sample C2	63
Figure 64: Details of cast-in-situ joints in sample C3	63
Figure 65: Details of cast-in-situ joints in sample C4	64
Figure 66: Details of the central prefabricated segment in sample C1	64
Figure 67: Details of the central prefabricated segment in sample C2	65
Figure 68: Details of the central prefabricated segment in sample C3	65
Figure 69: Details of the central prefabricated segment in sample C4	66
Figure 70: Location of longitudinal cuts in sample C4	67
Figure 71: Orthophoto of section AA	67
Figure 72: Detail of two consecutive lateral segments	67
Figure 73: Reinforcement layout in lateral prefabricated segment	67
Figure 74: Orthophoto of section a) BB and b) CC	68
Figure 75: Geometric dimensions of section BB	68
Figure 76: Principal reinforcement layout in sections a) BB and b) CC	69
Figure 77: Detail of the hooked bar type B	69
Figure 78: Additional reinforcement layout in sections a) BB and b) CC	70
Figure 79: Detail of inclined type C bar	
Figure 80: Detail of the hooked bar type D	71
Figure 81: Detail of the hooked bar type E	71
Figure 82: Orthophoto of section DD	
Figure 83: Reinforcement layout in section DD	72
Figure 84: Reinforcement layout in section DD a) principal and b) additional	
Figure 85: Detail of the bar type F	
Figure 86: Type D bars hooked inside the lateral prefabricated part	
Figure 87: Degradation of reinforcement in cast-in-situ joint	
Figure 88: View of degradation level	
Figure 89: Transverse scan with the georadar of the slab C1 on the front side	76

Figure 90: Transverse scan with the georadar of the slab C1 on the centre	77
Figure 91: Transverse scan with the georadar of the slab C1 on the back side	
Figure 92: Longitudinal scan with the georadar of the slab C1. Left – span 1, Right – spa	
Figure 93: Longitudinal scan with the georadar of the slab C1, span3	
Figure 94: Transverse scan with the georadar of the slab C2 on the front side	
Figure 95: Transverse scan with the georadar of the slab C2 on the centre	
Figure 96: Transverse scan with the georadar of the slab C2 on the back side	•
Figure 97: Longitudinal scan with the georadar of the slab C2. Left – span 1, Right – sp	
Figure 98: Longitudinal scan with the georadar of the slab C2, span 3	
Figure 99: Transverse scan with the georadar of the slab C3 on the front side	
Figure 100: Transverse scan with the georadar of the slab C3 centre	
Figure 101: Transverse scan with the georadar of the slab C3 back side	
Figure 102: Longitudinal scan with the georadar of the slab C3. Left – span 1, Right – s	
Figure 103: Longitudinal scan with the georadar of the slab C3, span 3	-
Figure 104: Transverse scan with the georadar of the slab C4 front side	
Figure 105: Transverse scan with the georadar of the slab C4 centre	
Figure 106: Transverse scan with the georadar of the slab C4 back side	
Figure 107: Longitudinal scan with the georadar of the slab C4. Left – span 1, Right – span 1,	
Figure 108: Longitudinal scan with the georadar of the slab C4, span 3	•
Figure 109: Test setup	_
Figure 110: Load history for test	_
Figure 111: Detail of the type 1 bar	_
Figure 112: Detail of the type 2 bar	
Figure 113: Detail of the type 3 bar	-
Figure 114: Detail of the type 4 and 5 bars	-
Figure 115: Detail of the type 6 bar	
Figure 116: Hardening/softening functions with linear softening: a – in compression; b	
tension	
Figure 117: Hardening/softening functions with exponential softening: a – in compress	_
in tension	
Figure 118: SOLID185 - 3D 8-Node Structural Solid	
Figure 119: 3D 8-Node Solid with REIN264 element	
Figure 120: Decomposition of force vector	
Figure 121: Model C1. Force-displacement curve for span 1	
Figure 122: Model C1. Force-displacement curve for span 2	
Figure 123: Model C1. Force-displacement curve for span 1, assuming μ=0.42	
Figure 124: Model C1. Force-displacement curve for span 2, assuming μ =0.42	
Figure 125: Model C2. Force-displacement curve for span 2	
Figure 126: Model C2. Force-displacement curve for span 3	
Figure 127: Model C2. Force-displacement curve for span 2, assuming μ=0.42	
Figure 128: Model C2. Force-displacement curve for span 3, assuming μ =0.42	
Figure 129: Model C3. Force-displacement curve for span 1	
Figure 130: Model C3. Force-displacement curve for span 1, assuming μ =0.42	
Figure 131: Model C3. Force-displacement curve for span 1, assuming μ =0.42	104
Figure 132: Model C4. Force-displacement curve for span 3	
Figure 132: Model C4. Force-displacement curve for span 3, assuming μ=0.42	_
Figure 133: Model C4. Force-displacement curve for span 3, assuming μ=0.42 Figure 134: Model C4. Force-displacement curve for span 3, assuming μ=0.2	
Figure 135: Damage - μ relationship	
1 1201 ο 1991 ο απιαξο η τοιαποποπιμ	10/

List of Tables

Table 1: Partial safety factors for permanent loads in operational and transitory verification	30
Table 2: Partial safety factors for permanent loads in adequate verification	30
Table 3: Partial safety factors with traffic as main action	30
Table 4: Partial safety factors with wind as main action	30
Table 5: Partial safety factors for resistance characteristics of materials in operational and	
transitory conditions	31
Table 6: Summary of geometric dimensions	34
Table 7: Load values for schemes 2,3	39
Table 8: Types of sensors	39
Table 9:Summary of Compression Test Results on H/D=1 samples	84
Table 10: Summary of the Modulus tests results	86
Table 11: Summary of the Compression tests results	86
Table 12: Summary of Tensile tests on reinforcement	89
Table 13: Coefficient n to describe ultimate strain	91
Table 14: Input values for concrete properties	-
Table 15: Input values for steel properties	
Table 16: Concrete geometry dimensions in model	
Table 17: Reinforcement in longitudinal and transverse directions	95

List of Equations

Equation 1: Relative stress at start of nonlinear hardening	91
Equation 2: Plastic strain at uniaxial compressive strength	91
Equation 3: Ultimate strain in compression	91
Equation 4: Tensile strength of concrete	_
Equation 5: Biaxial compressive strength of concrete	-

1. Introduction

Reinforced concrete has played a major role in construction history since its origin in the mid-to-late nineteenth century. By combining the compressive strength of concrete with the tensile capacity of steel reinforcement, it became the dominant construction material during the twentieth century. Reinforced concrete is used extensively in residential, industrial, and infrastructural projects and in all types of structural elements.

Since its invention, reinforced concrete has been the subject of extensive research. Over time, the material properties deteriorate under the influence of use and environmental conditions. Concrete is prone to cracking and deformations due to shrinkage and creep. The type of loading also influences the durability of a reinforced concrete structure since repeated loading leads to fatigue. Depending on environmental exposure, it is affected by moisture, chemical attacks and freeze-thaw cycles caused by extreme temperatures. Carbonation or salt penetration causes depassivation of steel bars, and the reinforcement starts to corrode. Corrosion of bars is accompanied by the increase in volume, which causes spalling of concrete cover. In addition to material degradation, existing structures were designed according to the standards active at the time of construction, not considering modern requirements for current loads, seismic and fire resistance.

Improvements in understanding of material behaviour and simultaneous revision of requirements lead to the need for assessment of existing structures. Assessment provides information about the current condition of the structure and its ability to withstand modern loading requirements and service conditions. Ecological aspects also play a role in decision making regarding existing structures. In most cases, extending the service life of structure is more sustainable than demolition and new construction. Along with reducing carbon emissions, retrofitting reduces construction waste, preserves cultural and historical heritage, and saves costs compared to the new construction.

Assessment is performed using:

- visual inspections to locate visible cracks, spalling and deformations
- geometrical surveys to measure dimensions and construction details
- non-destructive and destructive tests to determine material properties
- numerical analysis using finite element models

Load testing complements other methods by directly verifying load capacity or providing information for verification of structural model. In practice, very often results of final element models diverge from those of loading tests. This is happening because of assumptions, simplifications, and incomplete input data.

Despite advances in finite element modelling and testing, the difference between observed and predicted behaviour remains. Present work focuses on comparing experimental load tests performed in the laboratory with analytical models to identify the sources of divergence and improve the reliability of structural assessment.

2. Assessment of existing structures

Many structures approach the end of their design life, and assessment becomes more and more important. Evaluating existing structures allows to make an informed decisions regarding safety, functionality, and potential interventions. In addition, new sustainability goals promote the preservation and reuse of existing structures, reducing environmental impact, and conserving resources.

Current EN Eurocodes mainly focus on the design of new structures and offer limited guidance on the assessment of older constructions. For this purpose, New European Technical Rules for the Assessment and Retrofitting of Existing structures have been developed for existing structures. These rules concern all types of buildings, bridges, and civil engineering works, and take in account all relevant loads and environmental actions. They complement the EN Eurocodes by distinguishing between the design of new structures and the assessment or retrofitting of existing ones. The rules provide procedure for evaluating structural safety and planning interventions.

At the national level, Italy has issued Guidelines for the classification and risk management, safety assessment, and monitoring of existing bridges as mandatory code. Guidelines provide procedures for evaluating structural condition, load-carrying capacity, and required interventions. These guidelines align with European standards but include additional criteria to consider local specifics.

In this chapter, the assessment procedures provided by New European Technical Rules for the Assessment and Retrofitting of Existing structures [1] and the Guidelines for the classification and risk management, safety assessment, and monitoring of existing bridges [2] are reviewed.

2.1. New European Technical Rules for the assessment and retrofitting of existing structures

According to the European technical Rules an assessment of existing structures may be necessary in following cases:

- to evaluate structural resistance of existing structures in relation to the loads due to change in use of structure, operational changes or extension of its design working life
- repair of an existing structures that degraded over time due to environmental conditions or has sustained damage from accidental events such as impact, explosion, fire, or earthquake
- doubts about reliability of the structure

- rehabilitation of an existing building structure connected to the retrofitting of the building services
- requirements from authorities, insurance companies or owners or from a maintenance plan

For bridges, principles remain consistent and similar methodologies are applied. Additional aspects to consider are:

- reducing environmental impact through life cycle analysis
- estimating and optimizing costs with life cycle calculations
- integrating maintenance and management strategies
- conducting risk analyses

Part III of the Technical rules proposes a methodology for the structural assessment based on the principles of EN1990.

General assumptions for assessment consider that existing structure was designed in accordance with recognized engineering principles and built using proper workmanship and acknowledged professional practices.

The assessment of structure includes a series of procedures to determine current condition of the structure and future structural performance. The hierarchy of these procedures is presented in Table 3.1 of technical rules (Figure 1).

Table 3.1: Main components of assessment, structure management and interventions upon existing structures [1] and [8]

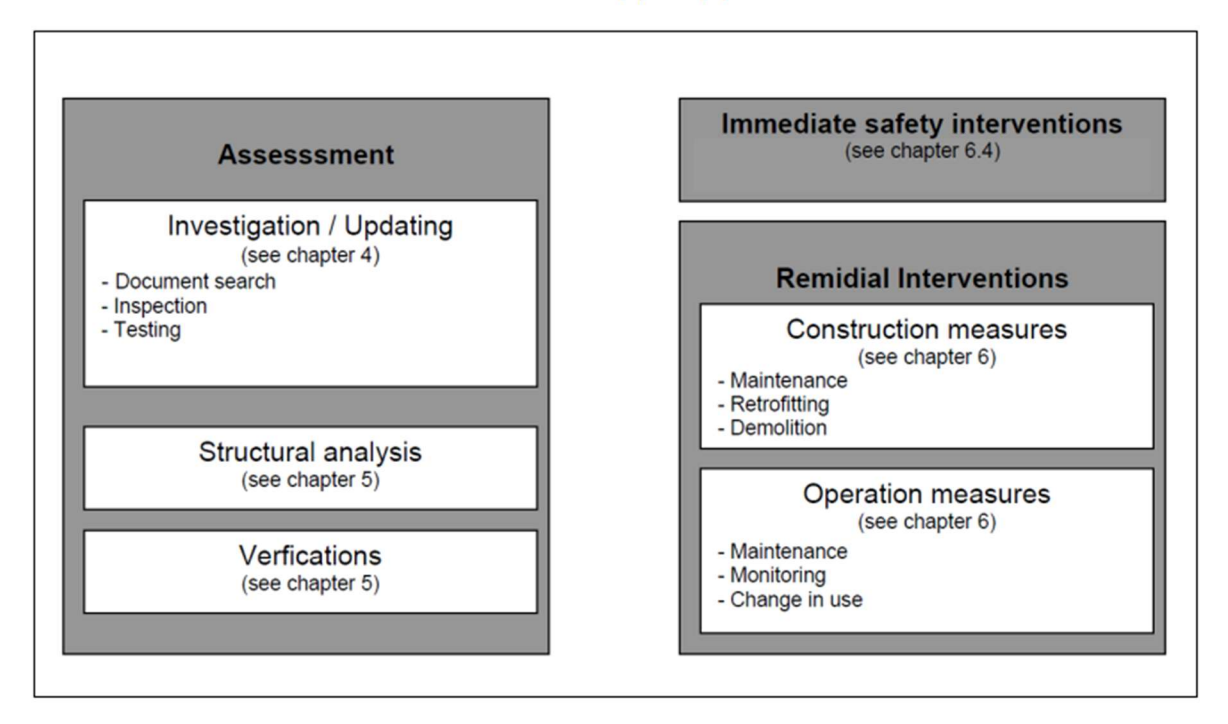


Figure 1: Main components of assessment

The goal of structural analysis is to evaluate the safety of a structure, and if required, its serviceability, considering remaining service life. The analysis also identifies potential interventions if required. Updated data on actions and resistances should be used to perform analysis.

2.1.1. Generic procedure

Table 3.2 of Technical Rules (Figure 2) shows the progression of stages of the assessment, considering updated information about condition of the structure.

Definition of requirements (see chapter 2 & 3) Specification of assessment objectives (see chapter 3.2.1) Identification of scenarios (see chapter 3.2.2) Operational measures Preliminary assessment (see chapter 3.2.3) Immediate safety Is safety clearly interventions ensured? yes Reporting results no Is further information required? yes Detailed assessment (see chapter 3.2.4) Reporting results Evaluation of results (see chapter 3.2.5) Remedial no Sufficient structural interventions performance? Reporting results Construction measures (see chapter 6)

Table 3.2: Generic procedure of assessment and retrofitting of existing structures.

Figure 2: Generic procedure of assessment and retrofitting of existing structure

2.1.2. Preliminary assessment

During the preliminary assessment study of documents is realized, followed by preliminary inspections and checks. Decisions on immediate interventions or on subsequent detailed assessment are made based on this information.

Original design documents provide vital information about existing structure, but the accuracy of documentation should be verified. Documents should also include information about previous interventions and history of exposure to significant environmental or seismic events, extreme loads, changes in soil conditions, or structural misuse.

Preliminary inspections are used to evaluate the structural system and recognize damage through visual observations, including visible deformations, cracks, spalling, and corrosion. Findings are recorded in qualitative grading system to describe the severity of damage (none, minor, moderate, severe, destructive, or unknown)

Preliminary checks are performed to identify critical deficiencies that could affect future safety and serviceability of the structure. Based on these checks, decision about further actions is made. In case of potentially dangerous condition, immediate interventions must be carried out. If there is any uncertainty about structural behaviour or clear deficiencies, further investigations are recommended.

2.1.3. Detailed assessment

During the detailed assessment all available documents should be reviewed. That includes drawings, specification, structural calculations, construction records and maintenance, details of modifications and information about soil conditions. It should be remembered that all the verifications have been done in accordance with standards present at the time of construction.

Detailed inspection of the structure and material testing are used to determine the dimensions of the structure and properties of materials in case of absence of original documentation or if its accuracy is uncertain.

Updated values of actions have to be determined in accordance with EN1991. If detailed structural analysis or inspection do not provide reliable results, testing of the structure can be used to measure properties or to predict load bearing capacity.

Verification of an existing structure should be performed to confirm a target reliability level that corresponds to the required structural response. If analysis shows insufficient resistance, remedial interventions must be planned. In some cases, the control or modification of the risk can be implemented. Risk control measures include load restrictions, monitoring and control, risk acceptance.

During the assessment of existing buildings, the knowledge level concept is applied. It states that depending on the level of detail of information obtained appropriate confidence factors are considered.

2.1.4. Material properties

Material properties must reflect the current condition of the structure, considering the deterioration and any past actions such as fire or overloads. When partial safety factor is applied the characteristic value of the strength must be use, whereas deformation properties, such as elasticity, are assessed using mean values. Probabilistic approach can be used to combine available original data with results from tests, so testing is always required to confirm the accuracy of design documents.

To characterize the material properties both destructive and non-destructive test may be applied. Non-destructive techniques must always be calibrated against destructive tests to ensure reliability. Since laboratory conditions may not fully reflect on-situ behavior, conversion factors can be applied.

2.1.4.1. Non-destructive tests

Schmidt Hammer [3]

A Schmidt hammer (rebound hammer, Swiss hammer, concrete hammer), is used to measure the elastic properties or strength of concrete or rock. It works by recording the rebound of a spring-loaded mass hitting the surface of the material. The impact energy is fixed, and the rebound depends on the surface hardness. The rebound value is read by the equipment and converted into an estimated compressive strength using a standard chart.

The test method is defined in UNI EN 12504-2 (2001). It is usually performed near core drill locations so results can be compared, and correction factors applied. This is done also because the reliability of rebound test is low. To improve reliability, it should be combined with other tests, such as ultrasonic or compressive tests.

Ultrasonic Tests [3]

This test correlates the speed of elastic waves traveling through a structural element with the material's compressive strength. The emitting probe produces sonic or ultrasonic impulses at a predetermined frequency. The receiving probe detects these impulses and measures their transit time using a quartz counter. Knowing the distance between the probes allows calculation of the wave propagation speed. The accuracy of measurements is influenced by material density, moisture content, presence of metal

reinforcement, reflections from structural surfaces, cavities or discontinuities, and porosity.

SONREB Tests [3]

The SONREB method (SONic + REBound = ultrasound + sclerometer) was developed to reduce errors in ultrasonic and Schmidt Hammer tests. Moisture content in the material causes the sclerometric index to be underestimated and the ultrasonic speed to be overestimated. As concrete ages, the sclerometric index rises while the ultrasonic speed decreases. Using tests together helps to correct some of the errors present when each method is applied alone.

2.1.4.2. Destructive tests

Core Drilling [3]

Core drilling involves extraction of the cylindrical samples from a structural element using a drill with a diamond-tipped crown. Each core is subjected to compression test to determine compressive strength. At least three cores are usually required. The cylinders must have a height equal to twice their diameter and flat surfaces. When different aspect ratio of cylinder is used, appropriate correction factors should be applied.

Rebar Extraction [3]

The reinforcement bars are extracted to obtain material characteristics. The correct extraction procedure provides that a new rebar is first welded, and the piece of rebar to be tested is cut. The testing protocol follows UNI EN ISO 15630-1. Rebars should be taken from the structural portions of elements where they are less stressed.

2.1.5. Geometrical properties

When assessing existing structures, the actual dimensions of structural members must be considered. If original drawings are available, they can be used to determine dimensions, but their correspondence to the real situation must be checked. In case of doubt, dimension obtained directly by inspection and measurement are used.

2.1.6. Structural model

If the structural properties are not sufficiently understood, or if dimensions and material properties cannot be established by measurements, testing may be required. The structural model must represent the actual condition of the structure. Updates on the model are based on the information obtained regarding degradation and permanent deformations. Partial or complete static load tests or dynamic tests can be applied, but they must be used when there is no alternative.

Inconsistencies between behaviour during testing and results of a simulation must be clarified. It should be mentioned that structural behaviour at test load level may differ from response at ultimate limit state. The effects of deterioration and defects on resistance and deformation capacity should be quantified and updated.

2.1.7. Structural analysis and verifications

The evaluation and assessment are performed equivalent to the design of new structures, using updated information and conditions of use during the remaining working life. Structural safety, serviceability and durability must be verified using reliable model and clear limit state function.

Comparison of actual reliability to the target values can be performed by means of:

- the partial factor format or the global resistance format,
- the probabilistic format,
- risk analysis.

Structural analysis for the assessment of existing structures must follow the basic principles of EN1990, while using updated values for materials, geometry, and actions obtained from inspections and tests. Different analysis methods are available, and the choice depends on the type of structure, material, and the accuracy required to reflect actual structural behaviour. The main methods are:

- Linear elastic analysis assumption that structure behaves elastically up to failure.
- Linear elastic analysis with limited redistribution allow partial redistribution of internal forces to reflect ductility in certain elements.
- Plastic analysis assumes sufficient ductility and redistribution, enabling the use of plastic capacity.
- Non-linear analysis considers both material and geometric non-linearity, providing the most realistic representation of behaviour.

The model must be consistent with the real behaviour of the structure. Using models outside their valid range may lead to unsafe conclusion.

Linear and plastic analysis are usually checked using the partial factor format from Eurocodes, which accounts for uncertainties in loads and resistances. Non-linear analysis requires more advanced approaches, such as probabilistic methods or risk analysis, because uncertainties and redistribution effects are more significant. In some cases, a global resistance format may be applied. The partial factor approach can also be applied but only when a small redistribution of internal forces and moments is needed, with factors adjusted to account for the effects of nonlinear behaviour. Non-linear analysis demands knowledge of the actual deformation capacity of the structure.

2.1.7.1 Verifications based on partial factors

The partial factor format considers uncertainties from different sources during assessment. Following inequality should be fulfilled for each limit state:

$$g(F_{act}, f_{act}, a_{act}, \theta_{act}, C) \ge 0$$

Where:

g is the limit state function; F_{act} is the assessment value of actions; f_{act} is the assessment value of material properties; a_{act} is the assessment value of geometrical quantities; θ_{act} is the assessment value of model uncertainties; C is the serviceability constraints.

2.1.7.2 Verifications based on global resistance

The safety verification can be performed in the domains of actions or actions effects. In the domain of actions, it should be verified that:

$$\gamma_{G,act}G_{k,act} + \gamma_{Q,act}Q_{k,act} + \gamma_{P,act}P_{k,act} \leq \frac{q_{u,act}}{\gamma_{R,act}}$$

Where:

 $\gamma_{G,act}G_{k,act}$ is the assessment value of permanent actions; $\gamma_{Q,act}Q_{k,act}$ is the assessment value of variable actions; $\gamma_{P,act}P_{k,act}$ is the assessment value of pre-stressing; $q_{u,act}$ is the failure load estimated by means of non-linear analysis with the actual mean values of the material resistances.

 $\gamma_{R,act}$ is the actual global resistance factor which accounts for the uncertainties in the resistance model;

Considering the domain of actions effects, it should be verified that:

$$E\left(\gamma_{G,act}G_{k,act} + \gamma_{Q,act}Q_{k,act} + \gamma_{P,act}P_{k,act}\right) \leq \frac{R\left(\frac{q_{u,act}}{\gamma_{R,act}}\right)}{\gamma_{Ract}}$$

Where:

E is the effect of actions;

R is the resistance:

 γ_{Ract} is the actual partial factor for model uncertainties on the resisting side; $\gamma_{R,act}$ is an actual global resistance factor taking into account the randomness of the structural response;

2.1.7.2 Verifications based on probabilistic format

The reliability of structure is assessed by probability of failure or the reliability index β . This safety format shall be applied in accordance with the principles and recommendations laid down in JCSS Probabilistic Model Code and in JCSS Probabilistic Assessment of Existing Structures.

The procedure for assessment of probability of failure consists of the following steps: development of appropriate structural model, randomization of input variables (actions, material properties, dimensions etc.) represented by random variables or field with spatial variability, and probabilistic analysis of structural performance using analytical, numerical, or simulation-based techniques. The outcome is an estimate of reliability of structure. Random variables that should be updated based on the actual condition of the structure include actions (incl. model uncertainties), material properties, geometrical properties, structural model (incl. model uncertainties), and deterioration models.

2.1.8. Interventions

Interventions may be categorized as immediate interventions, retrofitting, replacement of entire structure or individual parts, decommissioning and dismantling. Alternatively, to construction methods, operation measures may be implemented. It includes acceptance of current condition, limitation in use, additional safety provisions, more detailed investigations, new or revised monitoring and maintenance strategies.

Monitored values must be compared with threshold values, determined by the probability of failure.

Retrofitting is a measure used to achieve required structural performance, and it may involve repair or upgrading. The goal of repair is to restore the intended structural resistance by fixing or replacing damaged members, or by adding new ones. By upgrading, structural performance must increase beyond the originally intended level.

Urgent safety measures are implemented when immediate risk to public safety occurs. It includes evacuation of people, decommissioning of the structure, restrictions of use and access, and intensified monitoring.

Remedial measures are determined with respect to the importance of the structure, damage potential, nature of structural failure, possibility of monitoring and controlling, cost-risk considerations, and the possibility of damage limitation. Measures can be operational or constructional in nature. Apart from already mentioned operational measures, limitation of live loads, installation of automatic warning and safety equipment, and introduction of evacuation plans can be implemented.

2.2. Guidelines for the classification and risk management, safety assessment, and monitoring of existing bridges

Assessment of existing structures in Italy is regulated by the NTC 2018 [4], which includes a dedicated Chapter 8 on this topic. It covers the procedures for safety verification of existing structures, defines the required level of retrofitting when necessary, and includes a section specifically on seismic design.

Based on NTC 2018, the Ministry of Infrastructure and Transport issued in 2020 the Guidelines for the classification and risk management, safety assessment, and monitoring of existing bridges, which focus specifically on bridges. In 2022, complementary Operating instructions [5] were issued to ensure uniform and immediate implementation of the Guidelines. This chapter is mainly based on 2020 Guidelines.

2.2.1. Multilevel Approach

The Guidelines propose the multilevel approach for the assessment of existing bridges. It includes 6 levels. The level of detail, cost of investigations and complexity of analysis increase from Level 0 to Level 5, while the number of bridges that are assessed decreases. The multilevel approach and the relationships between levels of analysis are presented in Figure 3 [Source 6].

Level o. Census.

Level o includes the cataloguing procedure, during which the number of structures and their main characteristics are identified. Data is collected from technical and administrative documents, including geometry, location, year of construction, structural system, and the role in the transportation network.

During this stage, bridges can be grouped into macro classes to define order of priority for visual inspections.

Level 1. Visual Inspections.

During visual inspections, standardized defect sheets are used to describe cracks, corrosion, and other forms of structural degradation. This step also includes the description of the main characteristics such as structural systems, materials, general geometry, and data on hydraulic and geomorphological conditions. During this step critical elements are identified and inspected when possible.

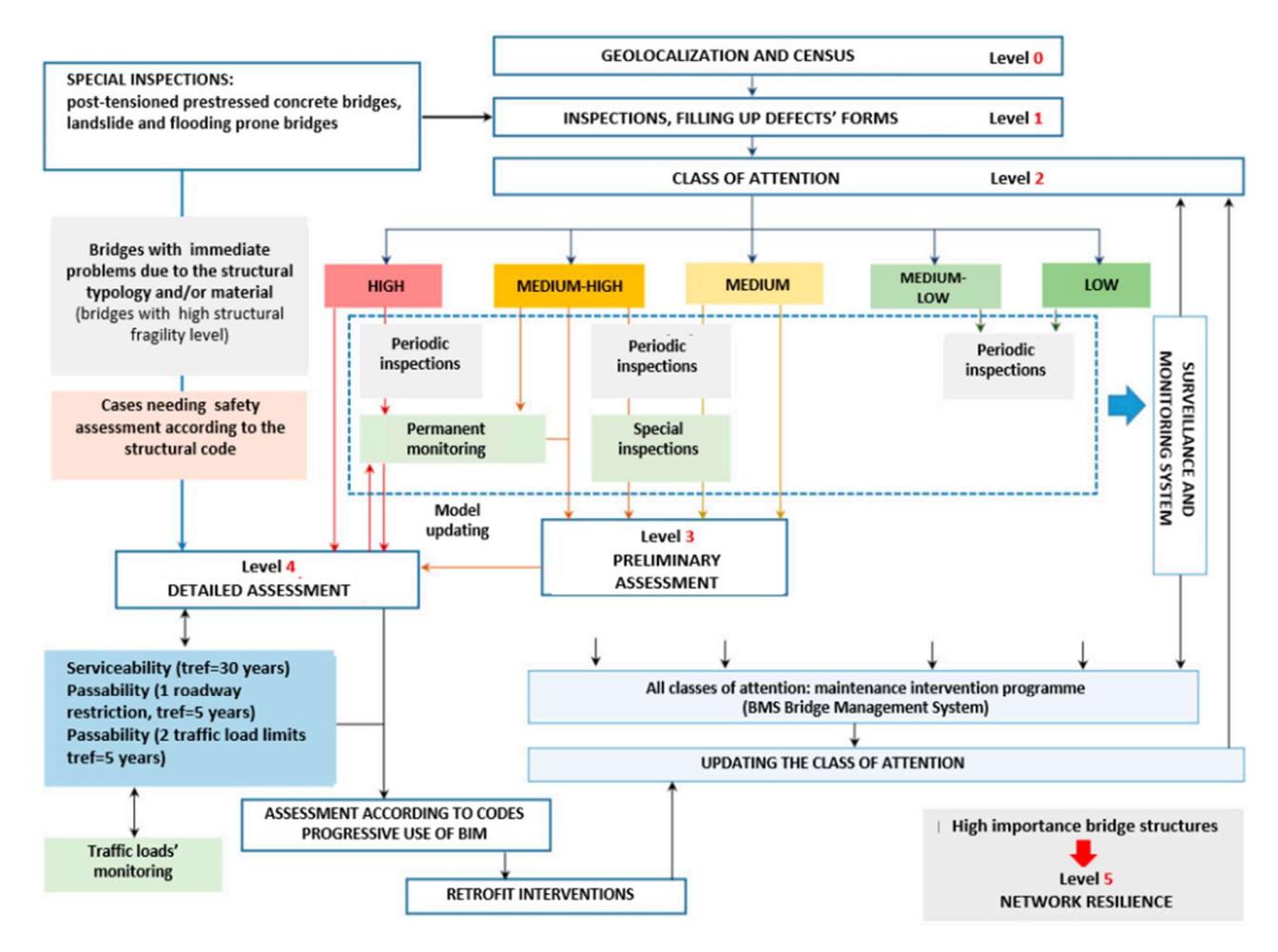


Figure 3: Multilevel approach and relationships between levels of analysis

Level 2. Attention classes.

Collected data is used to assign each bridge to an attention class (CdA). Four main types of attention classes are considered: structural and foundational, seismic, landslide, and hydraulic. Each type is evaluated independently and assigned to one of the following attention classes: High, Medium-High, Medium, Medium-Low, Low, as a function of hazard, vulnerability, and exposure (Figure 4). Attention classes for the four types are then combined to determine the overall attention class. Depending on the attention class frequency of periodical check is established. Continuous monitoring is provided for Medium-High, High attention class bridges. The attention class must be redefined after interventions.

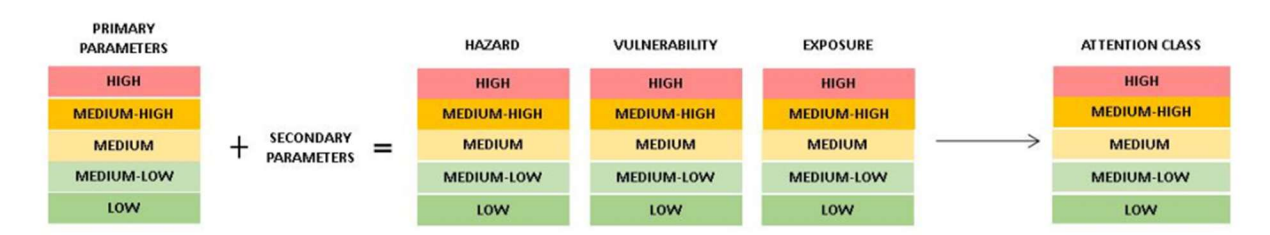


Figure 4: Logical flow for determining the attention class

Level 3. Preliminary assessments.

Level 3 is a preliminary assessment performed to evaluate deteriorated structural elements observed during visual inspection and to identify possible causes. It should be applied to bridges with Medium-High and Medium attention classes. This step is also used to approximately evaluate structural capacity by comparing the capacity of structure based on the standards at the time of construction with current requirements. The main structural elements, such as slabs, beams, piers, and abutments must be considered. In general, by comparing traffic loads, bridges designed for military loads are comparable to modern requirements, while the civilian traffic loads have increased in current regulations. Preliminary assessments determine whether Level 4 verification is required.

Level 4. Accurate safety verification.

Level 4 includes advanced analyses, such as material testing, geotechnical surveys, structural modelling, and load calculations according to the current standards.

Levels 4 will be reviewed in greater depth, as it is more relevant to the detailed structural assessment of slabs.

Level 5. Network evaluation.

It applies to bridges with significant transport importance and includes resilience analysis and socio-economic impact studies.

2.2.2. Level 4. Accurate safety verification

This chapter of the Guidelines is divided into three parts. The first part presents the fundamental concepts and strategies, knowledge acquisition and the definition of analysis levels. The second part provides procedures and measures necessary to obtain the understanding of the existing structure. And third part provide guidance for performing safety assessment, including modelling, analysis, and verification. Although the general principles are applicable to all structures, this chapter addresses specifically road bridges. In general, the procedures are intended to be adapted to each bridge.

2.2.2.1. Fundamental concepts and strategies for safety assessment

To understand the real behaviour of the structure the main objective is to reduce uncertainties related to the load definition, behaviour of materials and structures. In other words, to obtain appropriate level of knowledge of structure. It is achieved by progressive detailed investigations and testing, ensuring increase in accuracy and representation of real behaviour.

Reference time is introduced as a time frame for which the assessment is performed. At the end of this period assessment has to be repeated to ensure appropriate level of safety. Degradation caused by environment is more important in bridges than in buildings, especially if proper maintenance was not provided. Therefore, it is important to consider state of degradation of structure in case the resisting capacity declined.

According to NTC 2018 safety assessment is carried out in case of evident reduction of the resistant and / or deforming capacity of the structure or of some of its parts due to:

- significant degradation and decay of the mechanical characteristics of the materials, significant deformations consequent also to problems in the foundation;
- damage caused by environmental actions (earthquake, wind, snow and temperature), by exceptional actions (shocks, fires, explosions) or by abnormal operating and use situations;
- proven serious design or construction errors;
- change of the intended use of the structure or parts of it, with significant variation of the variable loads and / or passage to a higher class of use;
- whenever the structural interventions referred to in § 8.4 are carried out

The case of a change in the magnitude of environmental action is excluded from the situations that require safety assessment. However, for bridges, hydraulic effects such as floods, scour, and landslides are often crucial for an accurate evaluation of structural safety. Regarding the not structural interventions, possible increase in permanent loads and durability problems have to be considered.

Also, the bridges with High attention class must be subjected to detailed investigations and safety verification.

Guidelines define following situations as a result of assessment:

- 1. Adequate. An existing bridge is considered adequate when the checks performed according to the Technical Standards are satisfied using the loads and partial safety factors specified in the standard.
- 2. Operational. A bridge is considered operational when the checks performed according to the Technical Standards are satisfied but using a reduced reference time for the evaluation of partial safety factors. In the Guidelines, the reference period is taken as 30 years.
- 3. Transitable. A bridge is considered to be transitable when the checks performed are satisfied over a short time period (max 5 years). During this time operational interventions are planned and executed. These include limiting permitted loads, restriction of bridge usage.

Safety assessment requires to obtain two indicative values ζ_E and ζ_V . ζ_E is the ratio of the maximum seismic action that can be tolerated by the structure and the maximum seismic action that would be used in the design of a new structure on the same ground and with the same characteristics (natural period, behaviour factor, etc.). ζ_V is the ratio between the maximum value of the variable vertical overload that can be supported by the i-th part of the structure and the value of the variable vertical overload that would be used in the design of a new structure.

Evaluation of ζ_E is performed for adequate level bridges, while for operational and transitable situations verification is performed with respect to static and geotechnical actions.

Regarding the ζ_V the situation is similar. It can be performed for bridges classified as adequate. For other levels, assessment is carried out with reduced reference time, usage restrictions and load limitations. Therefore, when evaluating the safety ratio, the vertical overload is considered specifically to the verification conditions.

In addition to vertical loads and seismic effects, safety assessment should consider floods and landslides impacts.

Assessment of state of degradation and planning of restorations are also part of the assessment. Seismic or hydraulic related interventions require appropriate planning. Non-seismic actions require immediate measures, due to connection to the operating conditions of the bridge.

2.2.2.2. Structural Characterization of the bridge.

Procedure for the in-depth analysis:

- 1. Historical-critical analysis
- 2. The analysis of the original project
- 3. Geometric and physical surveys
- 4. Geological characterization of the site
- 5. Definition of mechanical properties of materials and construction details

In case of hydrogeological risk verification additional investigations include:

- 6. Hydraulic assessment, including scour identification at piers and abutments and efficiency of flood mitigation or flow regulation works
- 7. Geomorphological assessment, meaning the identification of slope movements and presence and effectiveness of past stabilization interventions.

The historical-critical analysis is a collection and study of all available documentation related to the structure, including original design drawings, technical reports, construction records. It allows to understand the original design, evaluate the verifications performed according to the regulations in force at the time, and an assessment of construction procedures that could have affected the structural behaviour.

The geometrical survey can confirm the accuracy original drawings, if available. This allows for a reliable reconstruction of structural model. Observations on crack patterns combined with historical analysis, provide possible explanation for the mechanisms of deterioration.

Based on the results of above analyses, further investigations on construction details and materials are planned. These investigations include in situ tests on structural elements and in situ or laboratory testing of the materials. The aim of mechanical characterization of materials is to determine their strength and deformability parameters, which are essential for structural modelling, analysis and safety assessment. A progressive, in-depth investigations allow to focus on critical areas and minimize the extent of testing.

Analysis of structural elements located in riverbed in combination with the assessment of hydraulic and geomorphological conditions allows to estimate potential damage in the event of landslides and flooding.

In the absence of original documentation, investigations are directed to obtain information about the entire structure, while still minimizing number of tests performed. The detailed investigations are based on the results of preliminary checks to focus attention on critical parts of the structure. The procedures include in-situ test on structural elements, laboratory tests to obtain material properties, in-situ surveys to assess the durability state.

The number of tests carried out depends on the desired level of knowledge. Three levels of investigations are defined by the standard:

- 1. Limited investigations. Limited number of tests allows to check the correspondence of existing structure to the original drawings or regulations in force at the time of construction.
- 2. Extended investigations. A greater number of tests is performed in case of absence of original documentation, or if the results of correlation are not satisfactory.
- 3. Exhaustive investigations. A greater number of tests is performed to achieve a desired level of knowledge of the structure. For example, in most critical areas or when are uncertainties are present.

The number of investigations corresponding to three levels of investigations is determined by the responsible technician based on the information obtained and the results of preliminary checks.

Based on the insights carried out, three levels of knowledge are defined for the purpose of choosing the type of analysis and the values of confidence factors. The levels of knowledge are in order of increasing of obtained information KL1 (LC1), KL2 (LC2) and KL3 (LC3). Corresponding confidence factors are used to reduce the magnitude of mechanical properties. According to the NTC 2018:

- 1. Knowledge level 1 is achieved when the historical-critical analysis, the complete geometric survey and limited investigations on construction details, and limited tests on the mechanical characteristics of the materials are carried out. The corresponding confidence factor is FC = 1.35.
- 2. Knowledge level 2 is achieved when the historical-critical analysis, the complete geometric survey and extended investigations on construction details, and extended tests on the mechanical characteristics of the materials are carried out. The corresponding confidence factor is FC = 1.20.
- 3. Knowledge level 3 is achieved when the historical-critical analysis, the complete geometric survey and exhaustive investigations on construction details, and exhaustive tests on the mechanical characteristics of the materials are carried out. The corresponding confidence factor is FC = 1.00. Complete geometric survey and exhaustive knowledge of construction details are equivalent to the original design documents.

The level of knowledge of critical structural elements should always be KL3.

2.2.2.3. Safety assessment and verifications.

Stages of safety assessment are evaluation of actions (permanent, traffic, seismic), load combinations (static and safety combinations with corresponding partial safety factors),

evaluation of material parameters and partial safety coefficients, modelling of structure, structural analysis, resistance evaluation and safety checks.

The values of actions and their combinations correspond to those defined for the new construction, Permanent loads are determined based on direct geometric measurements and the density of structural and non-structural members. Partial safety factors may be reduced under certain conditions.

Variable loads and loading schemes in the case of Adequate bridge are described in the Technical Standards. For Operational verification, the same load schemes are applied, but with reduced partial factors related to the reduction of reference time. In the Transitable case, the load schemes are adapted to the new geometric configuration. When load limitation is enforced, appropriate load is assumed with partial safety factors depending on the control of load limitation.

Seismic action is considered in accordance with Chapter 3 of NTC. Hydrodynamic actions and slope stability verifications are specified in the Chapter 6 of NTC and related Circular.

Load combinations are specified by the Technical Standard for each limit state. For the ultimate state, the fundamental combination (1) is used, for serviceability limit state characteristic combination (2) is applied, and for seismic verification combination (3) is used.

$$\gamma_{G1} \cdot G_1 + \gamma_{G2} \cdot G_2 + \gamma_{P} \cdot P + \gamma_{O1} \cdot Q_{k1} + \gamma_{O2} \cdot \Psi_{O2} \cdot Q_{k2} + \gamma_{O3} \cdot \Psi_{O3} \cdot Q_{k3} + (...)$$
 (1)

$$G_{_{1}}+G_{_{2}}+P+Q_{_{k1}}+\Psi_{_{02}}\cdot Q_{_{k2}}+\Psi_{_{03}}\cdot Q_{_{k3}}+(...) \tag{2}$$

$$E + G_1 + G_2 + P + \Psi_{21} \cdot Q_{k1} + \Psi_{22} \cdot Q_{k2} + \Psi_{23} \cdot Q_{k3} + (...)$$
 (3)

Combination coefficients are specified in Chapter 5 of Technical Standard, while partial safety coefficients are determined considering the reduced uncertainties and the actual reference period. Partial safety coefficients in the Guidelines are calibrated using the Adjusted Partial Factor Method (APFM), based on the reliability index β . In general, bridges are classified as Consequence Class 3 (CC3) according to the EN 1990.

The reduction of partial safety factors for permanent loads is considered under three situations:

- 1. Standard conditions, assuming a load variation coefficient of 0.1
- 2. Statistical control of materials and geometries, with load variation coefficient reduced to 0.05
- 3. Condition 2 with reduced modelling uncertainties.

Tables 1,2 summarize the partial safety coefficients for the adequate, operational, transitory bridges.

Tabella 6.3.2– Fattori parziali di sicurezza per i carichi permanenti, $\gamma_{G'}$ per verifiche di transitabilità e operatività

CLASSE DI CONSEGUENZA	(1) CONDIZIONI STANDARD	(2) CON ACCURATO CONTROLLO STATISTICO DI MATERIALI E GEOMETRIA E COV<0,05	(3) COME (2) E CON ABBATTIMENTO INCERTEZZE DI MODELLO (§ 6.3.3.5)
CC3	1.26	1.16	1.10

Table 1: Partial safety factors for permanent loads in operational and transitory verification

Tabella 6.3.3– Fattori parziali di sicurezza per i carichi permanenti, $\gamma_{\rm G}$, per verifiche di adeguamento

CLASSE DI CONSEGUENZA	(1) CONDIZIONI STANDARD	(2) CON ACCURATO CONTROLLO STATISTICO DI MATERIALI E GEOMETRIA E COV<0,05	(3) COME (2) E CON ABBATTIMENTO INCERTEZZE DI MODELLO (§ 6.3.3.5)
CC3	1.35	1.25	1.20

Table 2: Partial safety factors for permanent loads in adequate verification

Partial safety factors for variable actions are reported for reference periods of 5 years and 30 years (Tables 3,4).

Tabella 6.3.4- Fattori parziali di sicurezza considerando come azioni principali le azioni variabili da traffico

Classe di conseguenza	Tempo di riferimento tref	Fattori parziali per le azioni variabili da traffico, γ_{ϱ}
CC3	5 anni (ponte TRANSITABILE, § 6.1.5.3)	1.20
	30 anni (ponte OPERATIVO, § 6.1.5.2)	1.20

Table 3: Partial safety factors with traffic as main action

Tabella 6.3.5 – Fattori parziali di sicurezza considerando come azione principale l'azione del vento

Classe di conseguenza	Tempo di riferimento tref	Fattori parziali per l'azione del vento, γ_Q
CC3	5 anni (ponte TRANSITABILE, § 6.1.5.3)	1.26
CCS	30 anni (ponte OPERATIVO, § 6.1.5.2)	1.50

Table 4: Partial safety factors with wind as main action

Partial safety factors for load schemes from Codice della Strada are extremely complex to evaluate. The guidelines provide three situations:

- Control of load exceedance is carried out on sample basis, either through documentation or direct weighing, following the systematic schedule over time. γcds,1=1.6.
- 2. Continuous control of load exceedance is implemented, either through documentation or direct weighing, with blocking procedures applied in the event of excess load. γ_{CdS,2}=1.35.
- 3. Same is 2 but weighing and blocking guaranteed by the owner or manager. $y_{CdS,3}=1.1$.

Depending on the depth of investigations reduction in model uncertainties can be achieved and partial safety factor can be reduced. It is applicable when accurate statistical control of the geometry of structure and direct unit weights measurements are available. Calibration of numerical models by means of static and dynamic tests also contribute to the decrease in model uncertainties.

The material properties are obtained through statistical evaluation, while the extents of dispersion must be considered. To respect both the Italian standards and Eurocodes, following formulation is suggested:

$$f_d = min\left(\frac{f_m}{FC \cdot \gamma_M}; \frac{f_k}{FC}\right)$$

Considering the specific conditions of bridges and that generally the FC is 1, using the average value for f_m is considered unsafe. To estimate the 5% fractile with limited number of samples, assumption of log-normal distribution is made.

The guidelines suggest following values as partial safety factors for material characteristics (Table 5). These values are proposed to use only on ordinary or prestressed reinforced concrete, steel, and steel-concrete composite structures.

Tabella 6.3.7- Fattori parziali di sicurezza per le caratteristiche di resistenza dei materiali, condizioni di Operatività e Transitabilità

Materiale	Fattore parziale
Calcestruzzo	$\gamma_c = 1.26$
Acciaio da c.a. e c.a.p.	$\gamma_s = 1.10$
Acciaio da carpenteria	$\gamma_a = 1.05$
Connettori Acciaio-calcestruzzo	γ_{v} = 1.15

Table 5: Partial safety factors for resistance characteristics of materials in operational and transitory conditions

Safety verification is performed by calculating values ζ_E and ζ_V .

Verifications of foundations are performed in the case of global instability or when one of the following occur:

- Foundation failure causes or previously caused the instability of structure
- Morphological conditions, modification of soil profile, or liquefaction cause overturning or sliding of the structure
- Seismic actions on foundations

Local shear verifications in lightly reinforced on non-reinforced concrete elements, may use following expression (MPa, mm):

$$V_{Rd} = \frac{0.3\sqrt{f_{ck}}b_W d}{\gamma_c (1 + 0.0022d)}$$

During the safety assessment any problems with durability must be considered, such as reduction in section of concrete, reduction in section of steel due to corrosion etc.

The verification of trafficability for exceptional vehicles is performed applying the partial safety factors for actions and materials, assuming a reference period of 5 years. If the vehicle load is known with certainty, partial factor may be taken as 1.10. The distribution of weight between the axles must be considered.

3. Tests on existing RC slabs

For confidentiality reasons, the exact name and location of the structure, titles and reference numbers of laboratory reports are not disclosed. The relevant information is present in this chapter.

3.1. Load tests

3.1.1. General information

The object of investigation in this study is the deck of the road tunnel. For laboratory testing, four segments of deck were extracted from the structure. The general cross-section is shown in the Figure 5. The samples were cut approximately 2.5 m in length in the direction parallel to the travel. The vertical partitions below the road were cut maintaining approximately 35 cm of height.

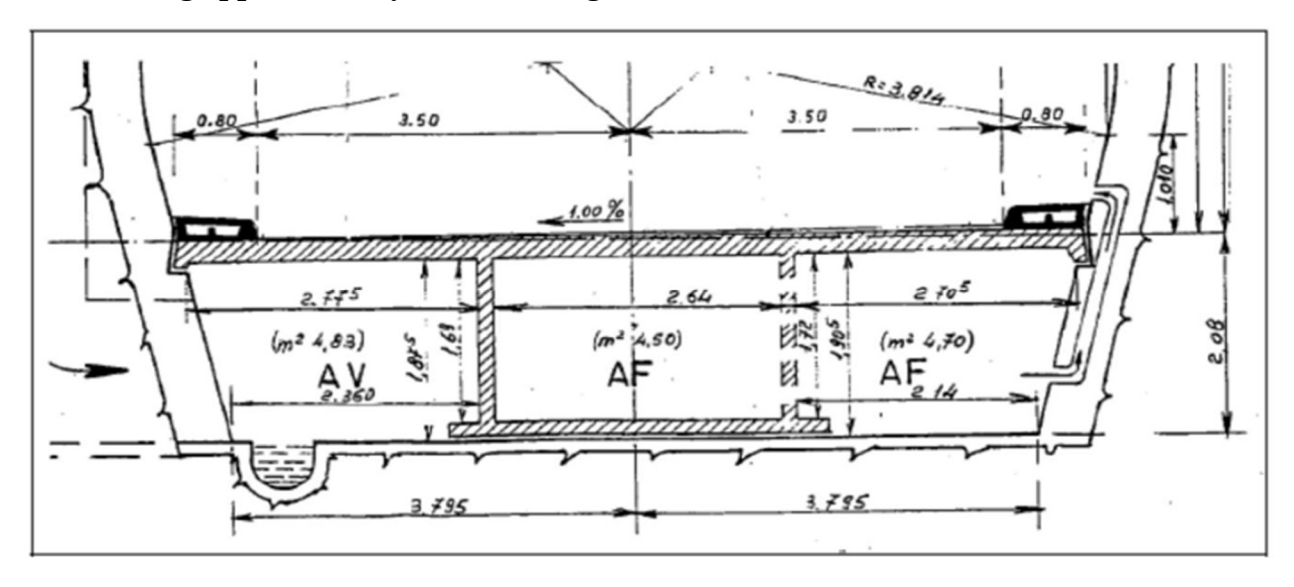


Figure 5: Characteristic cross-section of the deck

Load tests were performed using to the following static schemes 2 and 3, as reported in the NTC2018 [4], chapter 5.1.3.3.3 Load Schemes (Figure 6). Static scheme 2 was performed on two samples, while static scheme 3 was applied to the other two samples. For each static scheme, different ends of the structure were stressed during testing.

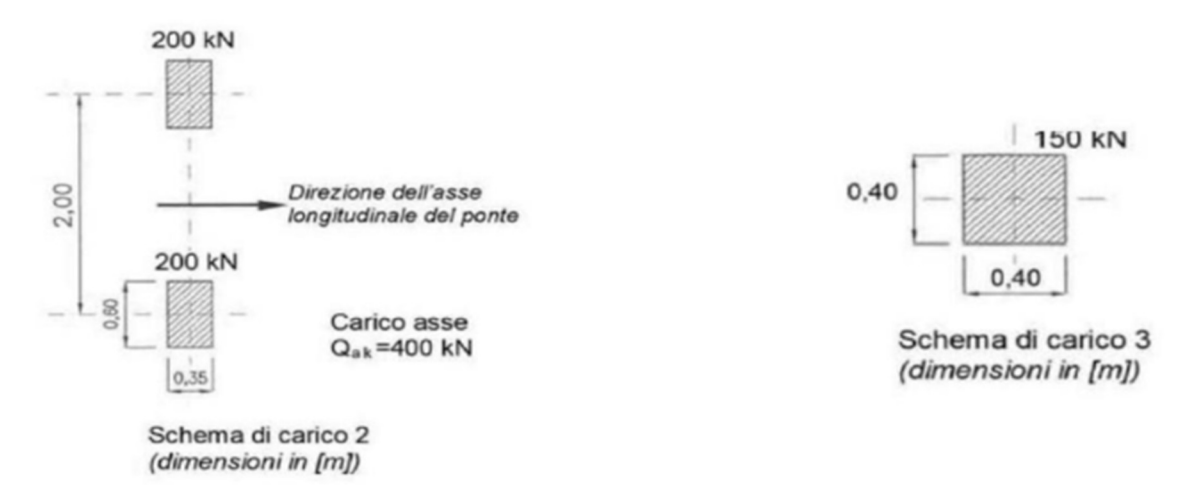


Figure 6: Load schemes 2 and 3, as reported in the 2018 NTC

3.1.2. Description of slots

All four samples have different dimensions. In the following table results of surveys are summarized, considering only concrete, excluding the thickness of asphalt.

misure	misure in mm		Solaio 2	Solaio 3	Solaio 4
BAP1	Fronte	100	115	105	100
	Retro	95	80	100	105
B _{AP2}	Fronte	130	155	145	145
	Retro	140	150	150	155
Варз	Fronte	145	160	150	145
	Retro	160	155	155	160
Вар4	Fronte	115	95	85	105
	Retro	100	95	90	100

misure in mm		Solaio 1	Solaio 2	Solaio 3	Solaio 4
L1	Fronte	2875	2845	2865	2858
	Retro	2873	2865	2835	2880
L2	Fronte	2813	2783	2793	2795
	Retro	2810	2788	2788	2793
L3	Fronte	2850	2883	2863	2865
	Retro	2850	2865	2878	2840
Ltot	Fronte	8645	8615	8615	8620
	Retro	8630	8605	8595	8615

misure in mm		Solaio 1	Solaio 2	Solaio 3	Solaio 4
H _{AP1}	Fronte	370	370	300	300
	Retro	370	370	300	280
HAP2	Fronte	380	340	350	350
	Retro	360	350	340	350
Нарз	Fronte	340	380	380	380
	Retro	350	380	380	380
Нар4	Fronte	280	290	380	380
	Retro	290	290	370	360

misure in mm		Solaio 1	Solaio 2	Solaio 3	Solaio 4
L1	Fronte	215	220	220	220
	Retro	220	210	200	200
L2	Fronte	230	220	220	220
	Retro	220	220	230	210
L3	Fronte	215	215	215	210
	Retro	220	215	210	195
B1	-	2500	2470	2480	2410
B2	-	2490	2530	2490	2460

Table 6: Summary of geometric dimensions

VISTA FRONTALE VISTA FRONTALE T T APPOGGIO 1 APPOGGIO 2 APPOGGIO 3 APPOGGIO 4

Figure 7: Summary of geometric dimensions.

3.1.3. Tests setup

Following the decision to perform 2 two-point bending tests and 2 one-point bending tests, following cases are identified:

- Slab 1: bending test according to the scheme 2 (span 1 and span 2)
- Slab 2: bending test according to the scheme 2 (span 2 and span 3)
- Slab 3: bending test according to the scheme 3 (span 1)
- Slab 4: bending test according to the scheme 3 (span 3)

According to the scheme 2, loading points are located at a distance of 1 m from the support. In this scheme central and adjacent spans are stressed.

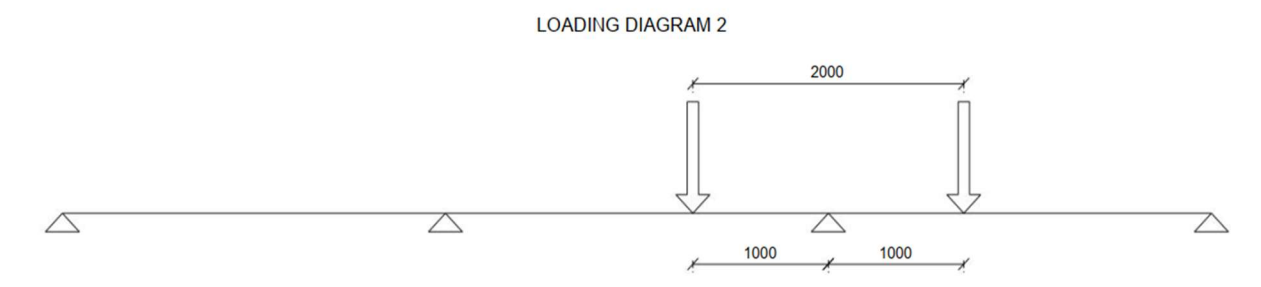


Figure 8: Loading scheme 2

Static scheme 3 involves stressing only lateral span, with application point in the centre of the span.

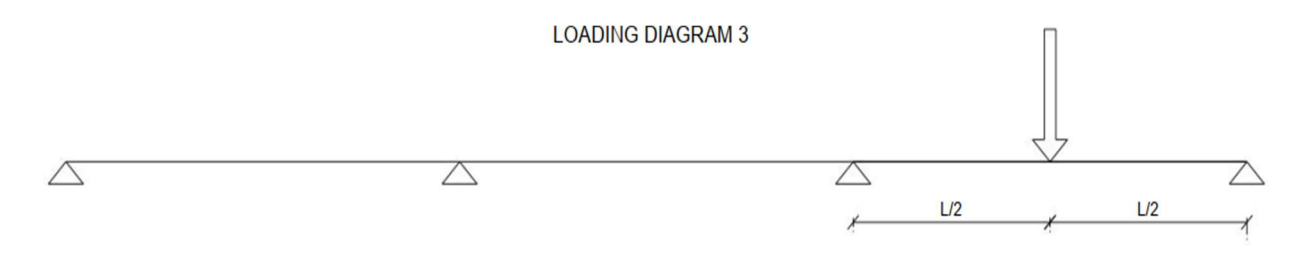


Figure 9: Loading scheme 3

All samples were positioned on steel profiles during the tests. To compensate for difference in support height, a series of steel plates were placed on steel profiles. This is visible in Figure 10. A layer of neoprene was used to compensate for irregularities of the surfaces.





Figure 10: Images of supports

The loading was applied using electromechanical jack with maximum capacity of 1000 kN. To simulate application of the load in two points spaced 1 m from the support, a distribution beam was connected to the jack. The distribution beam, in turn, was connected to the metal elements via cylindrical joints. The load was applied through the wooden elements with size 600x350 mm to simulate the required footprint.

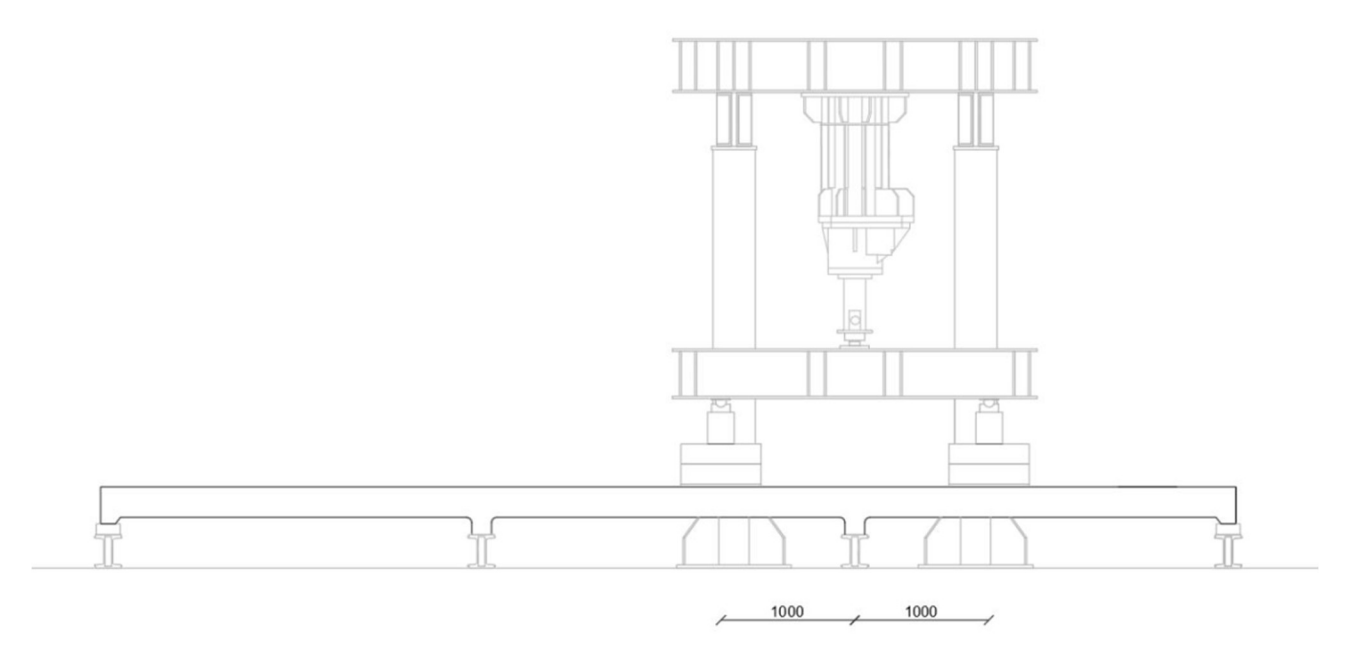


Figure 11: Test setup for scheme 2



Figure 12: General view of the test setup for scheme 2 and load cell detail

For scheme 3, the same electromechanical jack was used together with a steel column, which acted as a spacer to connect the head of the jack with point of load application. A

steel plate with dimensions 400x400mm was positioned between the column and the slab sample to simulate required footprint.

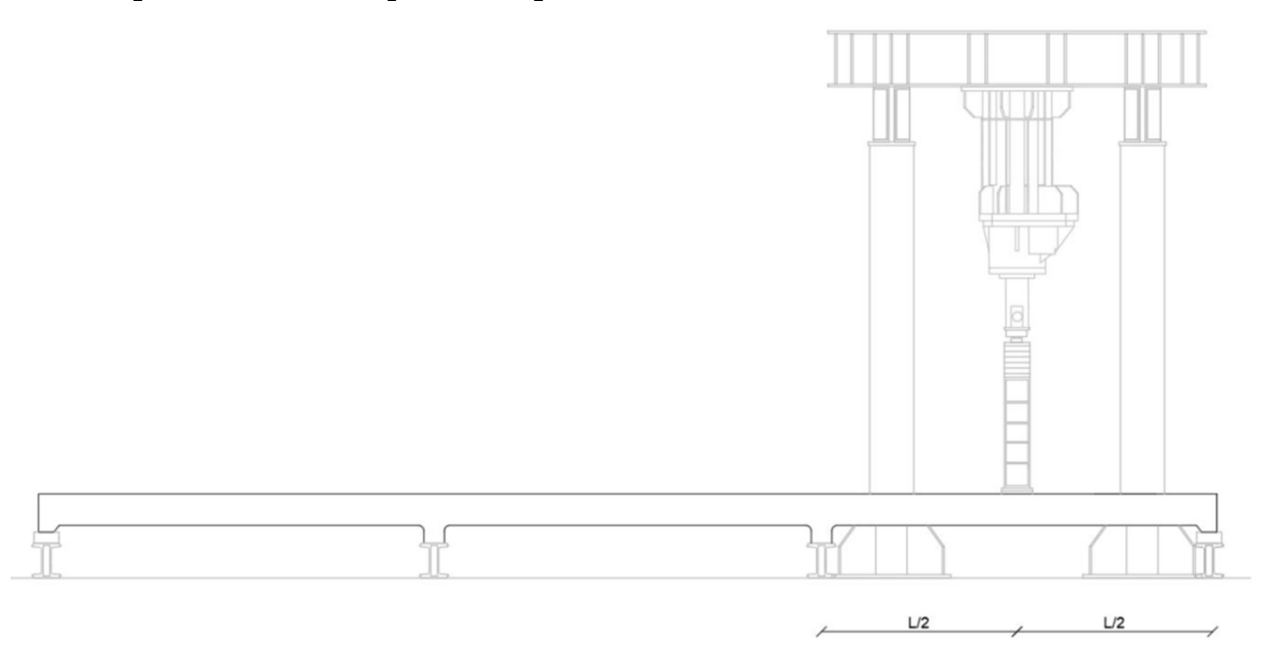


Figure 13: Test setup for scheme 3





Figure 14: General view for test scheme 3

3.1.4. Instrumentation and loading history

The measurement of the load for both schemes was performed by load cell with capacity of 1000 kN, positioned between the head of the jack and the distribution beam in scheme 2 and the column in scheme 3. Any elements placed directly on the sample above load cell is not registered by the cell. However, given the magnitude of the load, it can be considered negligible. Likewise, the self-weight of the samples was neglected.

The tests were performed under load control, with a loading rate of 2 kN/s. Samples were loaded with magnitudes of 0.5F, F, 1.5F and 2F of the required load. After repeating the load 2F three times, an overload cycle is applied till the element collapse. Load values are presented in Table 7.

Load value	Scheme 2, kN	Scheme 3, kN
0.5 F	200	75
1 F	400	150
1.5 F	600	225
2 f	800	300

Table 7: Load values for schemes 2,3

To monitor displacements, the samples were instrumented with transducers near the loading points and on the supports. Transducers were placed along the supports (two at the ends and one in the centre) adjacent to loading point and along the loading central line. The opposite support was monitored only in line with the loading point. Due to the number of measurements points, transducers of different capacity were used. The types of transducers are listed in Table 8, and their distribution in two load configurations can be observed in Figure 15 and Figure 16.

Type of transducer	Max disp, mm	Color
Inductive Standard Displacement Transducer (WA)	20	orange
Rectilinear Displacement Transducer with ball tip (PY2)	50	red
Rectilinear Displacement Transducer with cylindrical case (PZ34)	100	blue

Table 8: Types of sensors

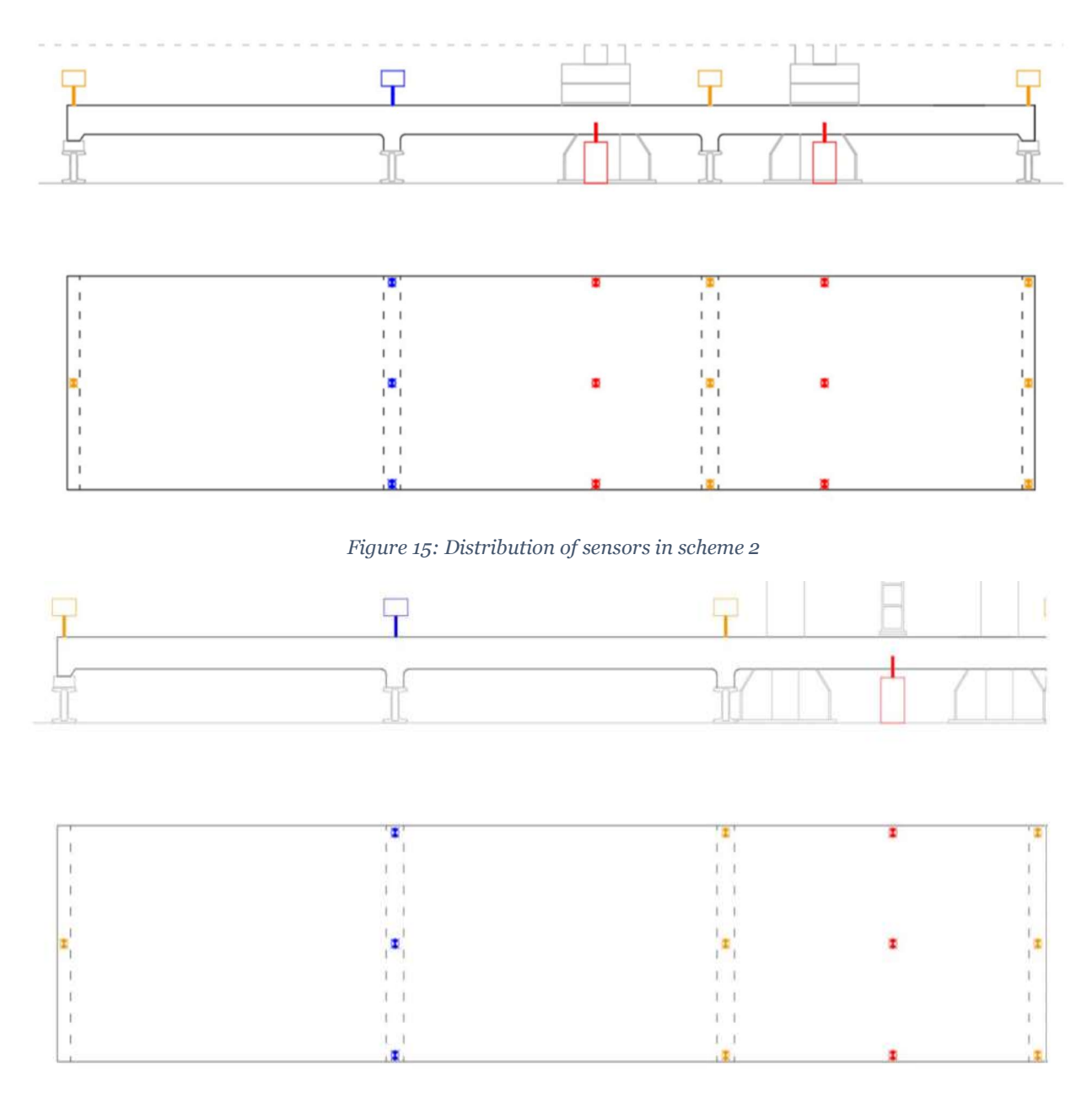


Figure 16: Distribution of sensors in scheme 3

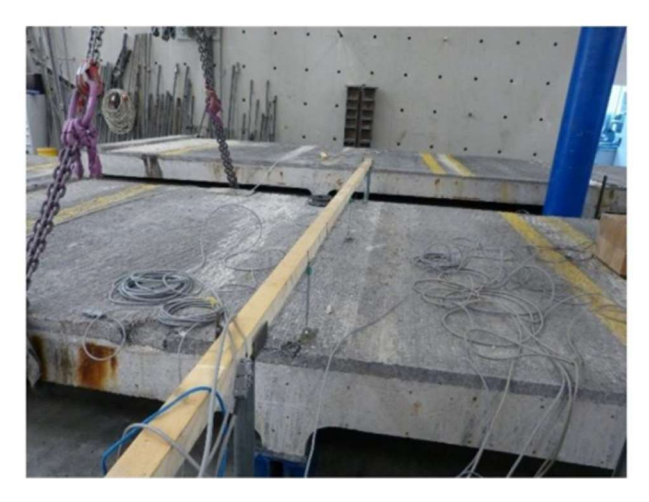




Figure 17: Sensors positioned to monitor the failure of the internal supports





Figure 18: Sensors positioned to monitor settlement at load application points

3.1.5. Results

Results obtained from the load tests are presented in the form of force-displacement graphs at the central point of load application. These graphs were corrected for support settlements. For static scheme 2 two, graphs are presented corresponding to the two loaded spans. For static scheme 3 only one graph is provided. In addition, to the graphs at the load application points, graphs showing the deflections in longitudinal (parallel to the traffic) and transverse direction are present (perpendicular to the traffic flow flow).

3.1.5.1. Sample 1

During visual inspections saline efflorescences was observed, likely caused by the humid environment. It presents a potential risk for corrosion of reinforcement. There is a crack pattern on span 1. The probable cause is transportation and handling of the sample. However, this pattern is between concrete and asphalt layers, and has minimal effect on structural layer.





Figure 19: View of tested spans 1 and 2 respectively





Figure 20: Left - view of span 3. Right: Crack pattern on span 1



Figure 21: Left - saline efflorescences on span 1. Right: Crack pattern on span 3

Static scheme 2 was performed on sample 1 with both span 1 and span 2 subjected to loading. The results are presented in the following graphs.

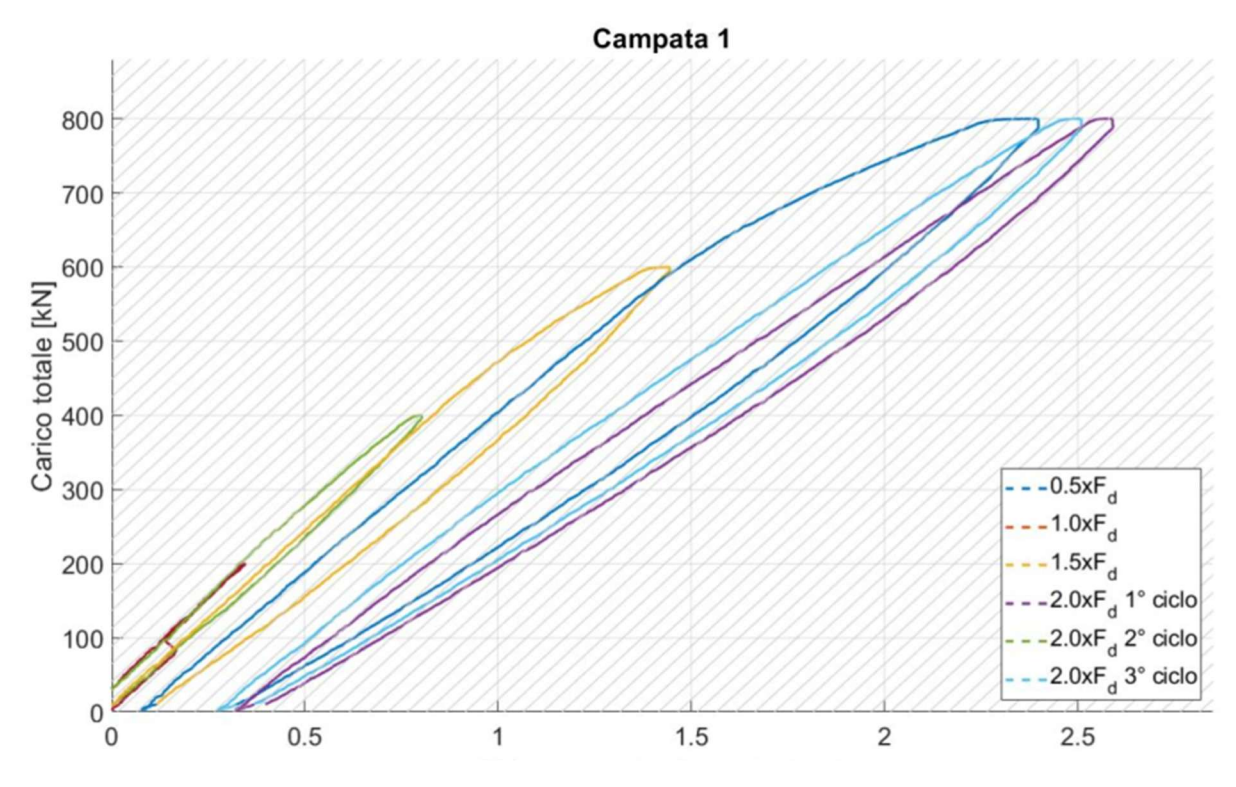


Figure 22: Force-displacement curve of span1

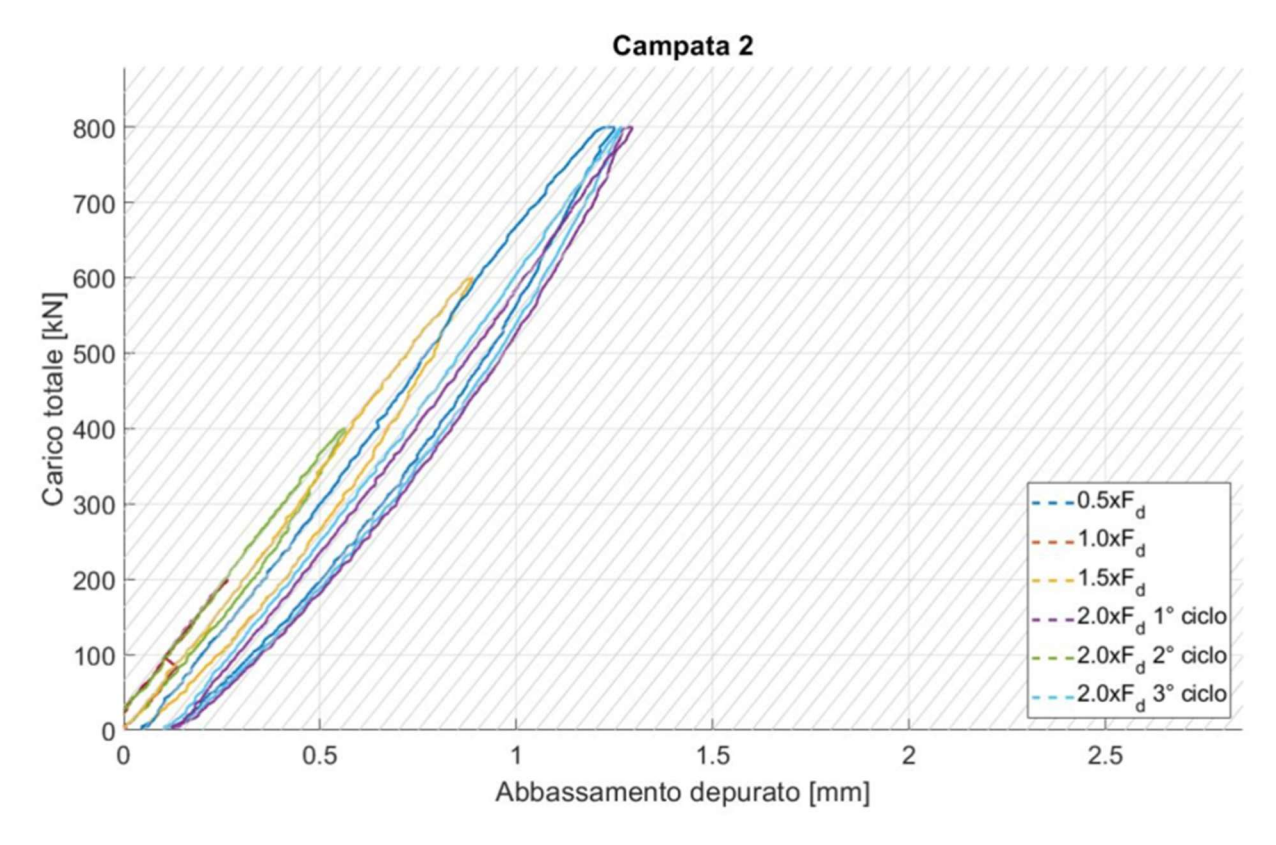


Figure 23: Force-displacement curve of span 2

It was observed that the maximum deflection of span 1 is approximately twice the magnitude of the deflection of span 2 (approximately 2.5mm compared to 1.3mm). For span 1, during the cycle corresponding to 1.5F, the accumulated and dissipated energy was significantly greater than in previous cycles, indicating that the elastic limit had been exceeded.

The following graphs present the deformations in the longitudinal and transverse directions along the central lines of loading. Settlements are observed at the supports adjacent to the loading points, while lifting occurs at the opposite support (Figure 24). In both directions, the expected maximum settlement is observed at the loading points.

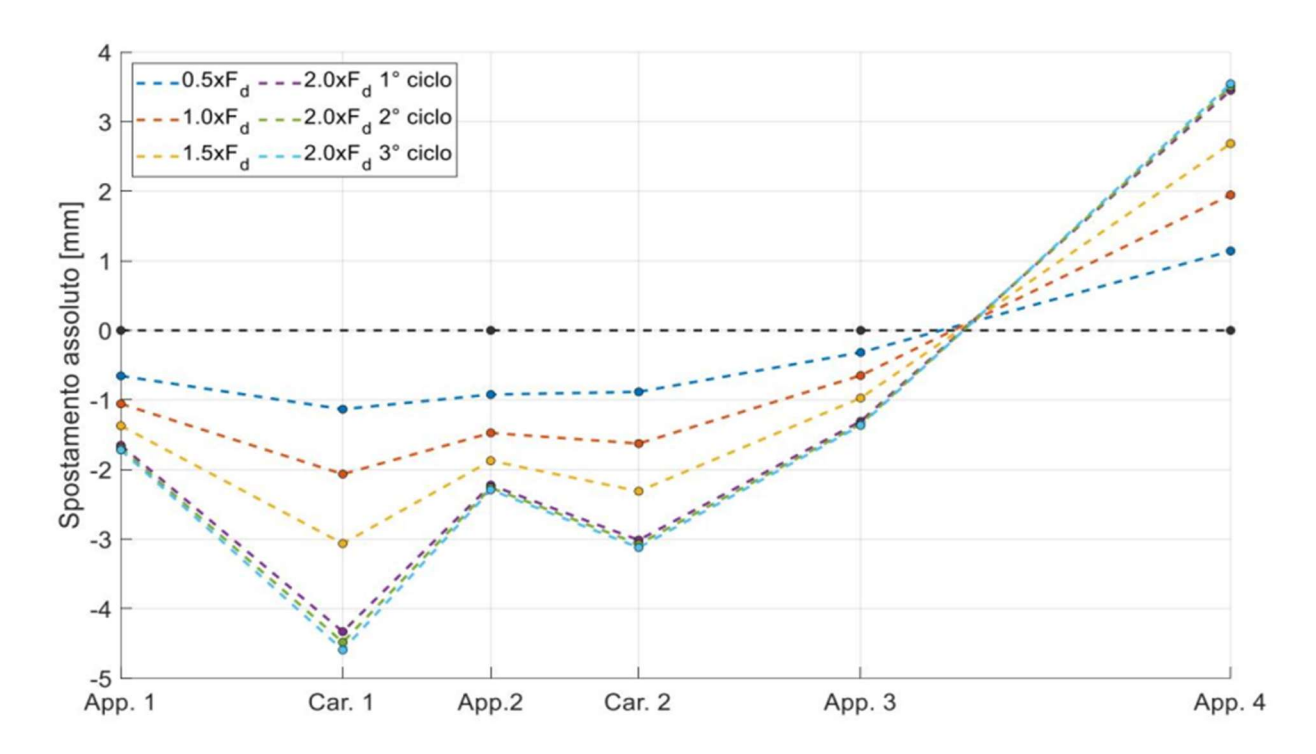


Figure 24: Deformations in the transverse direction

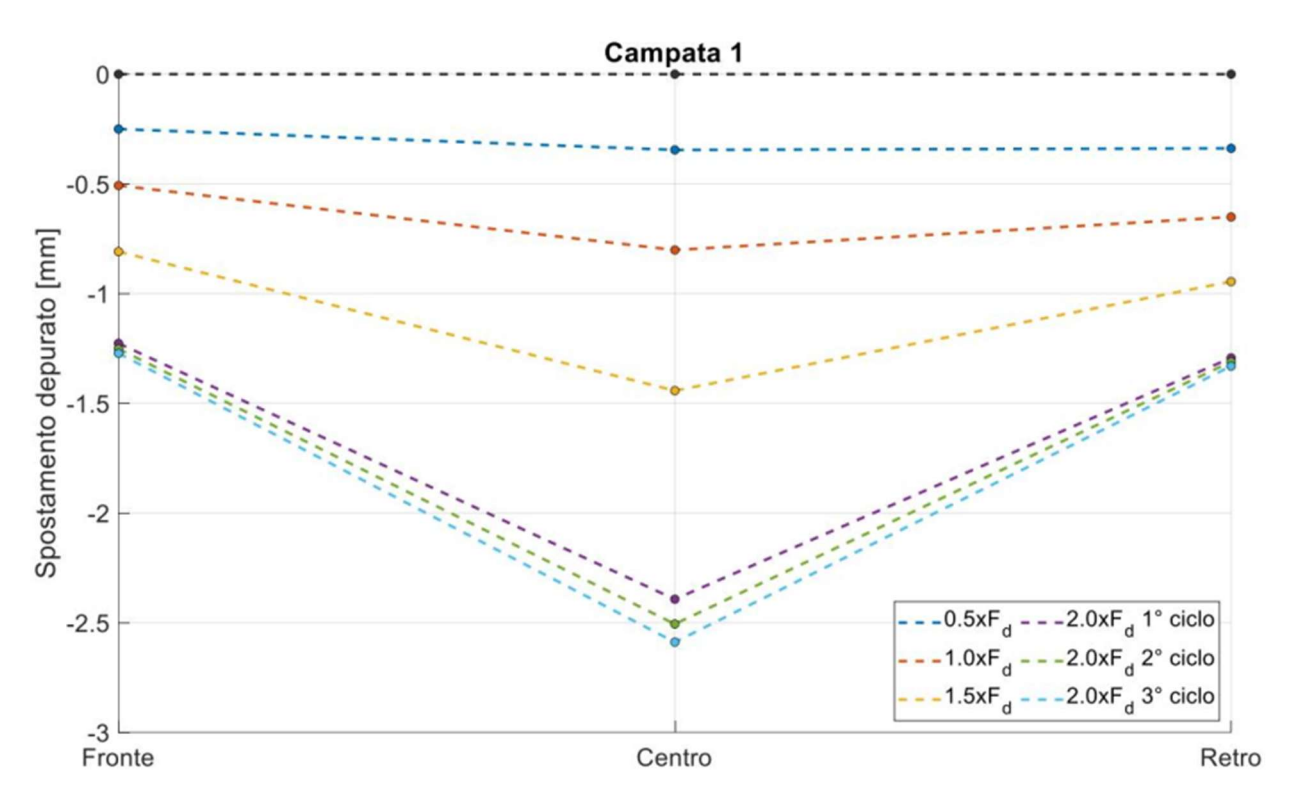


Figure 25: Deformations in the longitudinal direction of span 1

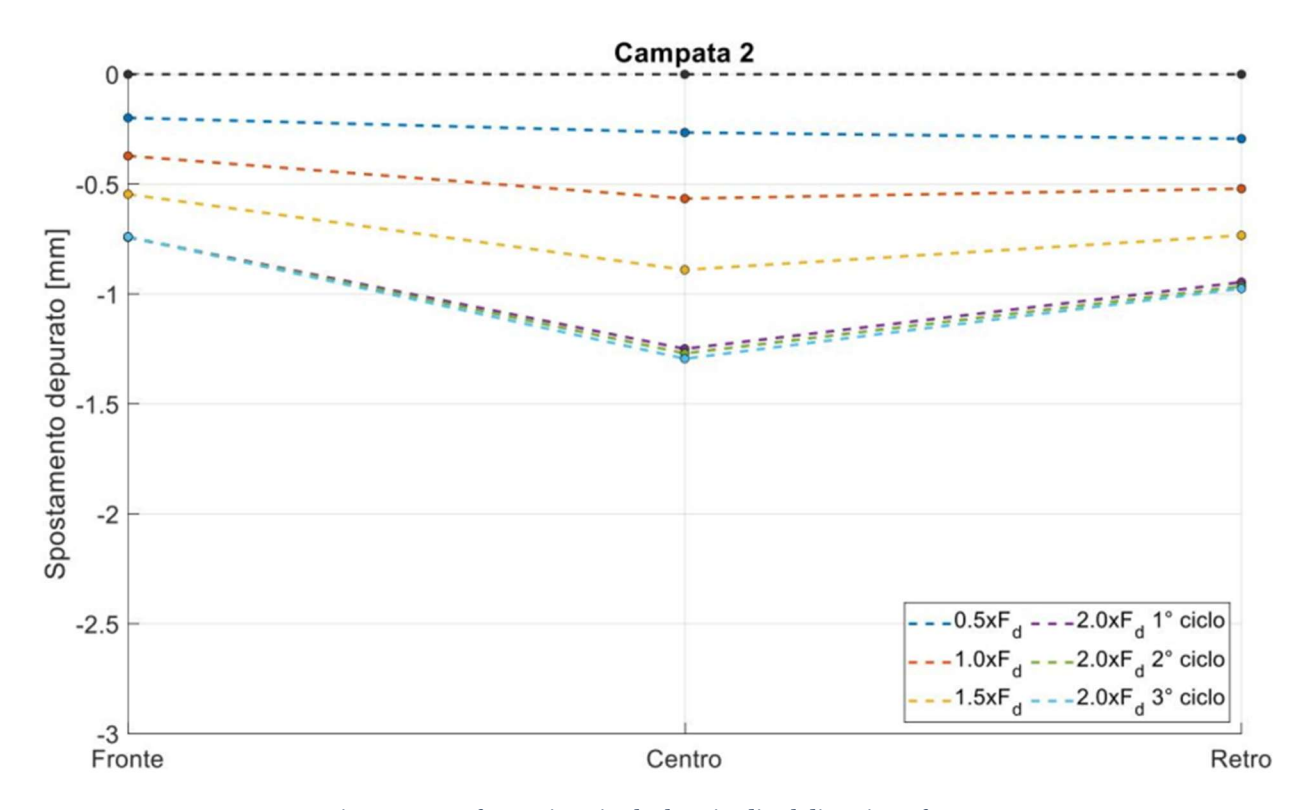


Figure 26: Deformations in the longitudinal direction of span 2

3.1.5.2. Sample 2

During visual inspections saline efflorescences was observed, likely caused by the humid environment. It presents a potential risk for corrosion of reinforcement. On the intrados of sample, the damage due to small demolitions is observed, probably carried out to inspect the corrosion of reinforcement.





Figure 27: Left: View of span 3. Right: Construction joint between span 2 and 3





Figure 28: Left: Small demolition in span 3. Right: View of not loaded span 1





Figure 29: Left: Construction joint between span 2 and span 1. Right: Efflorescence in span 1





Figure 30:Left: Small demolitions near loading point of span 2. Right: Crack pattern at span 3

Static scheme 2 was performed on sample 2 with both span 2 and span 3 subjected to loading. The results are presented in the following graphs.

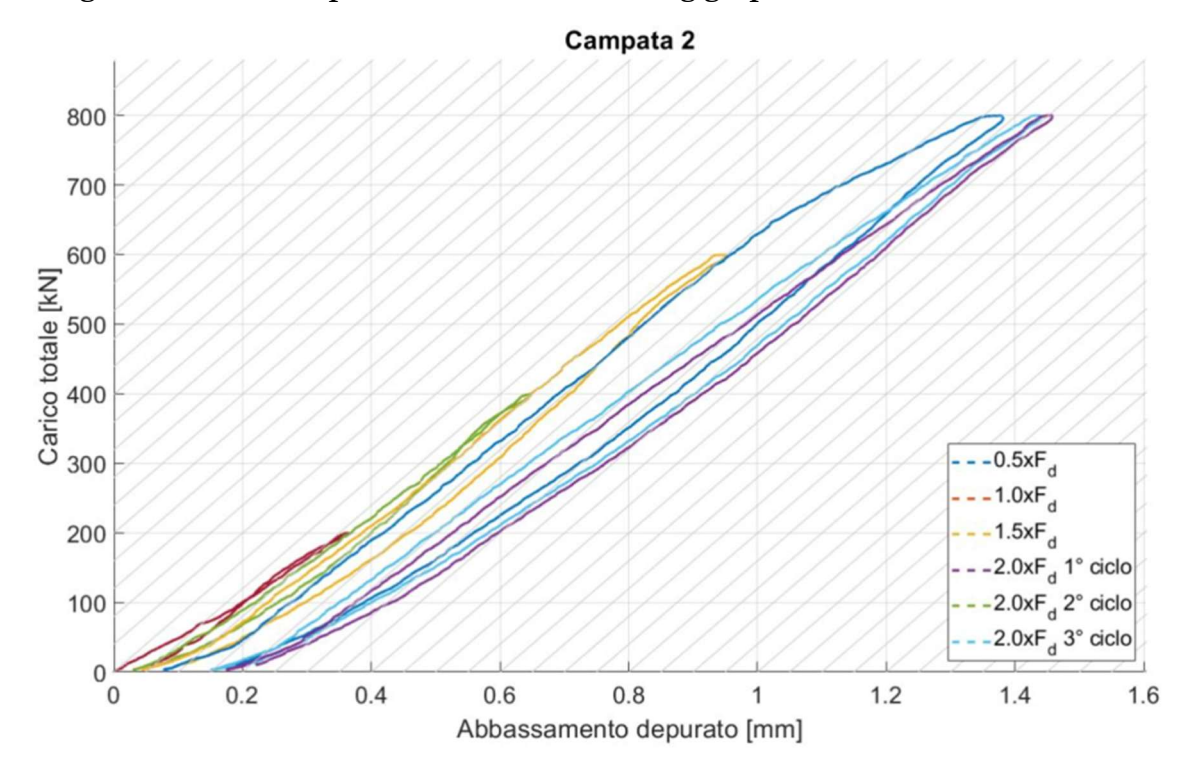


Figure 31: Force-displacement curve of span 2

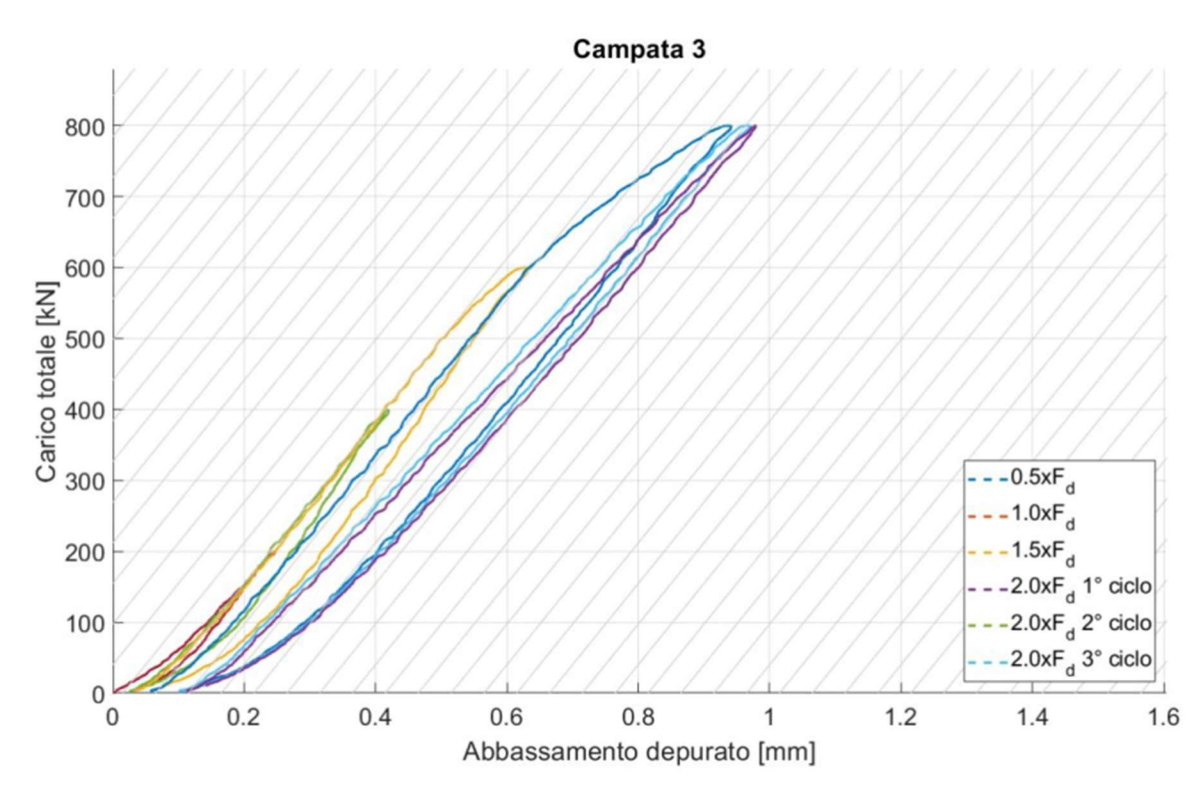


Figure 32: Force-displacement curve of span 3

A change in slope is observed in span 2 at a load of about 450 kN and in span 3 at 550 kN. In Sample 2, lateral span shows higher stiffness compared to central span.

The following graphs present the deformations in the longitudinal and transverse directions along the central lines of loading.

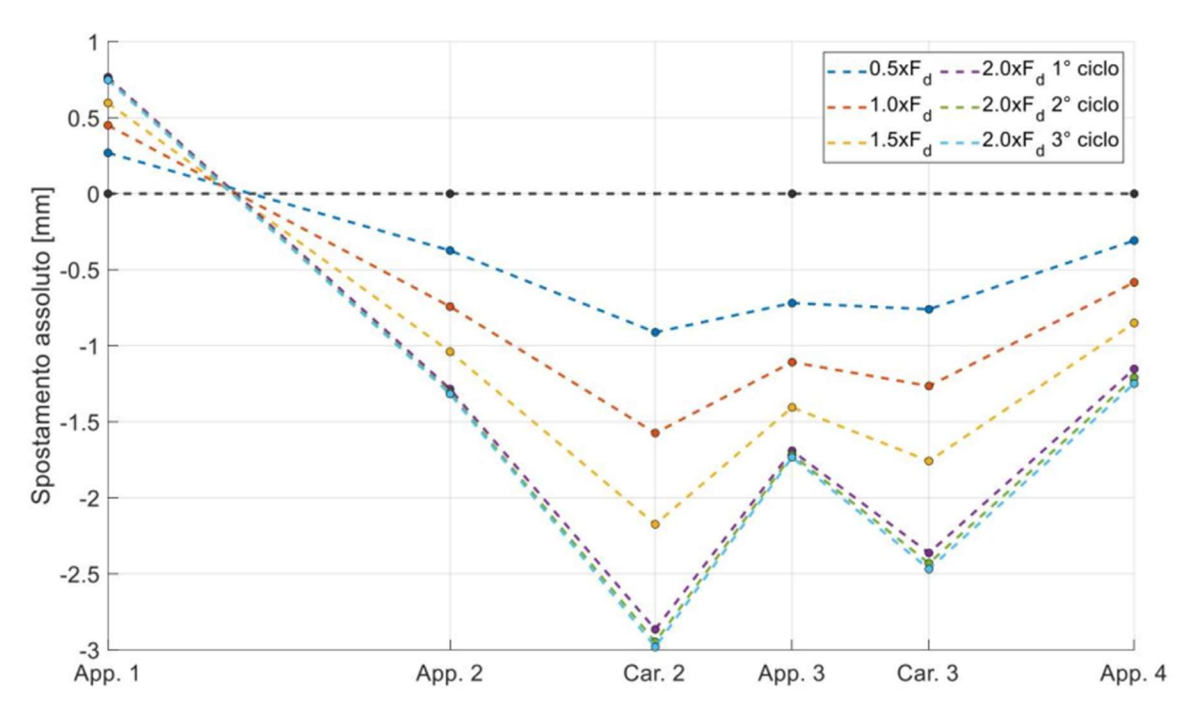


Figure 33: Deformations in the transverse direction

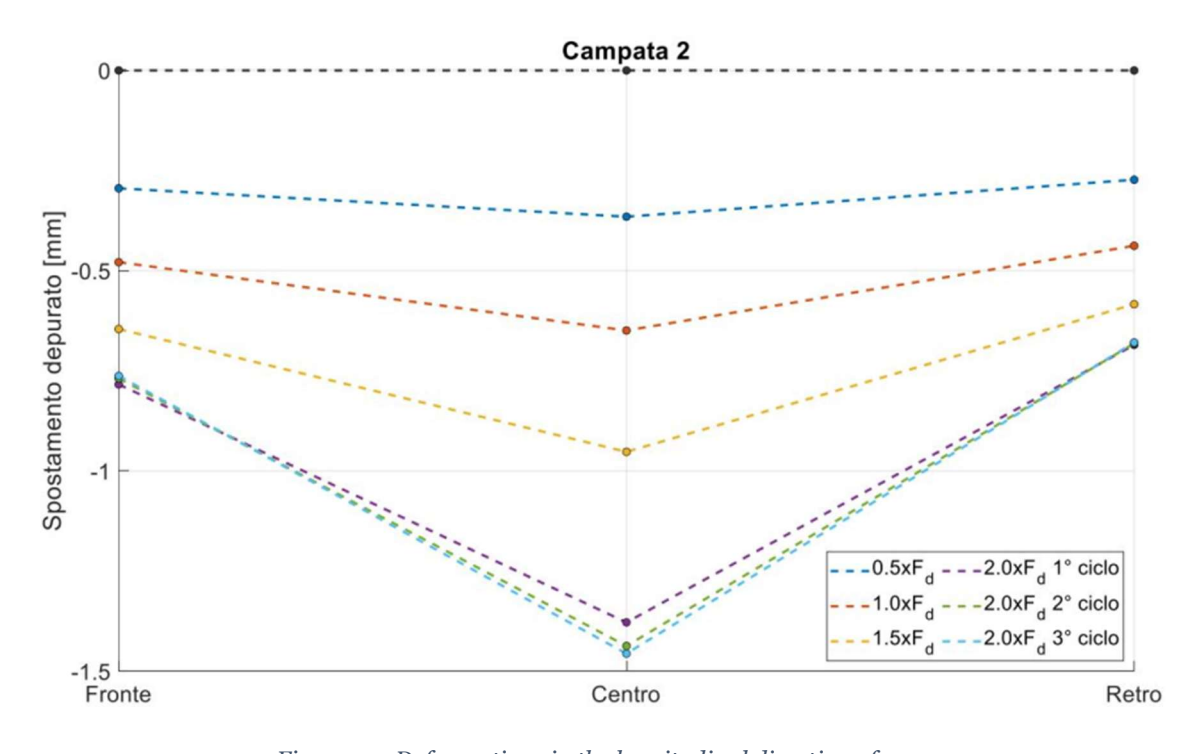


Figure 34: Deformations in the longitudinal direction of span 2

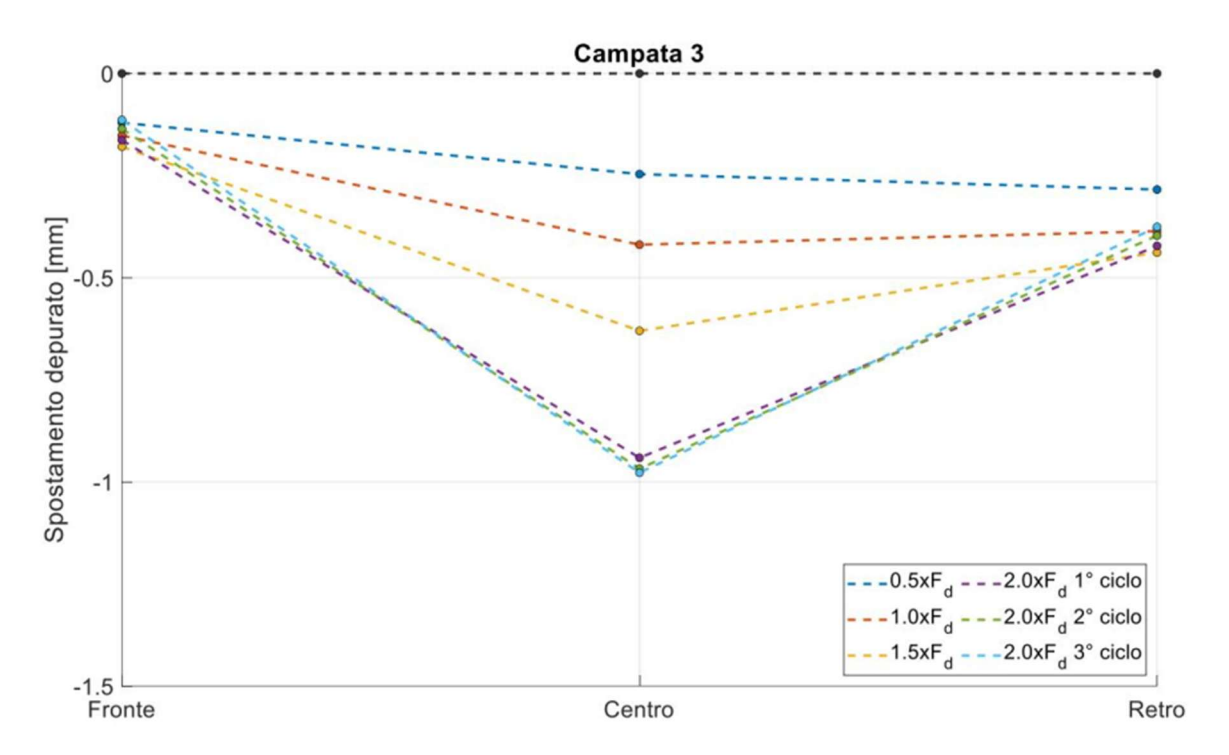


Figure 35: Deformations in the longitudinal direction of span 3

Settlements are observed at the supports adjacent to the loading points, while lifting occurs at the opposite support. In both directions, the expected maximum settlement is observed at the loading points.

3.1.5.3. Sample 3

During visual inspections saline efflorescences was observed, likely caused by the humid environment. On the intrados of sample, the damage due to small demolitions is observed, probably carried out to inspect the corrosion of reinforcement. In this case it does not affect the span under test. Span 1 has areas that show restoration with cement mortar.





Figure 36: View of span 1 and 2 respectively





Figure 37: Restoration on span 1





Figure 38: Left: Black spots on span 1. Right: Saline efflorescence on span 2

Static scheme 3 was performed on sample 3 with span 1 subjected to loading.

A decrease in stiffness is observed in loads above 75 kN, and it remains constant up to approximately 200 kN. A further change in stiffness occurs at the load of 250 kN (Figure 39).

In the transverse direction, the supports adjacent to the loaded span have settlements, while the opposite supports show uplift till 2F load. At 300 kN, the lateral support lowers (Figure 40). In both directions, the expected maximum settlement is observed at the loading points. Big differences in settlements of the front and back part indicate the rotation of the sample, likely due to the not regular support surfaces (Figure 41).

The results are presented in the following graphs.

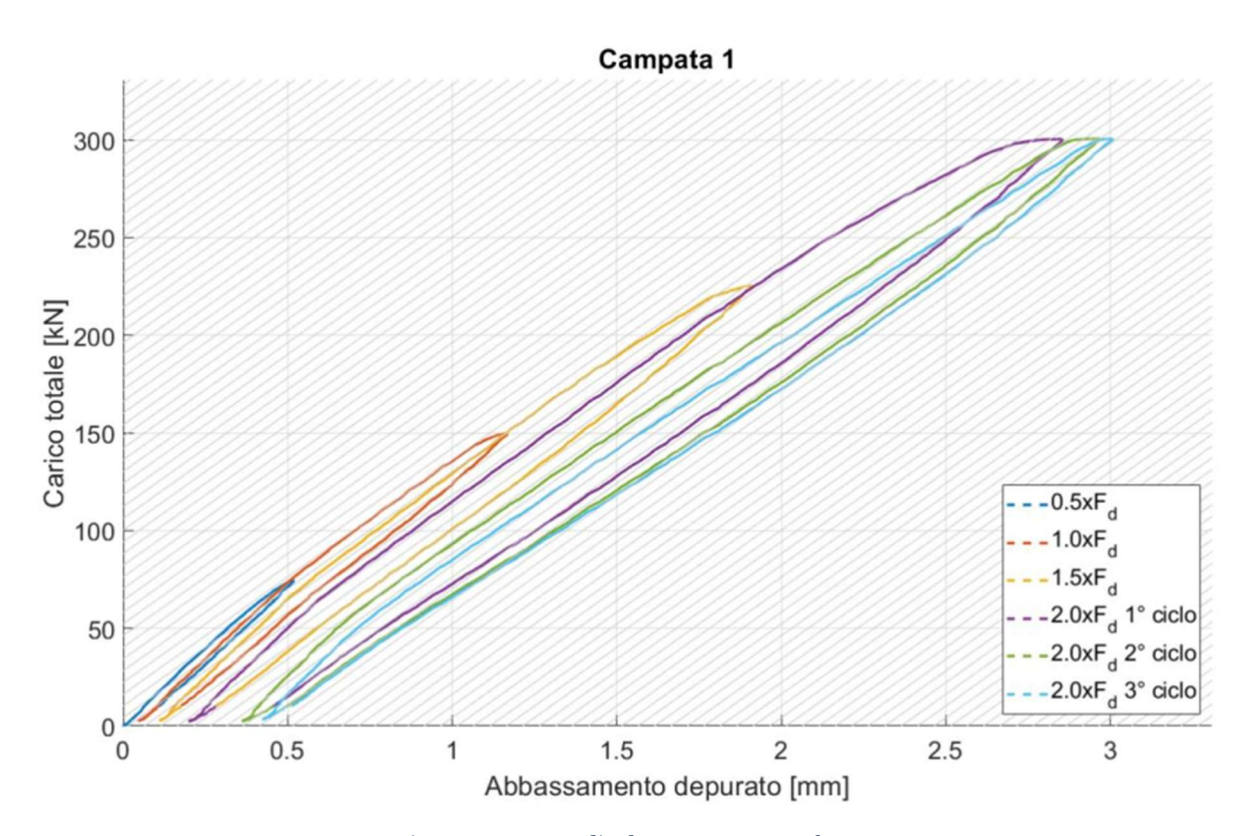


Figure 39: Force-displacement curve of span 1

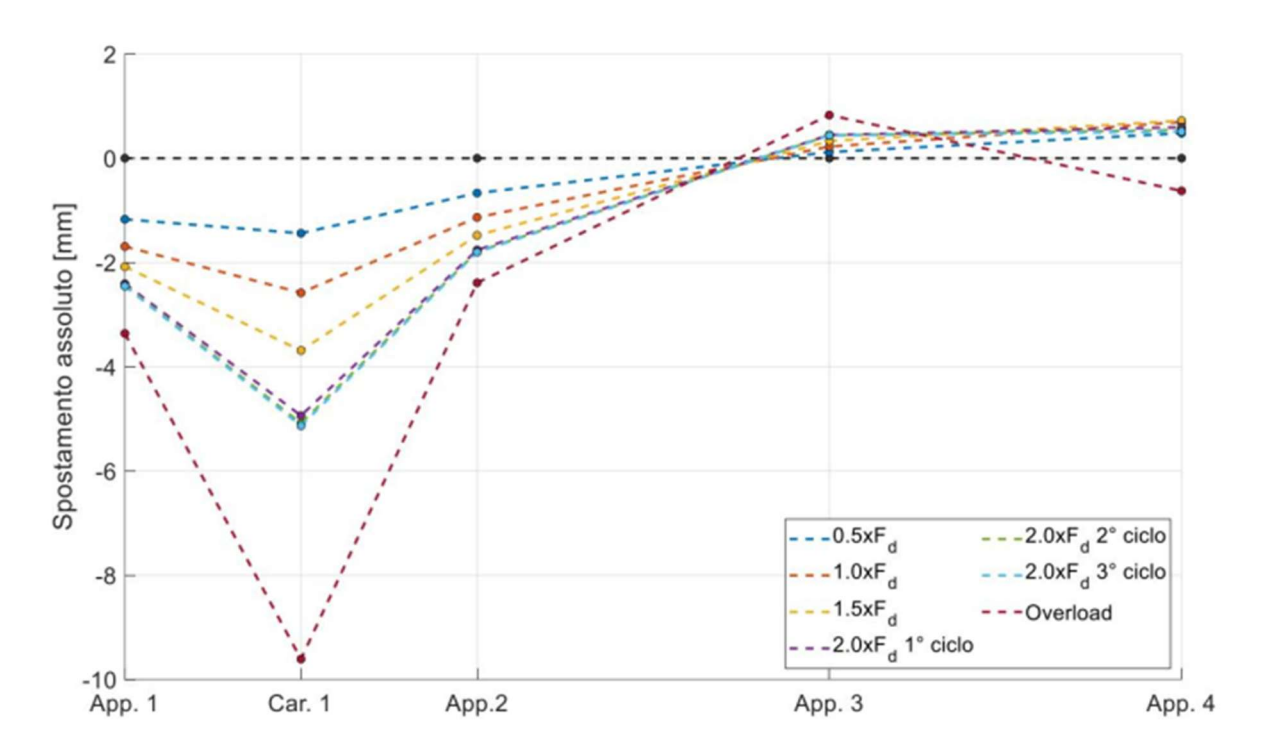


Figure 40: Deformations in the transverse direction

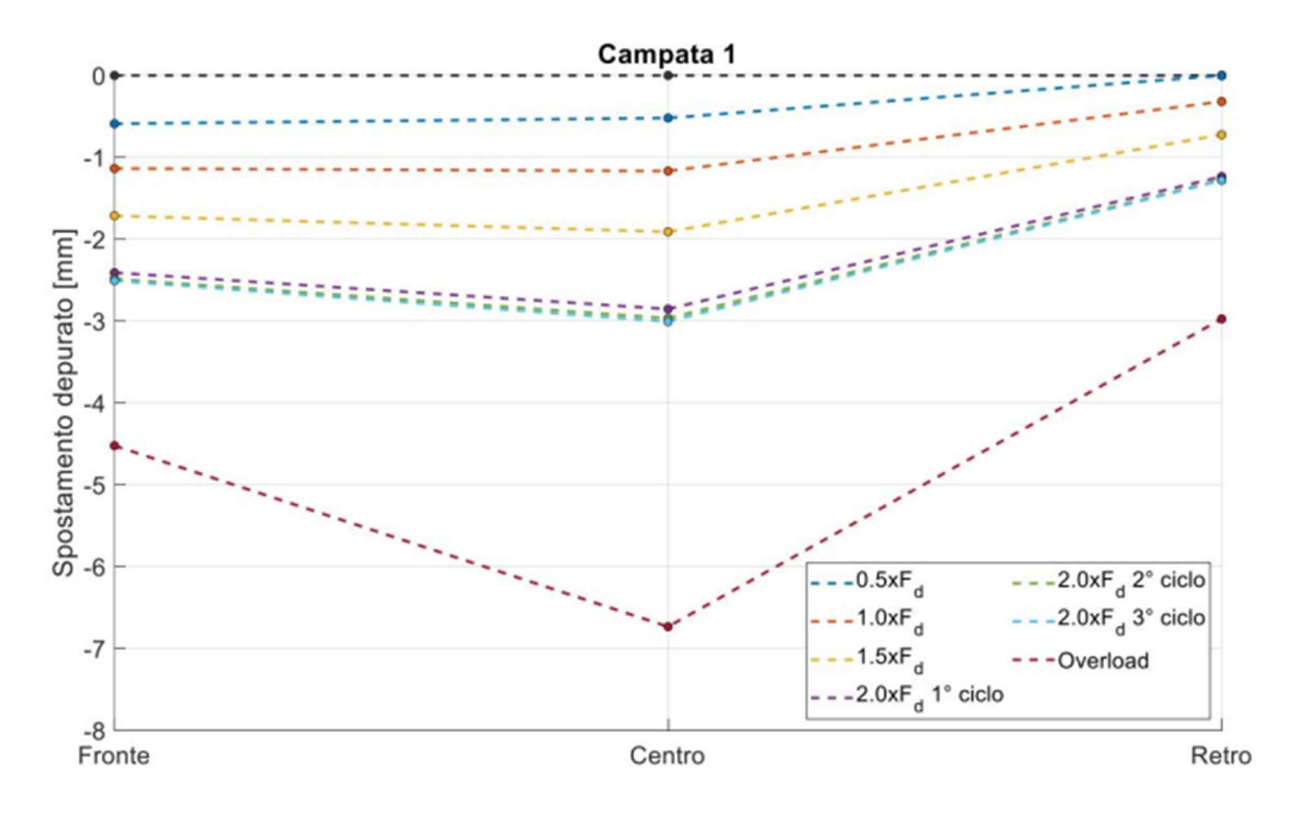


Figure 41: Deformations in the longitudinal direction of span 1

3.1.5.4. Sample 4

On the intrados of the tested span, damage due to small demolitions is observed, probably carried out to inspect the corrosion of reinforcement. A Significant crack is present on the front of the slab, corresponding to the cracking surface. The surfaces of the supports are discontinuous and inclined, especially support 3.





Figure 42: Span 3 and support detail





Figure 43: Significant crack pattern on the front of the slab





Figure 44: View of small demolition

Static scheme 3 was performed on sample 4 with span 3 subjected to loading.

Sample 4 shows elastic behaviour up to a load of 250 kN (Figure 45).

In transverse direction, the situation is like that of sample 3, where the opposite support experiences uplift (Figure 46). In both directions, the expected maximum settlement is observed at the loading points. Big differences in settlements of the front and back part indicate the rotation of the sample, likely due to the irregular support surfaces (Figure 47).

The results are presented in the following graphs.

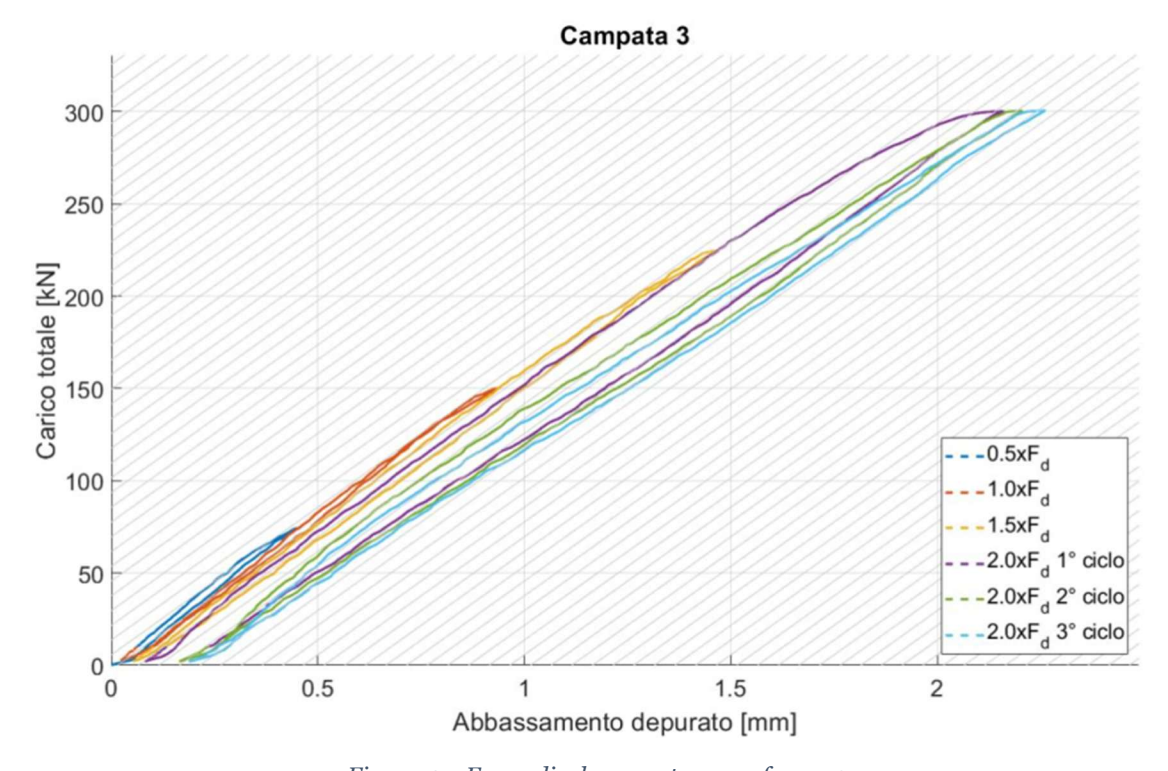


Figure 45: Force-displacement curve of span 3

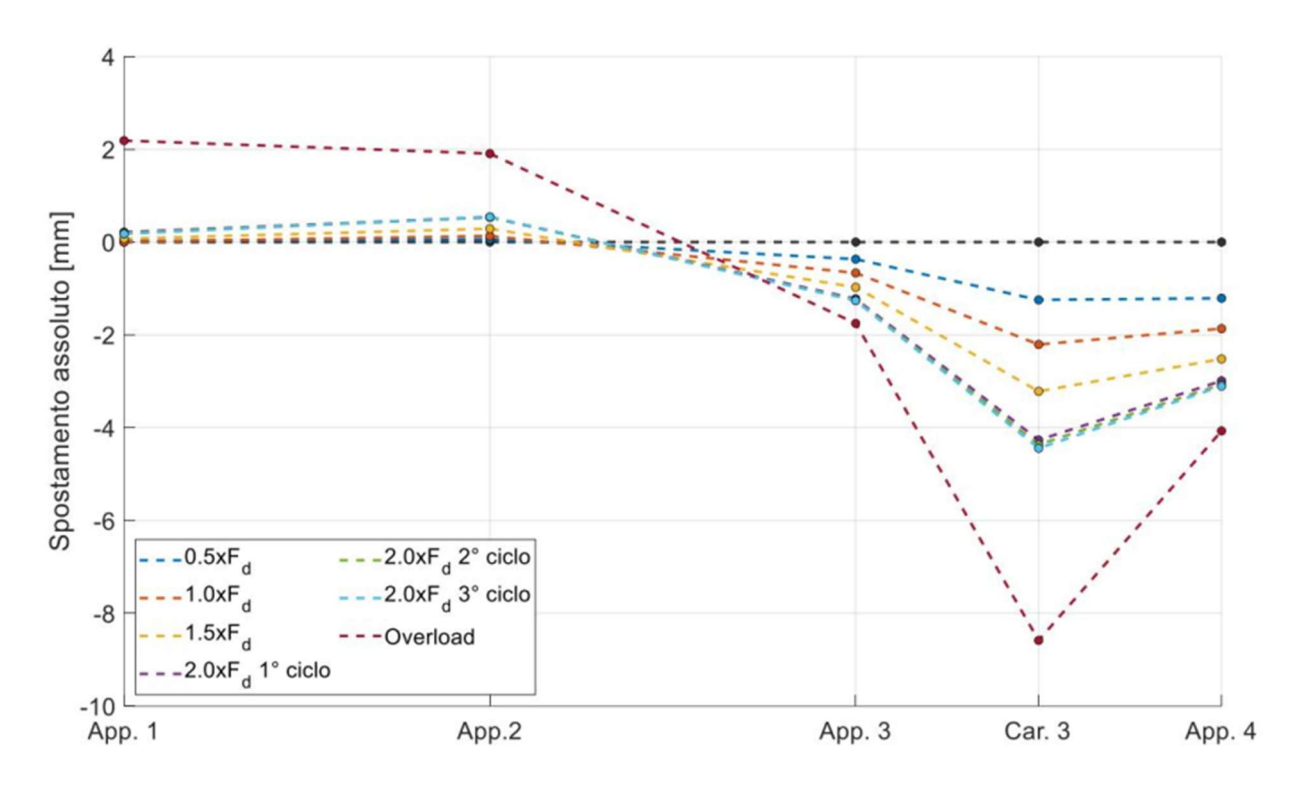


Figure 46: Deformations in the transverse direction

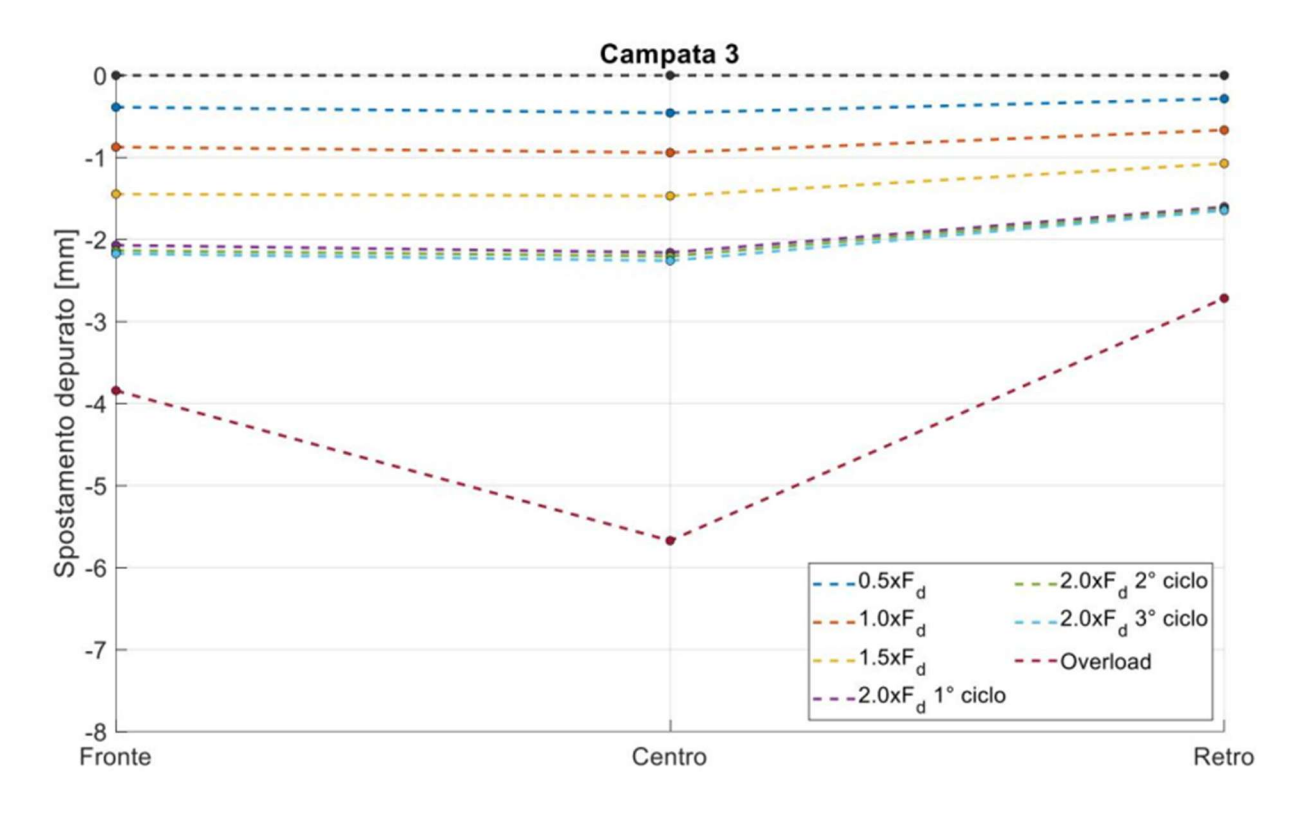


Figure 47: Deformations in the longitudinal direction of span 3

3.2. Surveys and Material tests

3.2.1. General information

Following procedures were performed on each of the samples:

- Geometrical survey of the cross section
- 6 scans with georadar (3 in the transverse direction and 3 in the longitudinal direction)
- collection of 3 concrete samples (from central precast part, lateral precast part, and cast-in-situ part)
- 6 reinforcement specimens for steel characterization

Since the specimens had already been subjected to load tests, material extractions were performed in the areas that were not subjected to loads or were affected only by minor stresses.

In the Figure 48, the approximate locations of concrete core extractions are marked.

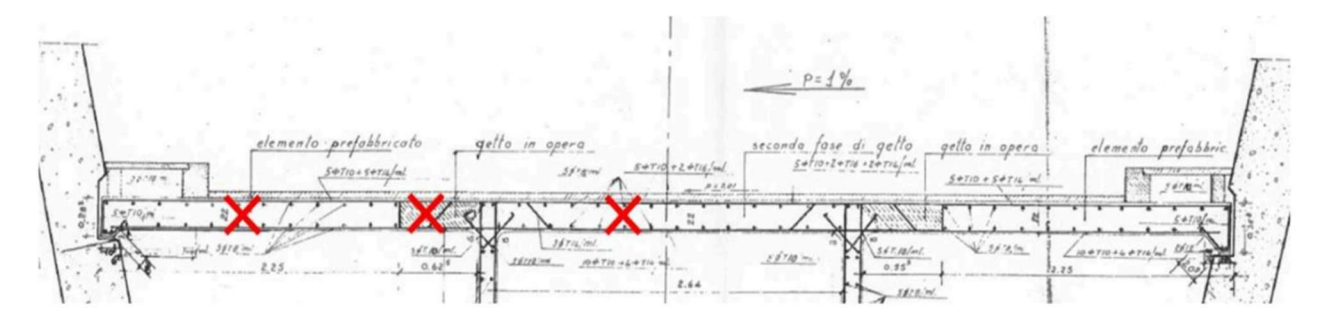


Figure 48: Approximate location of concrete core samples

To determine reinforcement layout in longitudinal direction one sample has been subjected to four cuts, 2 in cast-in-situ parts, one in prefabricated central and one in prefabricated lateral part (Figure 49).

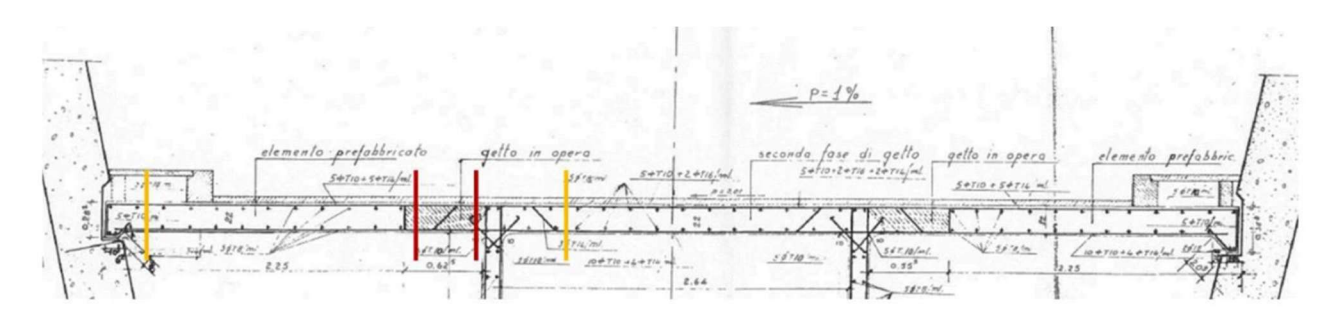


Figure 49: Location of longitudinal cuts (red in cast-in situ part, yellow- in precast parts)

3.2.2. Geometric survey

3.2.2.1. Transverse survey of the samples

The survey of all sections was carried out using digital photogrammetric techniques and the post-processing was performed with photogrammetric software, which allowed the 3D reconstruction of the object of interest.

Figures below (Figures 50, 51, 52, 53) show orthophotos of the reconstructed slabs. Each sample consists of a central prefabricated part and two lateral prefabricated parts connected to the central part by cast-in-situ joints.



Figure 53: Orthophoto of slab C4

The geometric dimensions of the slab are shown (Figures 54, 55, 56, 57), with a subdivision into precast and cast-in-situ areas. Casting joints have an almost vertical surface at the connection with central parts, while near the lateral parts, a v- shaped detail is present.

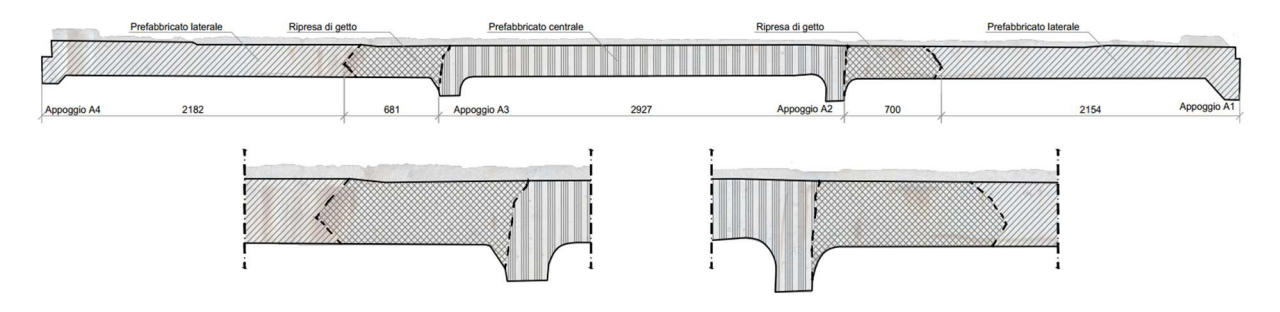
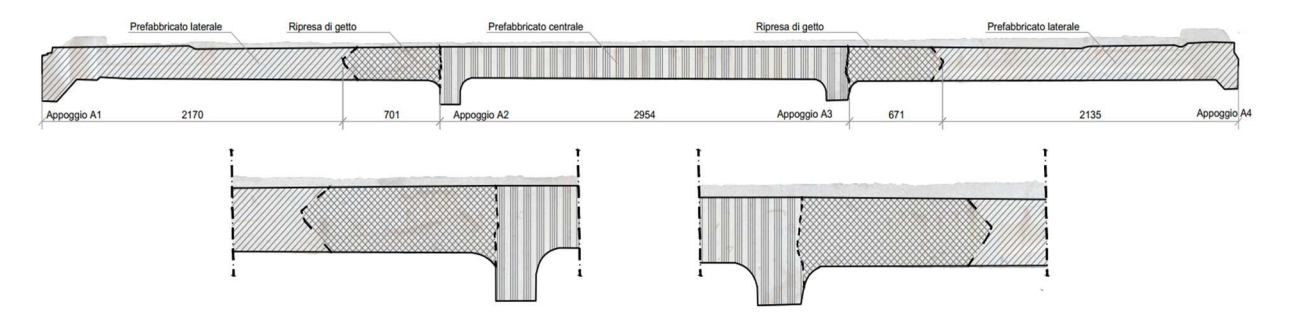


Figure 54: Sample C1 (lateral precast parts-oblique lines, central precast part-vertical lines, casting joint-rhombus)



Figure~55: Sample~C2~(lateral~precast~parts-oblique~lines,~central~precast~part-vertical~lines,~casting~joint-rhombus)

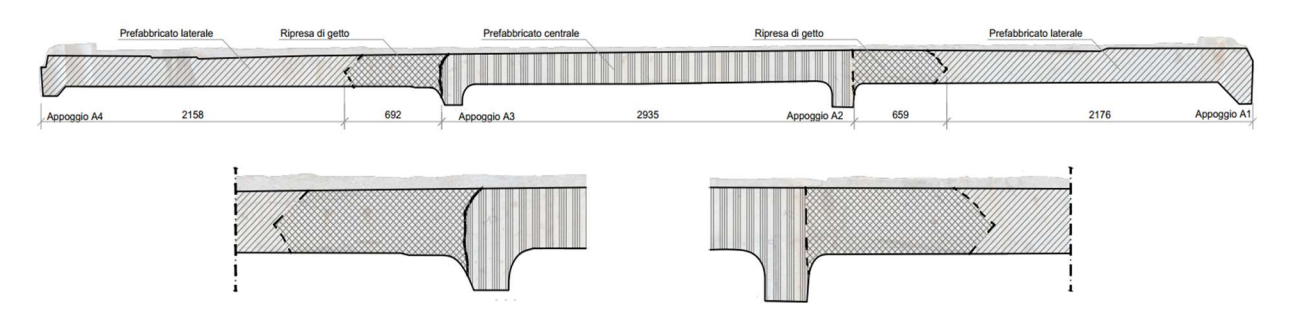


Figure 56: Sample C3 (lateral precast parts-oblique lines, central precast part-vertical lines, casting joint-rhombus)

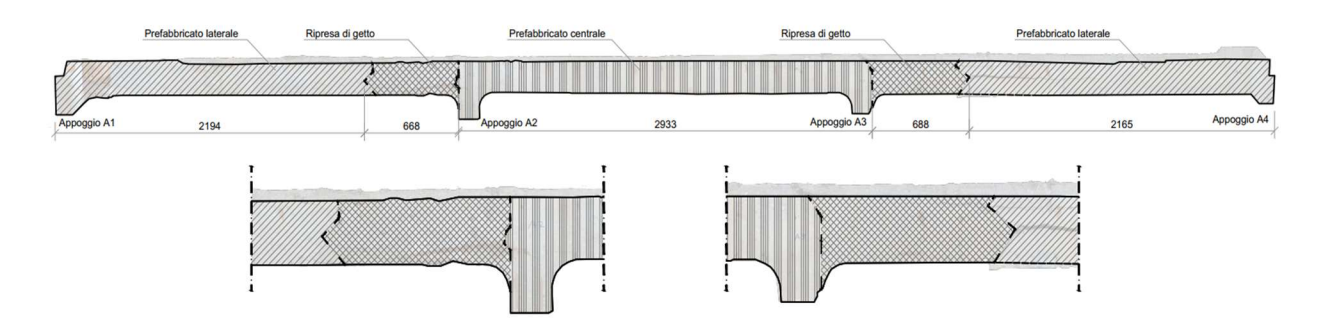


Figure 57: Sample C4 (lateral precast parts-oblique lines, central precast part-vertical lines, casting joint-rhombus)

In the figures below (Figures 58, 59, 60, 61) geometrical dimensions of concrete, patterns of reinforcement in longitudinal direction and covers of the lateral prefabricated elements are present.

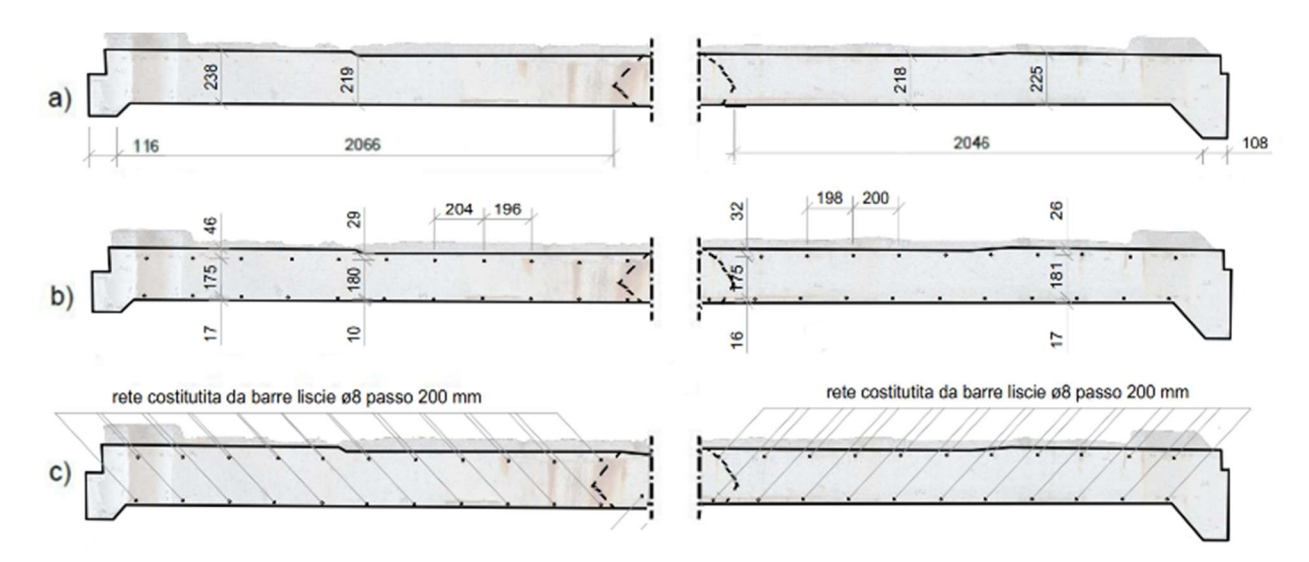


Figure 58: Details of lateral prefabricated segments in sample C1

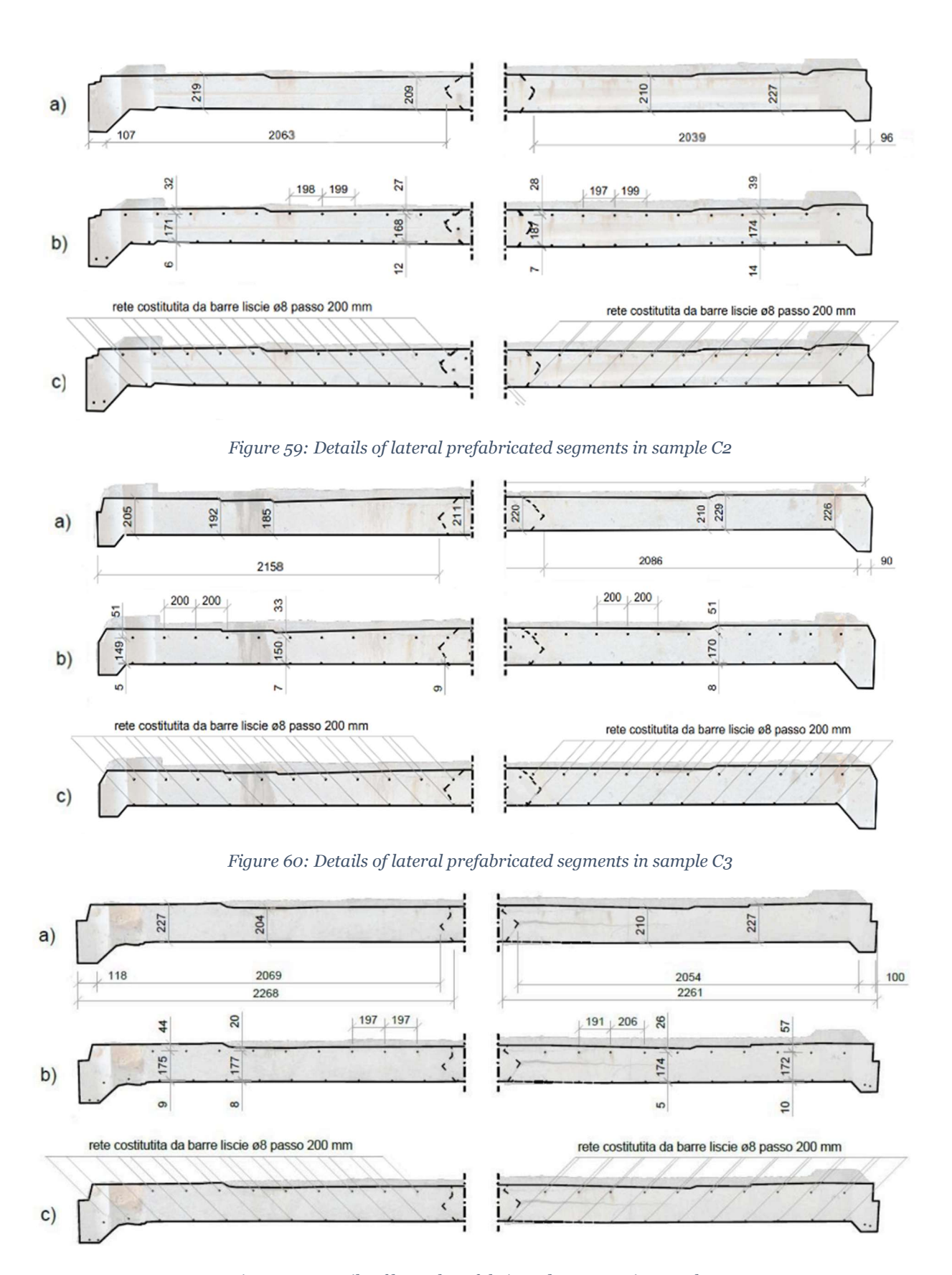


Figure 61: Details of lateral prefabricated segments in sample C4

The top surface of the concrete slab is irregular, with a stepped trend. This is perhaps due to the milling operation on asphalt layers, which sometimes affect the concrete layer. The concrete cover at the bottom is very small, possibly because the reinforcement has been placed directly on the formwork during fabrication. The constant spacing of 200 mm suggests that reinforcement mesh was used, which was confirmed during demolition.

Cast-in-situ joints were analyzed in a similar way. Figures 62, 63, 64, 65 show the details of the joints, their geometrical dimensions, and reinforcement patterns. As mentioned above, the interface with the precast parts differs. In the central part it is almost vertical, while near the lateral part a V-shaped detail is present. It should be noted that clear separation line between the prefabricated segments and the cast-in-situ joints is visible. The smaller aggregates in the joint parts indicate a different class of concrete compared with the precast parts. The reinforcement layout in the cast-in-situ joints is completely irregular and does not follow any pattern. For most reinforcement bars concrete covers are large. The reinforcement bars are not perfectly circular in shape, but they can be approximated as circular bars with a diameter of 8 mm.

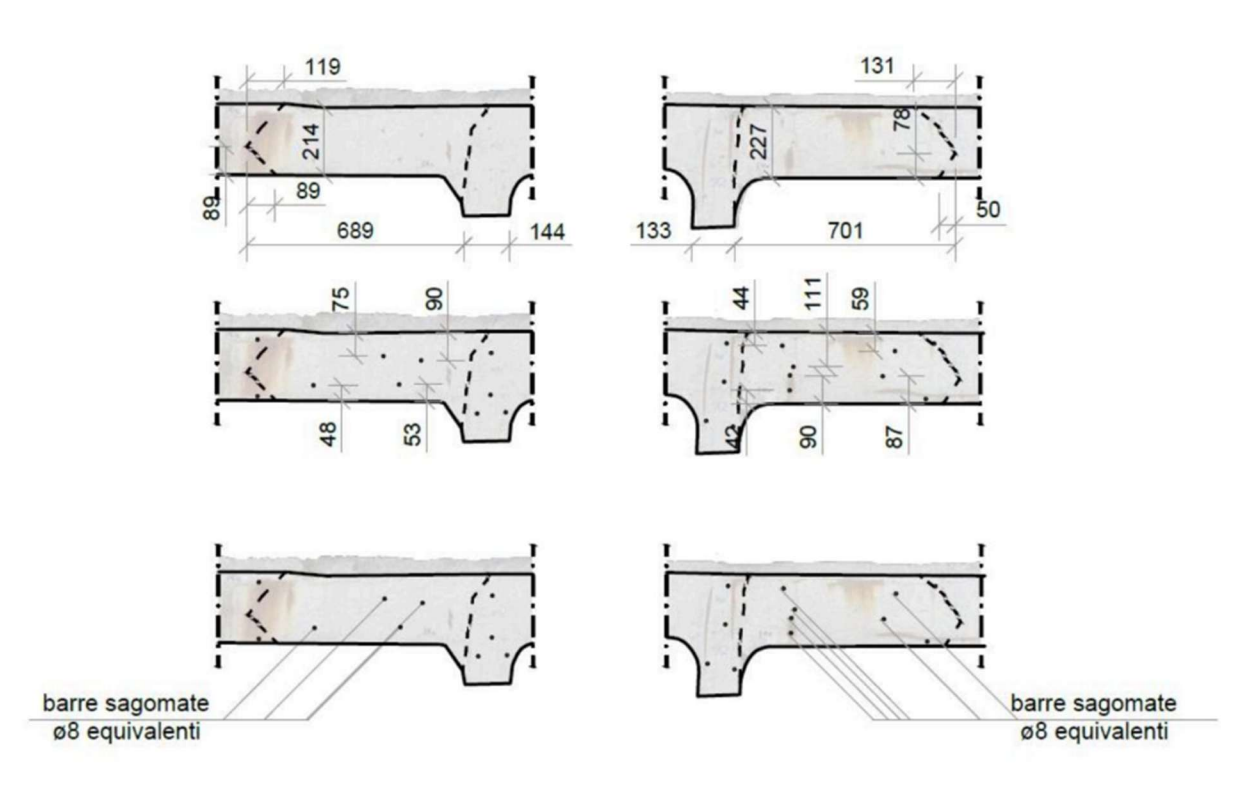


Figure 62: Details of cast-in-situ joints in sample C1

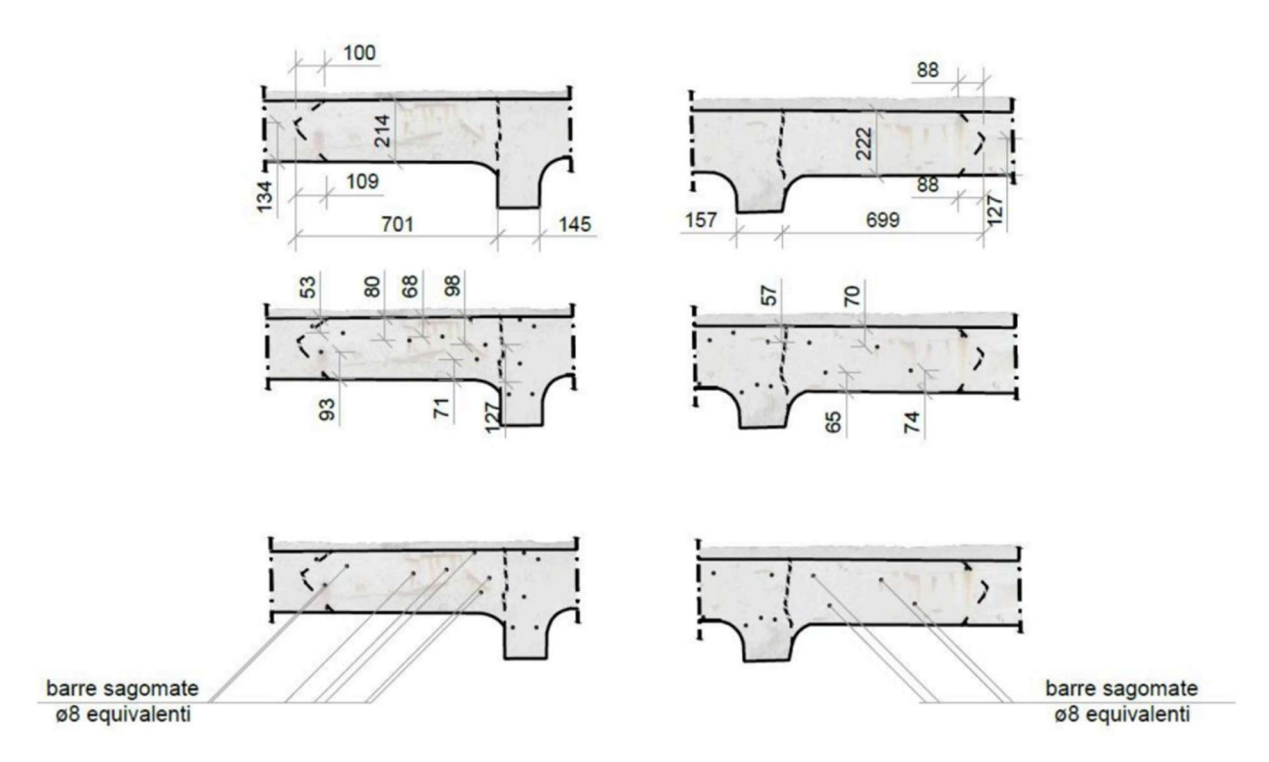


Figure 63: Details of cast-in-situ joints in sample C2

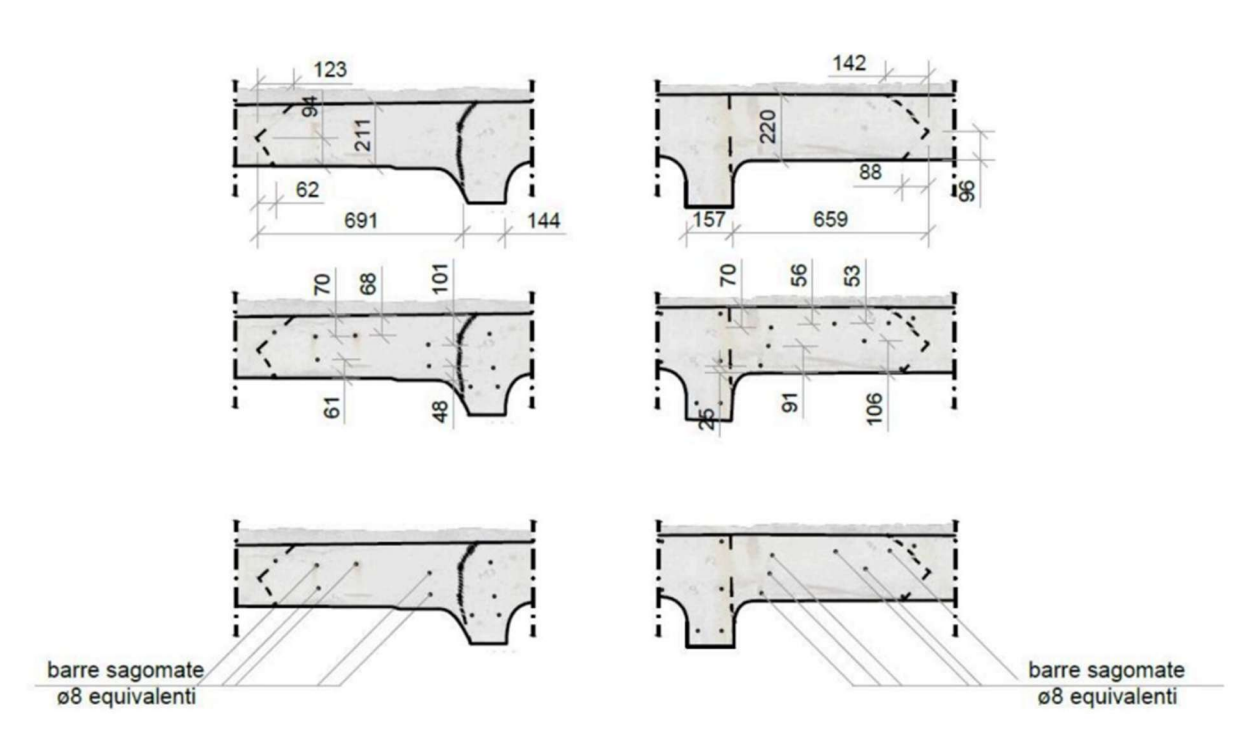


Figure 64: Details of cast-in-situ joints in sample C3

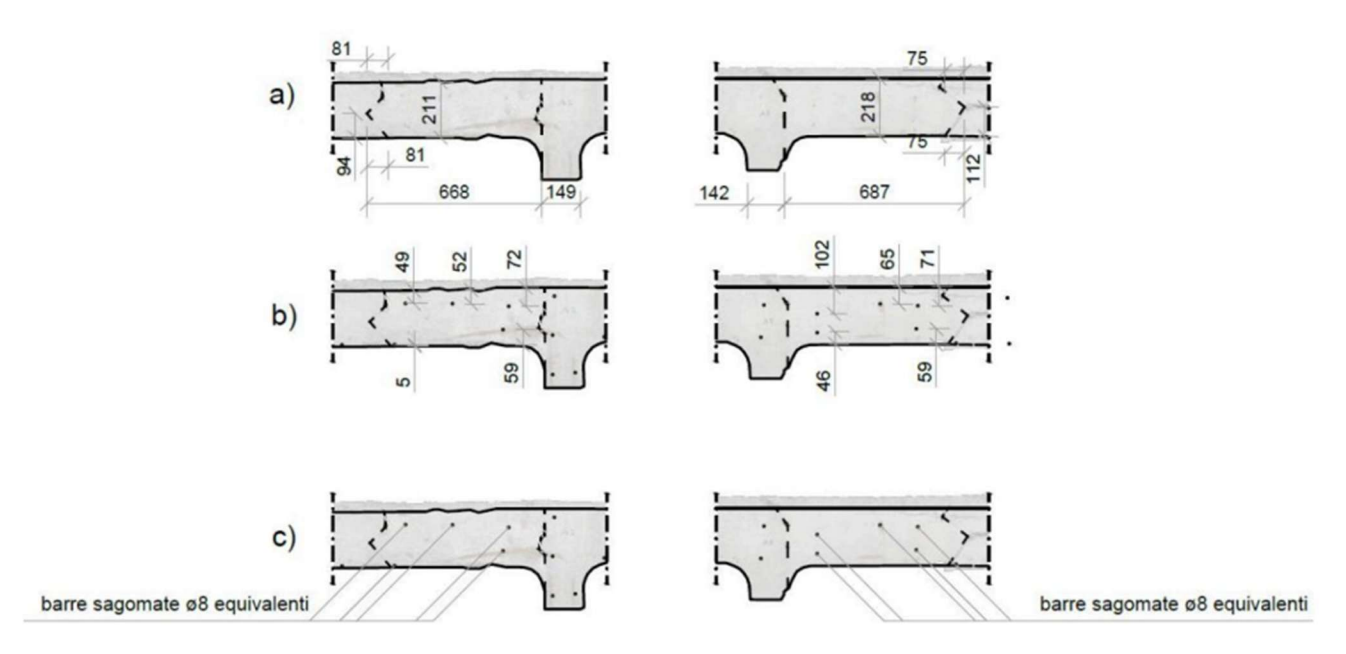


Figure 65: Details of cast-in-situ joints in sample C4

Figures 66, 67, 68, 69 present details of central prefabricated parts.

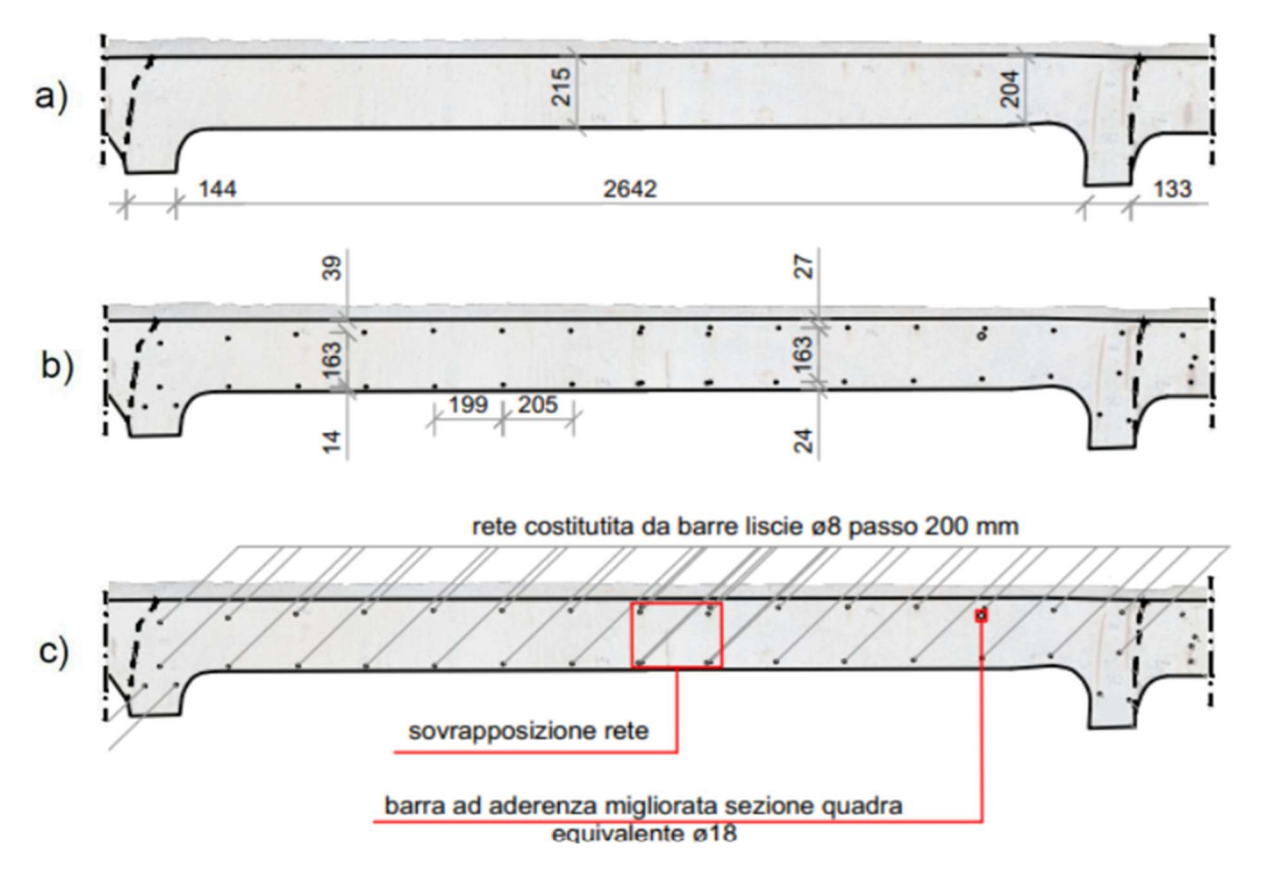


Figure 66: Details of the central prefabricated segment in sample C1

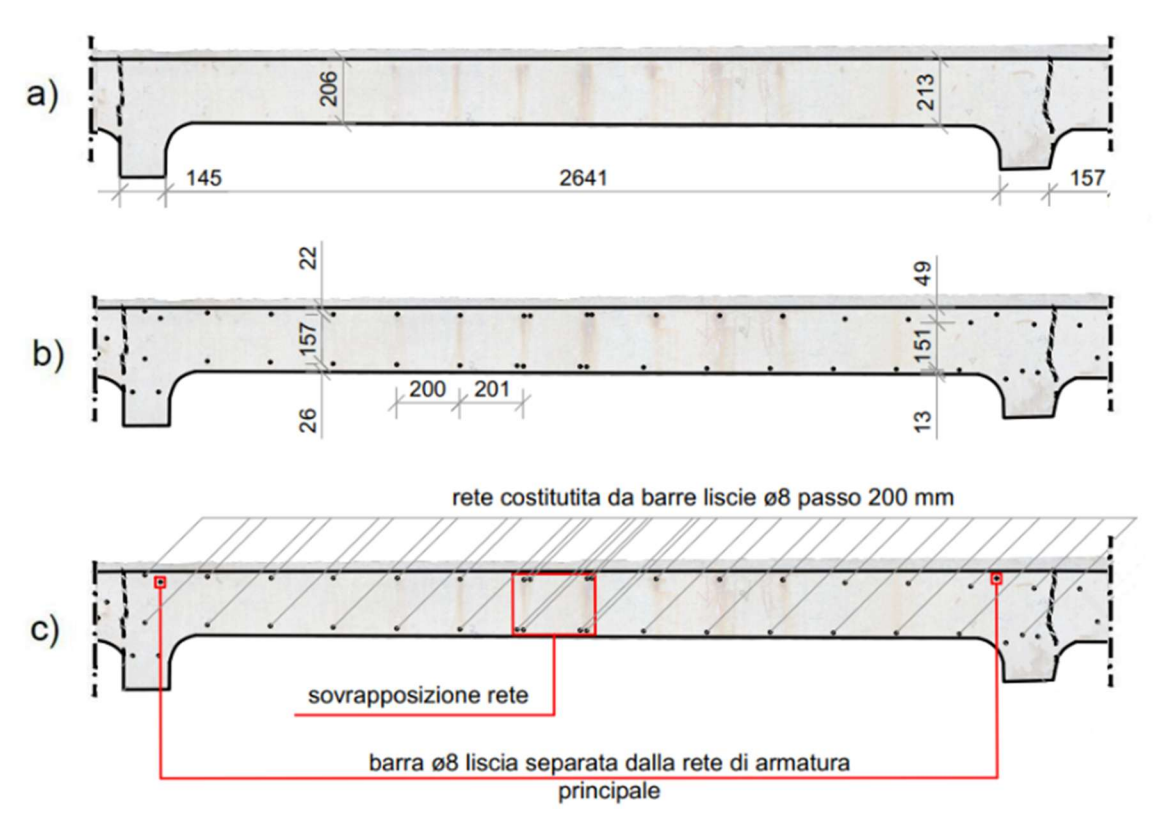


Figure 67: Details of the central prefabricated segment in sample C2

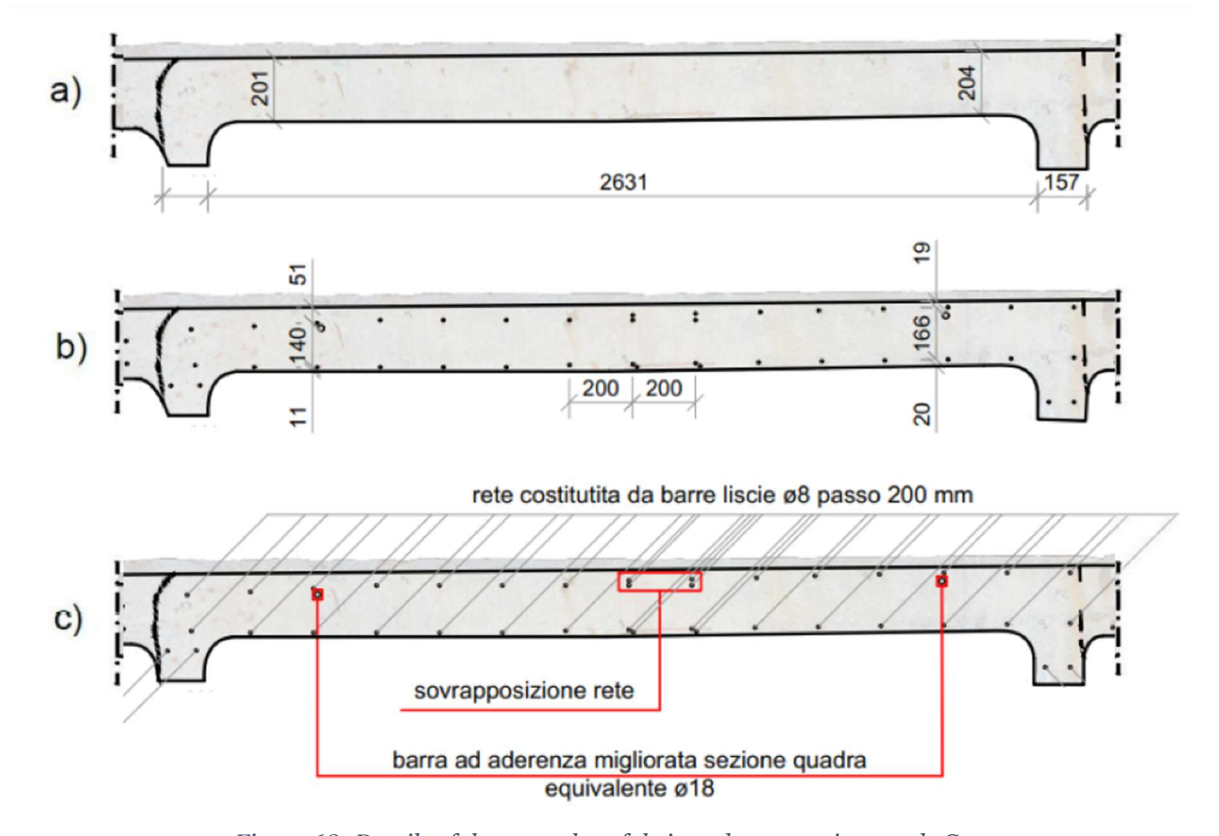


Figure 68: Details of the central prefabricated segment in sample C_3

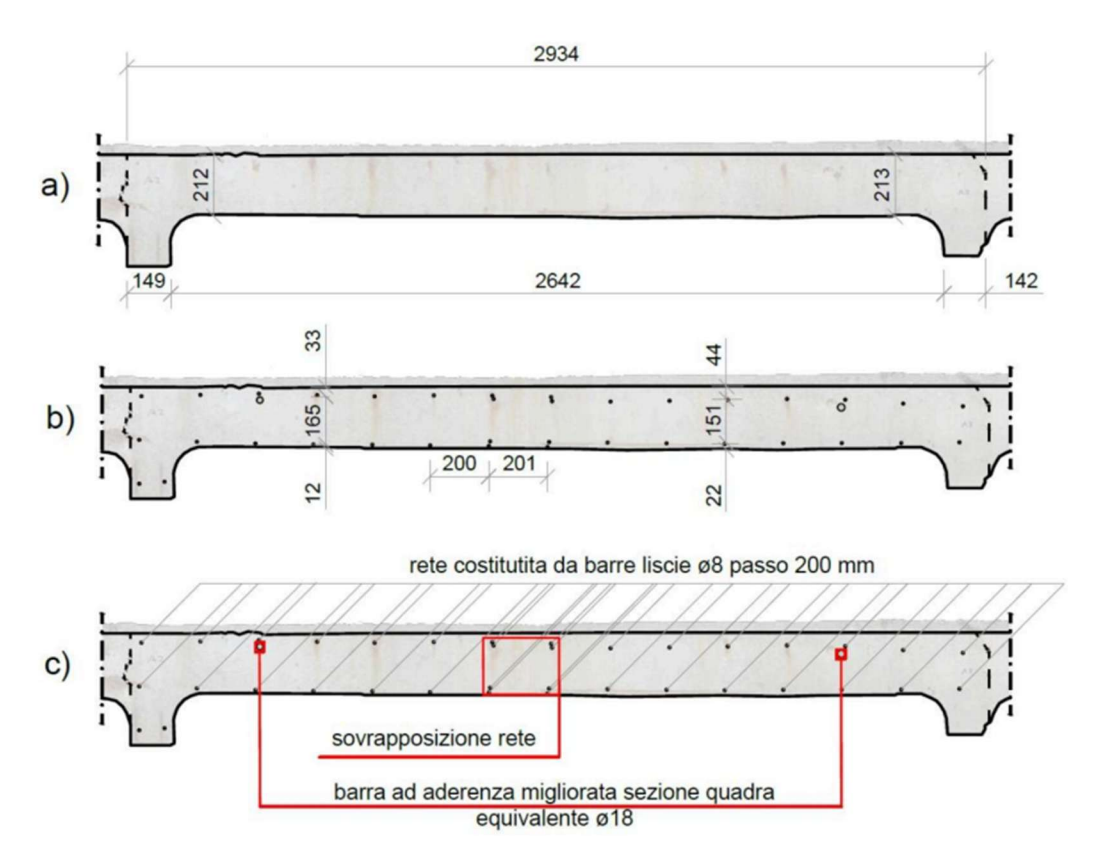


Figure 69: Details of the central prefabricated segment in sample C4

The top surface of the central prefabricated segment is relatively smooth, with only minor irregularities. The reinforcement bars are arranged in an orderly manner with an approximate spacing of 200 mm. Demolition confirmed the presence of top and bottom reinforcement meshes. Additional reinforcement was placed in the upper half of the segment. In sample C1, a single bar with a diameter of 18 mm was found. In sample C2, two bars with a diameter of 8 mm were present, while in samples C3 and C4, two bars with a diameter 18 mm were observed (Figures 66c, 67c, 68c, 69c).

3.2.2.2. Longitudinal survey of the sample C4

For the longitudinal investigation, four cuts were performed on the sample C4. Locations of cuts were chosen to examine the structural continuity, the integration between prefabricated segments, and the reinforcement layout.

Figure 70 shows the location of the sections made in sample C4.

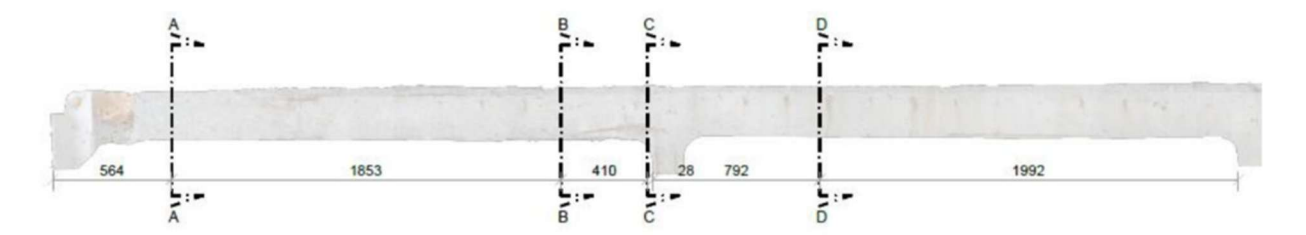


Figure 70: Location of longitudinal cuts in sample C4

Section AA – Lateral prefabricated segment:

Figure 71 shows and orthophoto of the section AA.



Figure 71: Orthophoto of section AA

The joint between consecutive lateral segments is shown in the Figure 72. The next figure presents the reinforcement layout and their spacing.

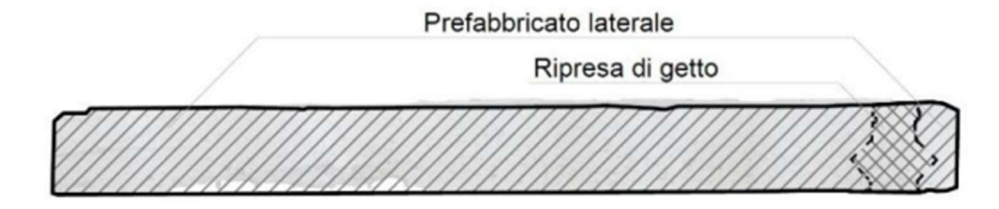


Figure 72: Detail of two consecutive lateral segments



Figure 73: Reinforcement layout in lateral prefabricated segment

A sequence of 10mm bars, spaced at 200 mm at the top of the slab and 100 mm at the bottom, forms reinforcement meshes with reinforcement found in the transverse analysis. In the joint, the reinforcement bars are irregularly arranged and disconnected from each other.

Sections BB, CC – Cast-in-situ joint:

Orthophotos of the sections (Figure 74) reveal the irregularities of the top surface. It may have been damaged by asphalt milling, as some of the bars are in direct contact with asphalt.

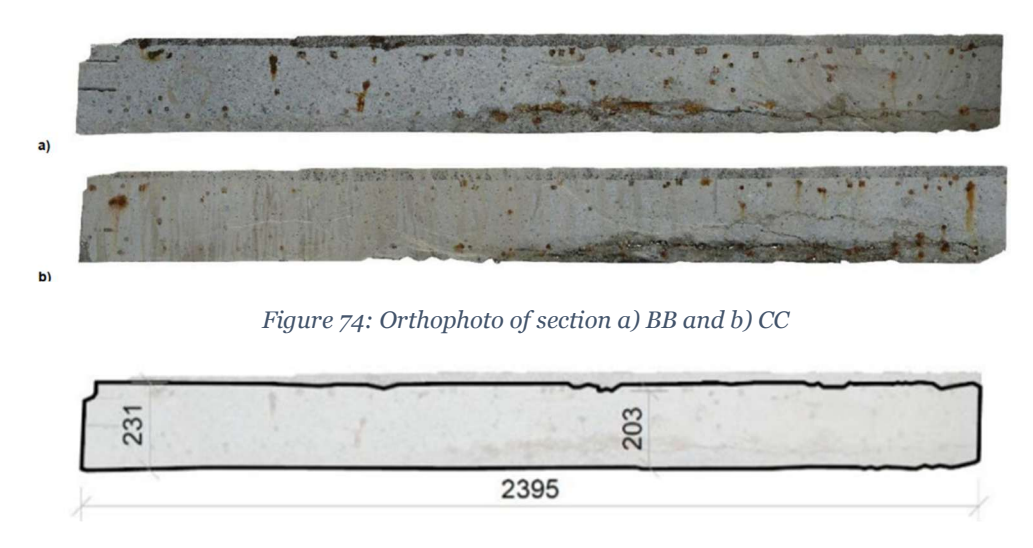
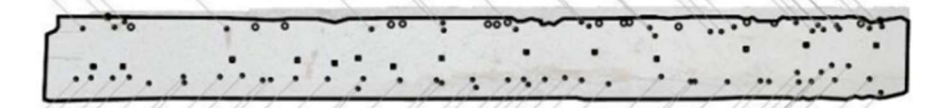


Figure 75: Geometric dimensions of section BB

During demolition, a dense presence of 10 mm diameter bars was observed. The number of bars on the intrados was greater than on the extrados. After dismantling the segment, it was noted that the reinforcement from meshes of the precast elements extended into the cast-in-situ joint and overlapped. Consequently, the number of bars should be twice that of prefabricated parts (Figure 76). Near section CC, in addition to the main mesh, a series of hooked bars (type B) with a diameter of 8mm, bent approximately 10cm into the joint, were observed (Figure 77). These hooked bars were irregular in the arrangement but were clearly visible during demolition.

continuazione della rete costruita da barre lisce ø10 passo 200 per la sovrapposizione dei prefabbricati TIP. A



continuazione della rete costruita da barre lisce ø10 passo 100 per la sovrapposizione dei prefabbricati TIP. A

a)

b)

continuazione della rete costruita da barre lisce ø10 passo 200 per la sovrapposizione dei prefabbricati TIP. A con ganci tipologia B



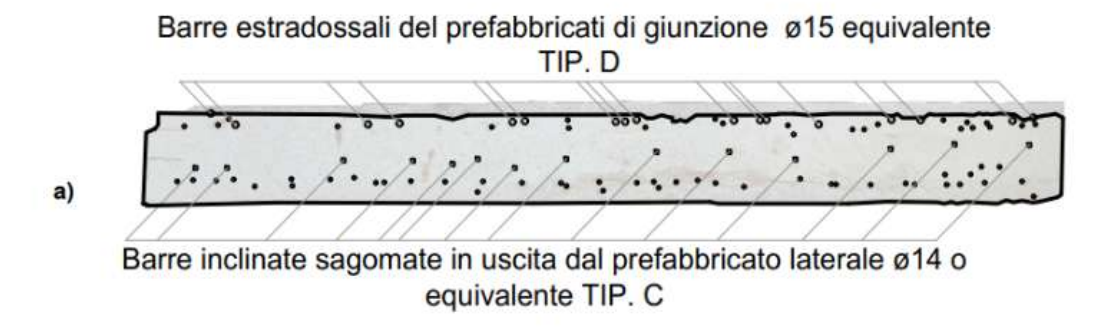
continuazione della rete costruita da barre lisce ø10 passo 100 per la sovrapposizione dei prefabbricati TIP. A

Figure 76: Principal reinforcement layout in sections a) BB and b) CC



Figure 77: Detail of the hooked bar type B

Figure 78 shows the presence of additional reinforcement not detected in section AA. Type C bars (Figure 79) extend from the lateral prefabricated parts and are bent diagonally into the cast-in-situ joint. In the upper half of the slab, a series of type D hooked bars with a non-circular shape and an approximate diameter of 15mm were observed (Figure 80). These bars are extended from lateral precast segment and bent at the opposite end of the joint.



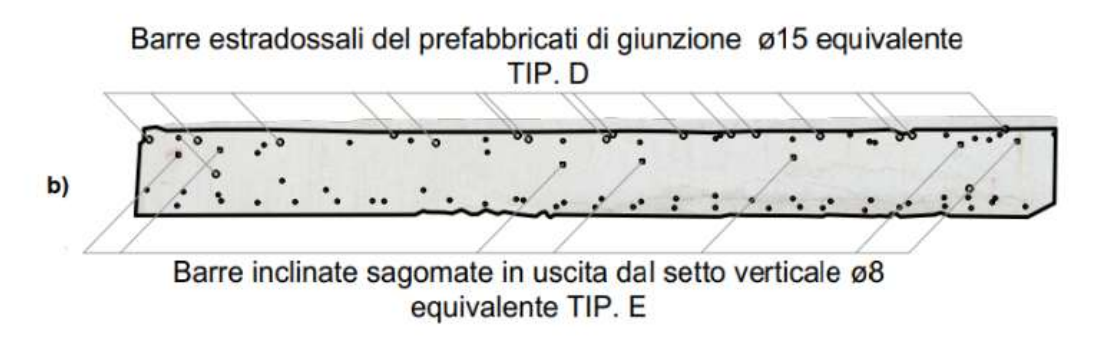


Figure 78: Additional reinforcement layout in sections a) BB and b) CC



Figure 79: Detail of inclined type C bar



Figure 80: Detail of the hooked bar type D

In section CC, type E bars were observed. These bars extend from the vertical partition of central prefabricated element and are bent at 90 degrees into the joint. The detail of this element is shown in Figure 81.



Figure 81: Detail of the hooked bar type E

Sections DD – Central Prefabricated Segment:

Figure 82 shows the orthophoto of the section DD.



Figure 82: Orthophoto of section DD

As previously noted, the section of the prefabricated part shows a more organized reinforcement layout (Figure 83).

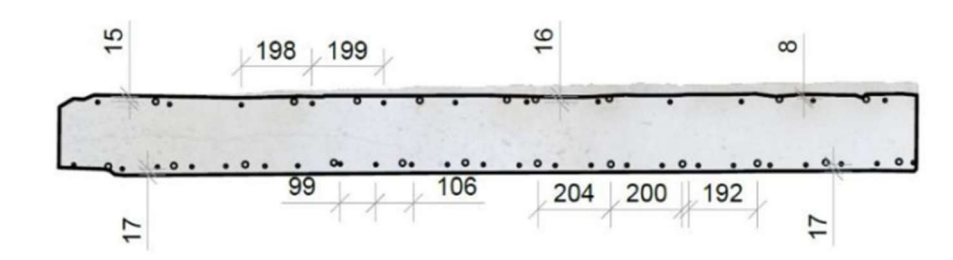


Figure 83: Reinforcement layout in section DD

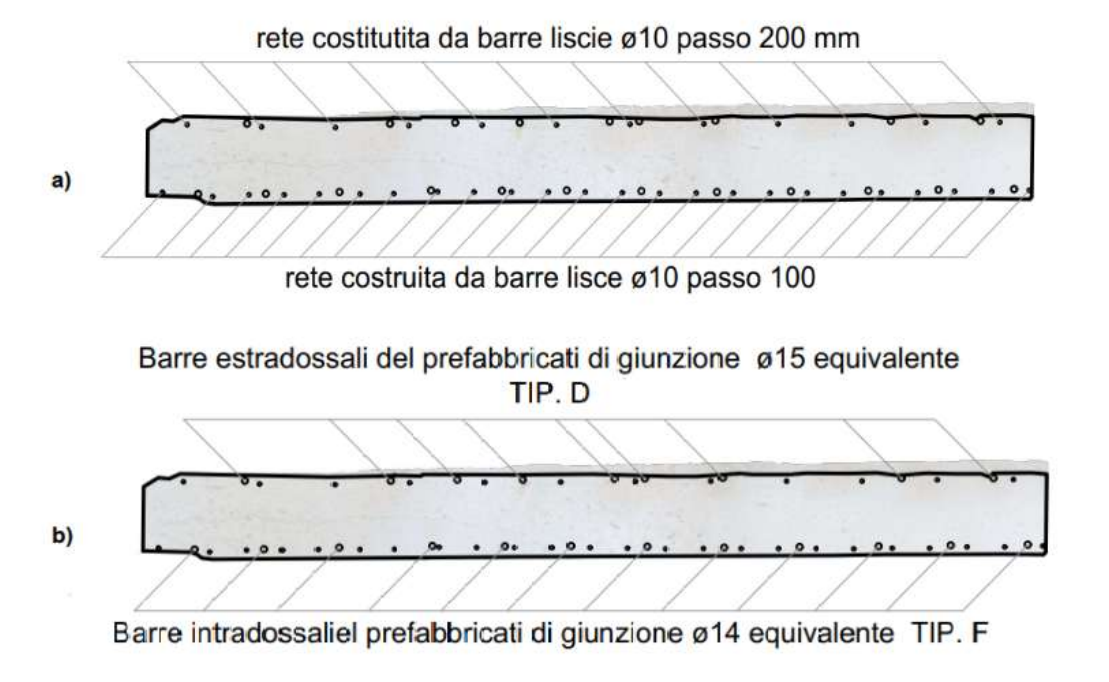


Figure 84: Reinforcement layout in section DD a) principal and b) additional

The principal reinforcement is the same as in the lateral part, forming meshes with a spacing of 100mm in the intrados and 200mm in the extrados (Figure 84a). Additional reinforcement on top consists of the previously mentioned type D bars, which extend from the central prefabricated segment into the cast-in-situ joint (Figure 84b). Type F reinforcement (Figure 84b) is on the level of the bottom mesh but stops approximately 15-20 cm before the vertical partitions.



Figure 85: Detail of the bar type F

3.2.2.3. General observations following the demolitions

Parts of structure were demolished to better understand the reinforcement layout and the state of the degradation of the material.

In Figure 86, it can be seen that type D reinforcement bars are hooked before the section AA in the lateral prefabricated segments, which explains the absence of additional reinforcement in the section AA.

It was also observed that the reinforcement bars in the cast-in-situ joint show a high level of degradation, whereas bars in prefabricated elements are generally not heavily corroded. In some cases, corrosion has completely compromised the reinforcement section, breaking the bar into two separate elements (Figure 88).



Figure 86: Type D bars hooked inside the lateral prefabricated part



Figure 87: Degradation of reinforcement in cast-in-situ joint



Figure 88: View of degradation level

3.2.3. Georadar Scanning

Georadar is a non-destructive method used to investigate structures using radio signals. The reflected signals are used to map embedded objects and internal characteristics.

In this study, georadar scanning was used to compare four samples and to determine whether the reinforcement layout was consistent among them. Three scans in the transverse direction were performed at the front, centre and back of sample. In the longitudinal direction, three scans were performed only in the centre prefabricated parts, because due to the high density of reinforcement in the cast-in-situ parts, the reading would be difficult to interpret.

By analysing transverse scans, a constant spacing of reinforcement was observed, confirming previously obtained information. The concrete cover is not uniform, but shows a linear trend, indicating that the reinforcement was arranged in the form of meshes.

Longitudinal scans were more difficult to interpret due to the high density of reinforcement, particularly in the lateral prefabricated parts, which contain greater amount of additional reinforcement.

Overall, the four samples have similar scanning profiles, suggesting that findings from earlier investigations can be extended to all samples.

3.2.3.1. Sample C1

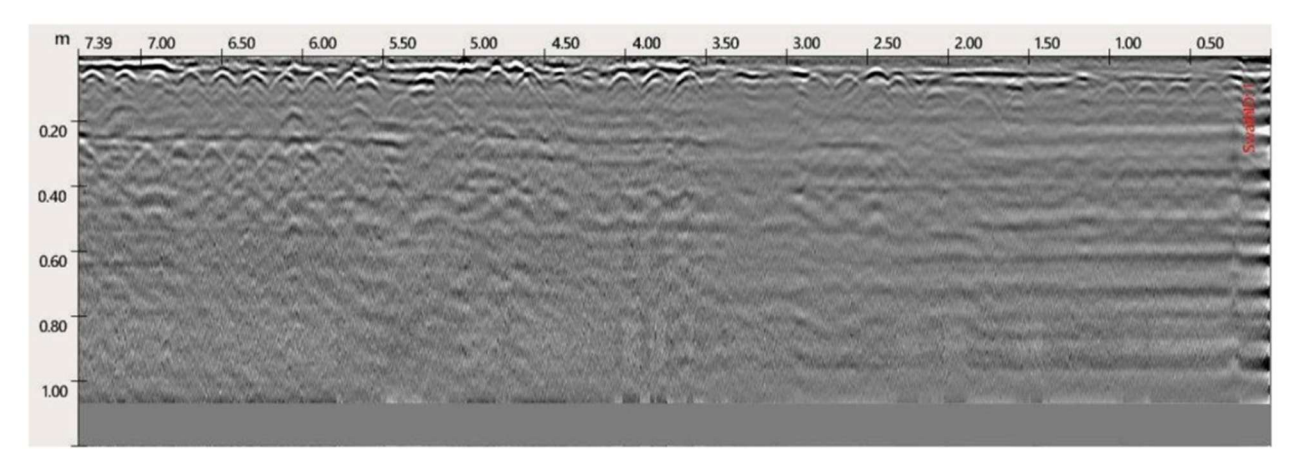


Figure 89: Transverse scan with the georadar of the slab C1 on the front side

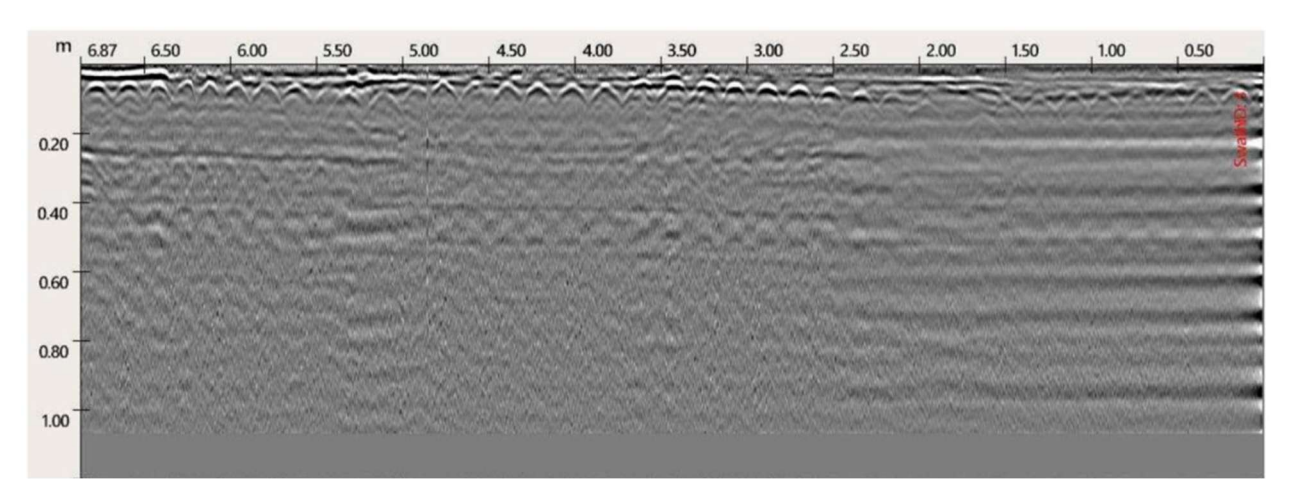


Figure 90: Transverse scan with the georadar of the slab C1 on the centre

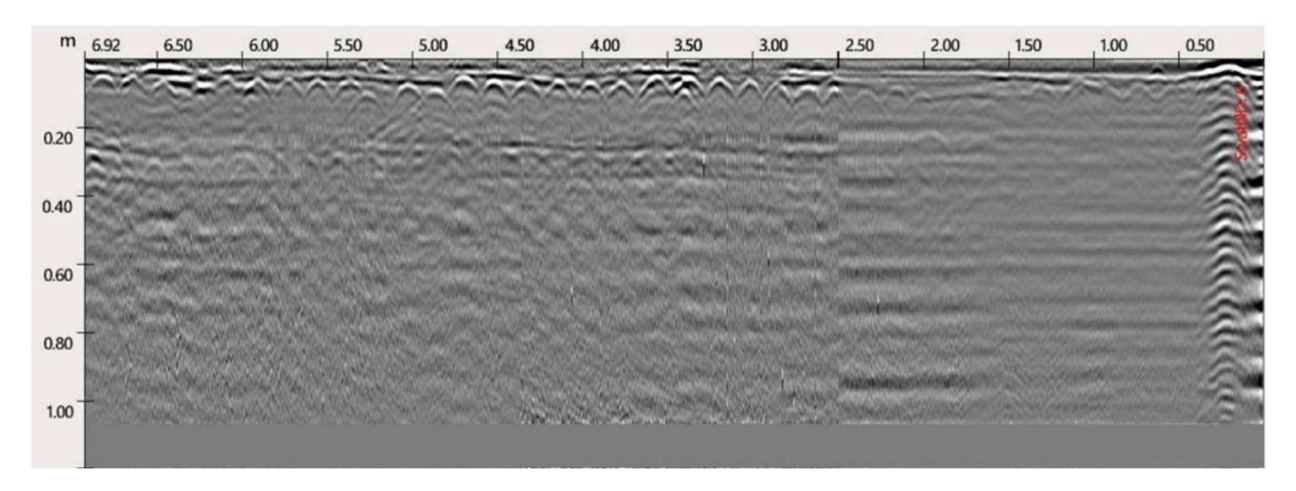


Figure 91: Transverse scan with the georadar of the slab C1 on the back side

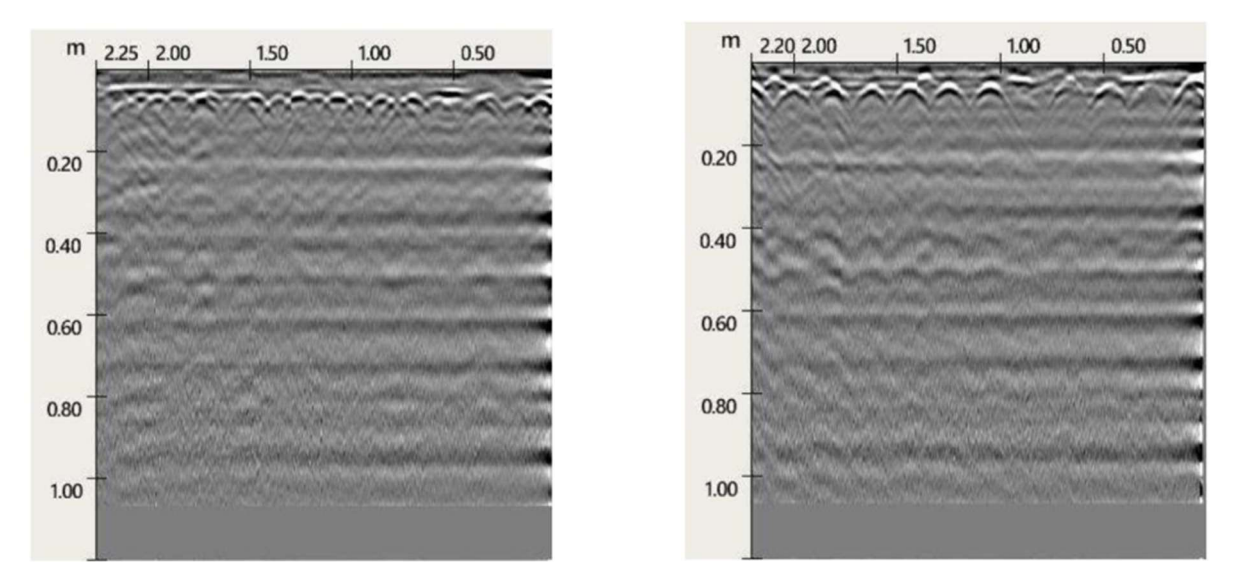


Figure 92: Longitudinal scan with the georadar of the slab C1. Left – span 1, Right – span 2

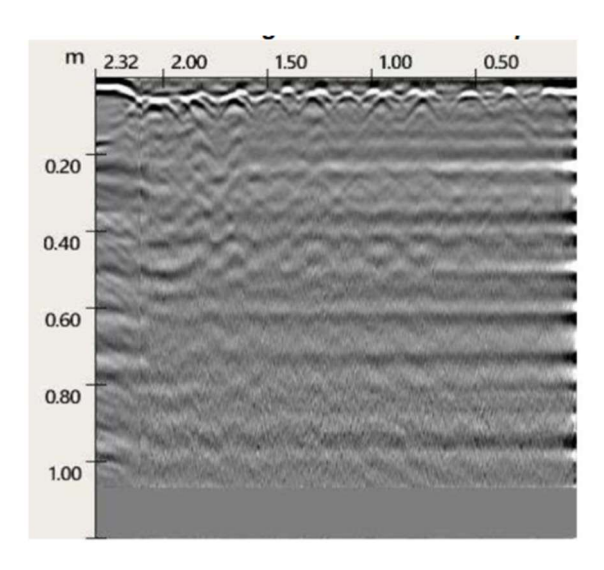


Figure 93: Longitudinal scan with the georadar of the slab C1, span3

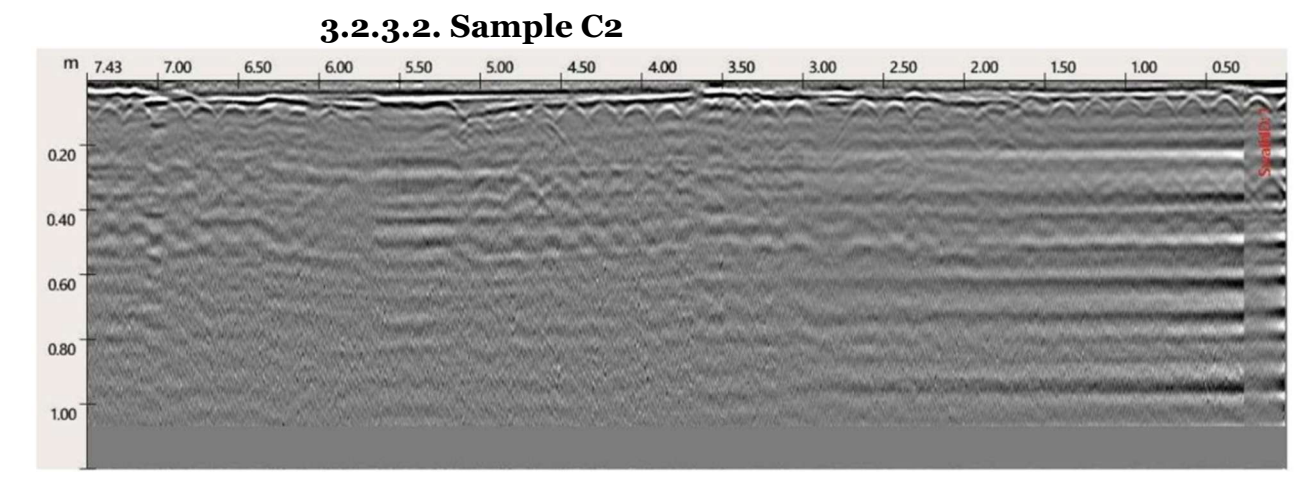


Figure 94: Transverse scan with the georadar of the slab C2 on the front side

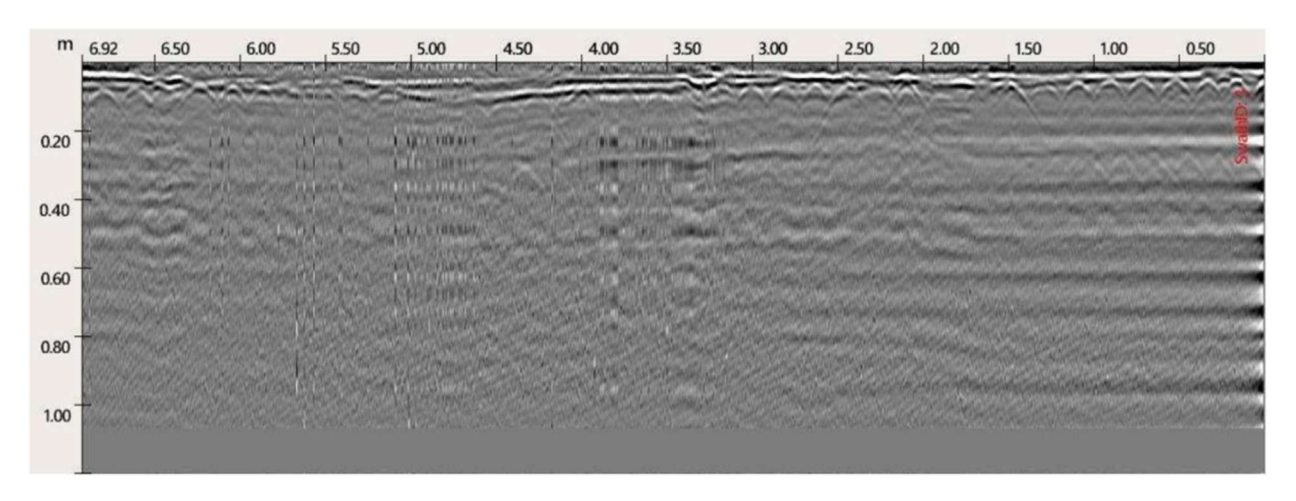


Figure 95: Transverse scan with the georadar of the slab C2 on the centre

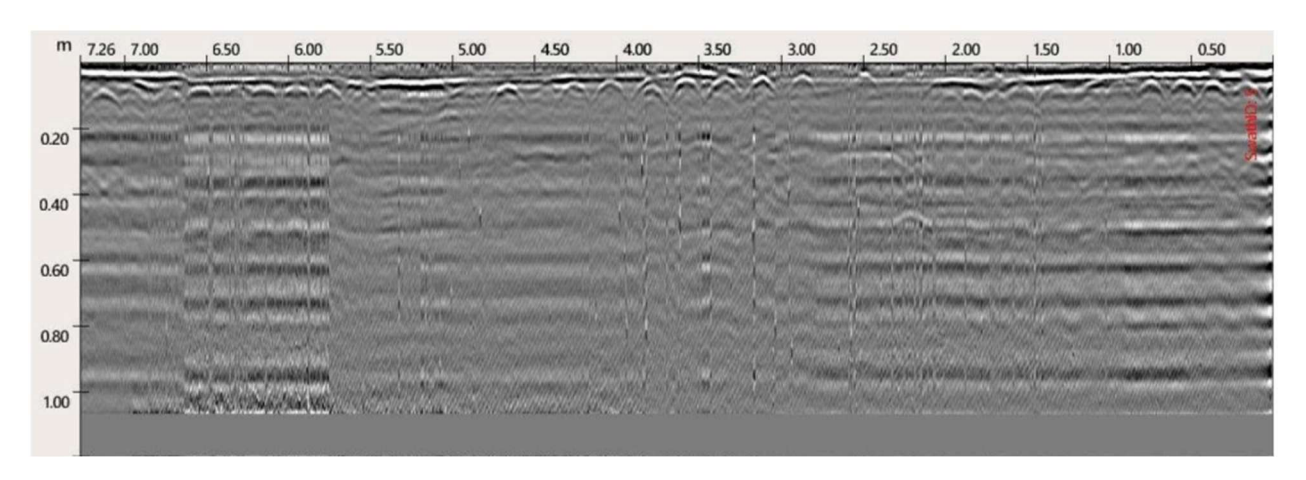


Figure 96: Transverse scan with the georadar of the slab C2 on the back side

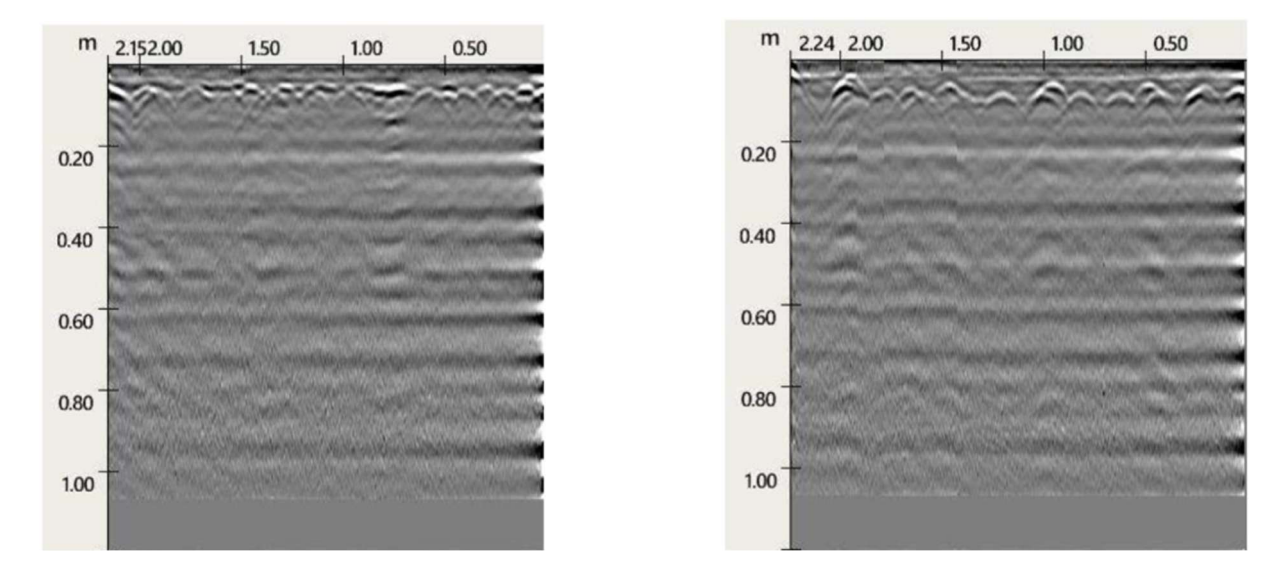


Figure 97: Longitudinal scan with the georadar of the slab C2. Left – span 1, Right – span 2

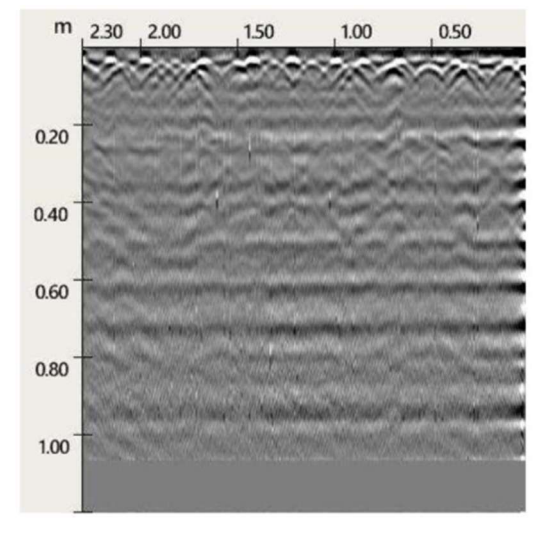


Figure 98: Longitudinal scan with the georadar of the slab C2, span 3

3.2.3.3. Sample C3

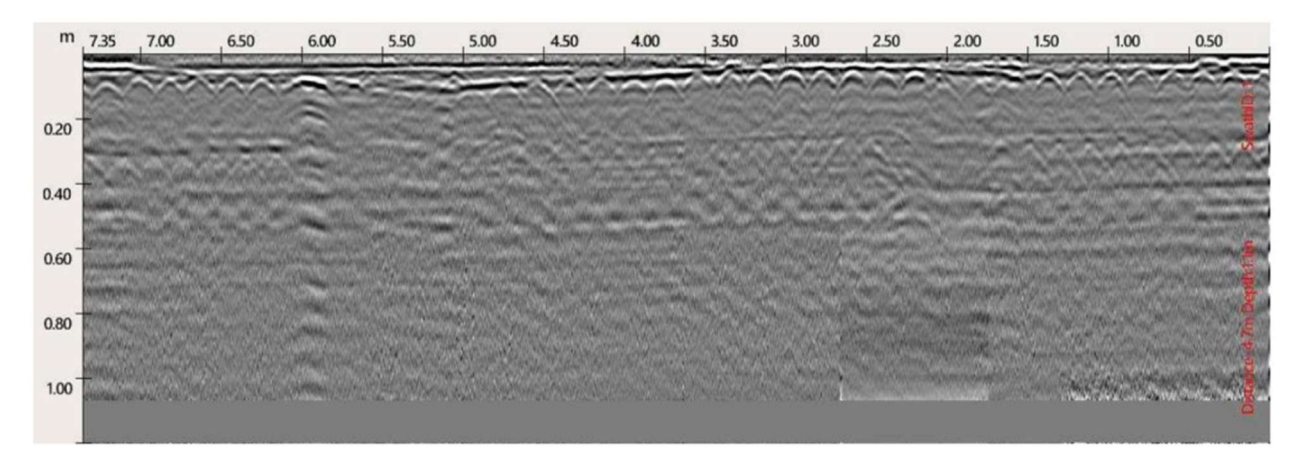


Figure 99: Transverse scan with the georadar of the slab C3 on the front side

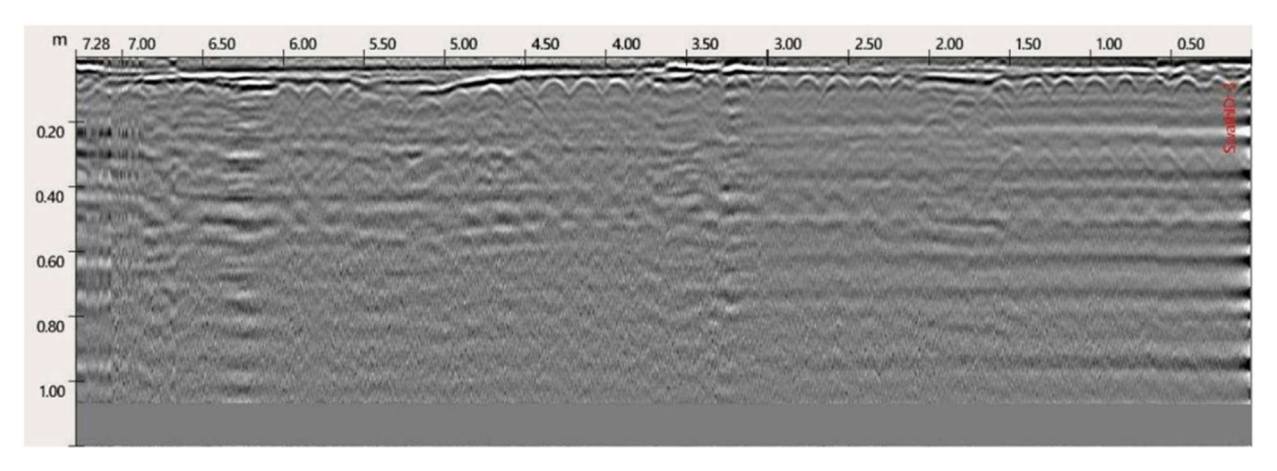


Figure 100: Transverse scan with the georadar of the slab C3 centre

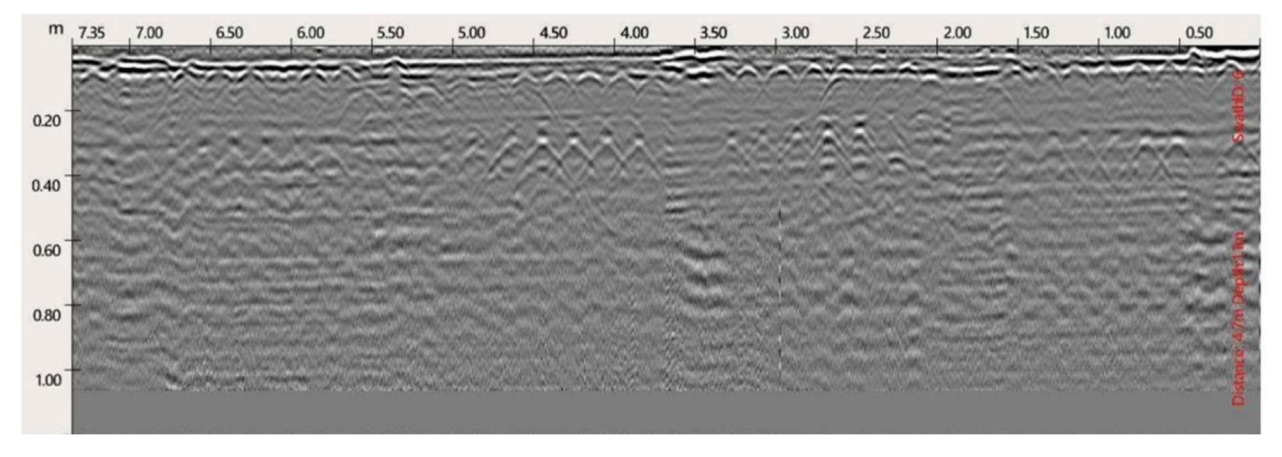


Figure 101: Transverse scan with the georadar of the slab C3 back side

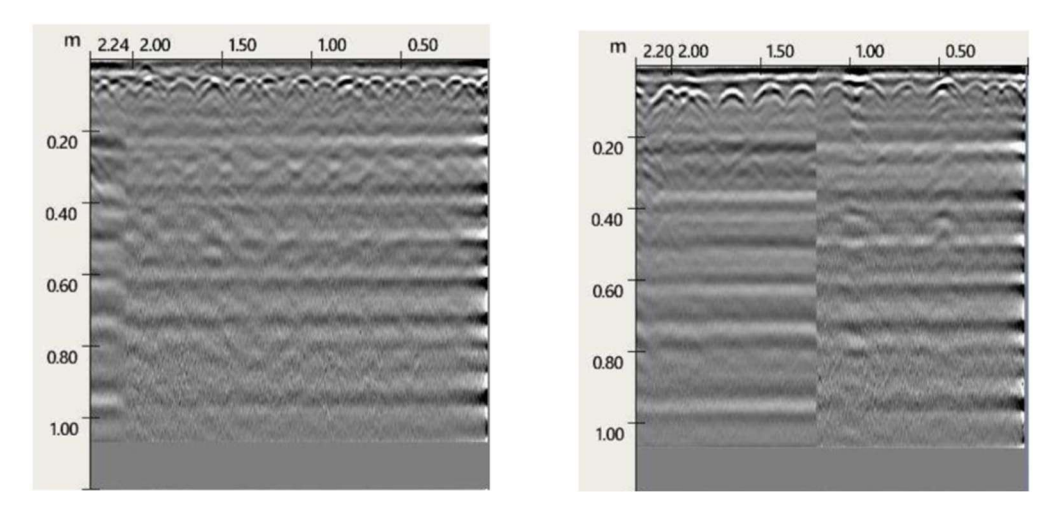


Figure 102: Longitudinal scan with the georadar of the slab C3. Left – span 1, Right – span 2

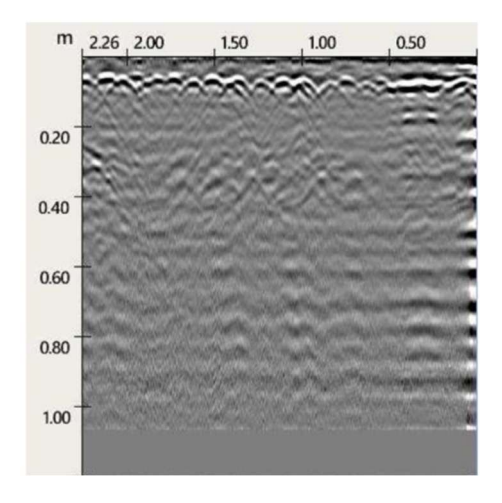


Figure 103: Longitudinal scan with the georadar of the slab C3, span 3



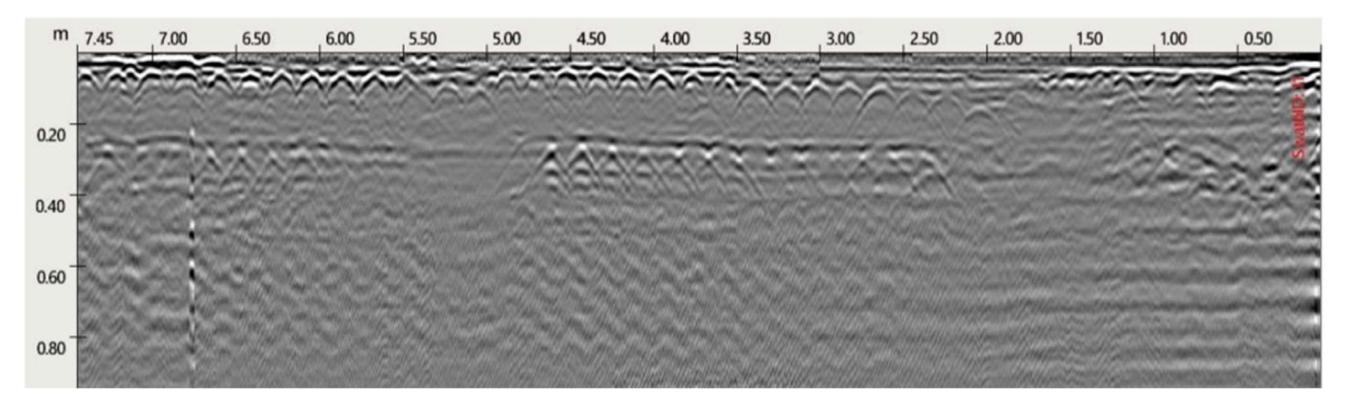


Figure 104: Transverse scan with the georadar of the slab C4 front side

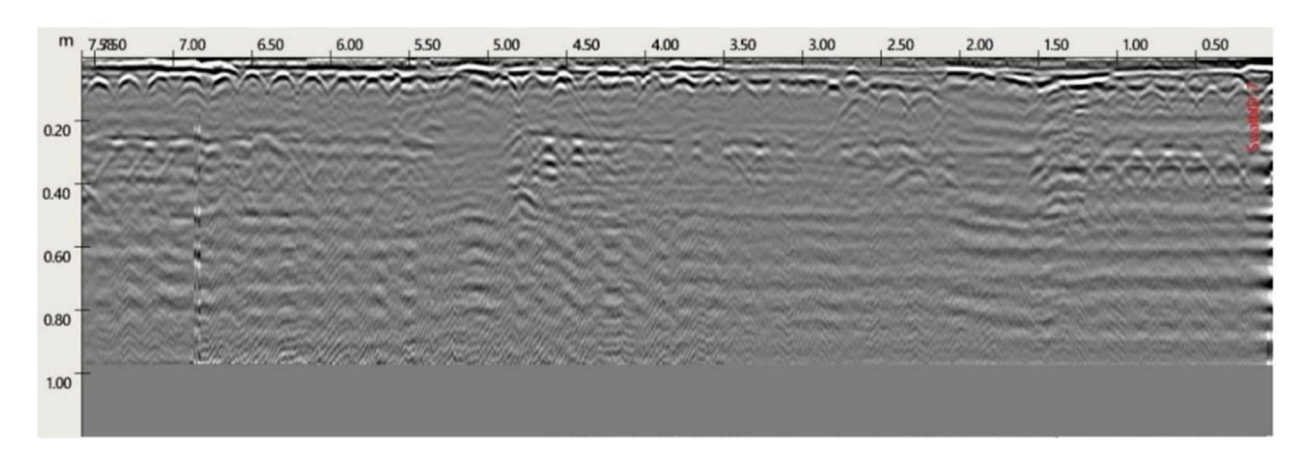


Figure 105: Transverse scan with the georadar of the slab C4 centre

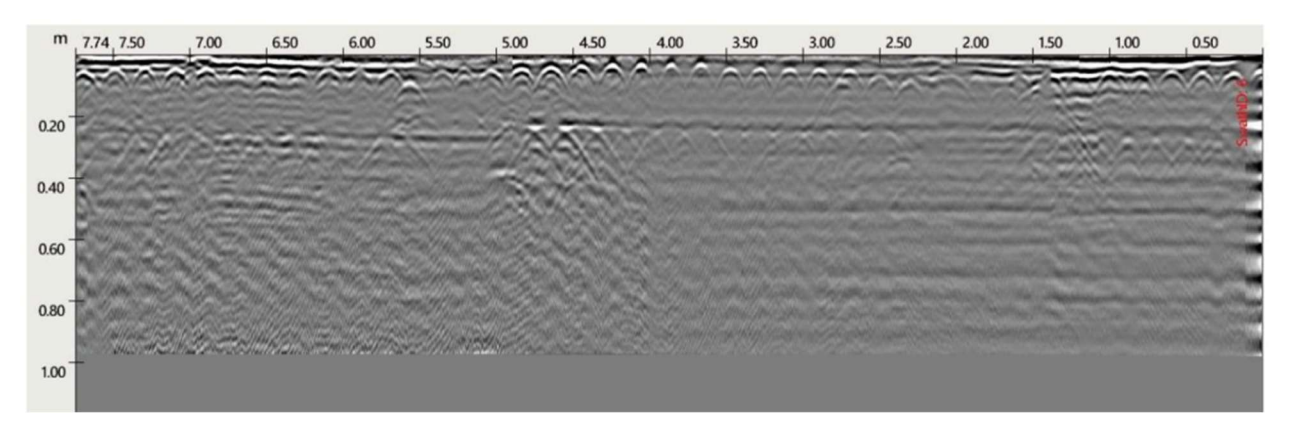


Figure 106: Transverse scan with the georadar of the slab C4 back side

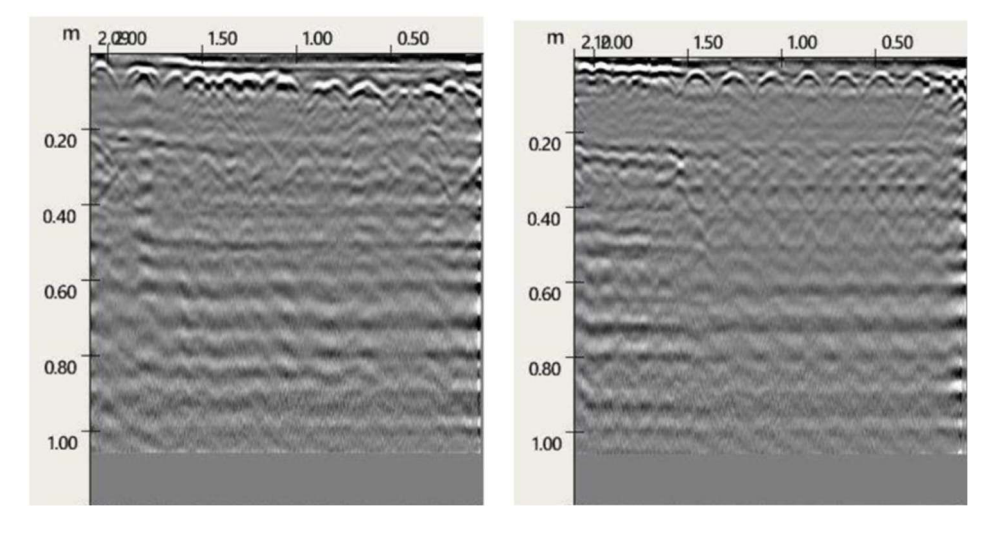


Figure 107: Longitudinal scan with the georadar of the slab C4. Left – span 1, Right – span 2

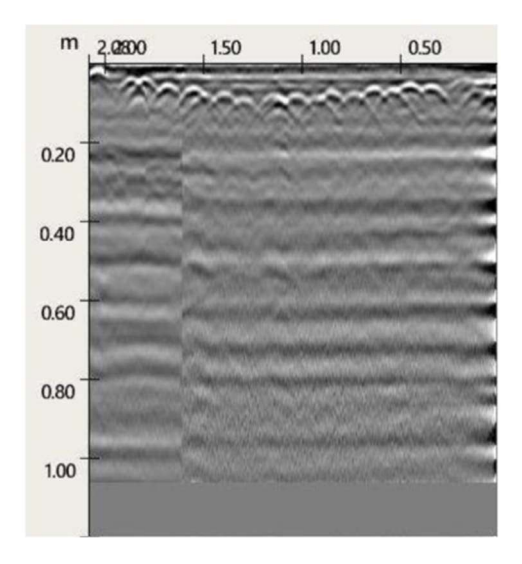


Figure 108: Longitudinal scan with the georadar of the slab C4, span 3

3.2.4. Material Tests

3.2.4.1. Concrete

For the characterization of concrete, compression and elastic modulus tests were performed on extracted cores from the lateral prefabricated part, the cast-in-situ part, and the central prefabricated part.

Cores with an H/D ratio of 1 were extracted from the least stressed portions of the slabs. From the precast parts, a diameter of 100mm was taken from sample C4, and 93 mm from the other samples. From the cast-in-situ parts, a diameter of 93mm was taken from sample C4, and 64 mm from the other samples. This difference is due to the difficulty of extracting larger cores without encountering reinforcement, given the high density of bars in these sections.

Compressive strength test

The extracted samples were prepared to meet the requirements of the reference standard (UNI EN 12390) regarding surface condition. Tests were performed using the CONTROLS AUTOMAX 5 testing machine, with a capacity of 1000 kN, applying a stress rate of 600 kPa/s until failure.

The reported in the Table 9 resistances do not include any correction coefficients. A noticeable difference is observed between the strengths of the prefabricated elements and cast-in-situ joints.

		Diametro	Alterna	II/D	A	Volume	Peso	Densità	Carias	Sforzo
Camp.	Localizzazione		Altezza	H/D	Area				Carico	
		[mm]	[mm]	[#]	[mm ²]	[mm³]	[g]	[kg/m ³]	[kN]	[MPa]
C1	Pref. Laterale	93	96	1.03	6793	652119	1575	2415.20	527.1	77.60
	Pref. Centrale	93	97	1.04	6793	658912	1625	2466.19	533.2	78.49
	Ripresa di getto	64	67	1.05	3217	215538	480	2226.98	137.8	42.84
	Ripresa di getto	64	66	1.03	3217	212321	477	2246.59	169.8	52.78
	Pref. Laterale	93	97	1.04	6793	658912	1630	2473.77	622.9	91.70
	Pref. Centrale	93	95	1.02	6793	645326	1589	2462.32	532.7	78.42
	Ripresa di getto (R)	64	66	1.03	3217	212321	470	2213.63	98.8	30.71
C2	Ripresa di getto (R)	64	66	1.03	3217	212321	467	2199.50	97.3	30.25
	Ripresa di getto (F)	64	67	1.05	3217	215538	479	2222.34	91.3	28.38
	Ripresa di getto (F)	64	65	1.02	3217	209104	466	2228.55	96.4	29.97
	Ripresa di getto (F)	64	65	1.02	3217	209104	460	2199.86	90.9	28.26
	Pref. Laterale	93	96	1.03	6793	652119	1565	2399.87	478.8	70.49
	Pref. Centrale	93	96	1.03	6793	652119	1614	2475.01	521.8	76.82
C3	Pref. Centrale	93	96	1.03	6793	652119	1617	2479.61	490.5	72.21
	Ripresa di getto	64	64	1.00	3217	205887	460	2234.23	153.1	47.59
	Ripresa di getto	64	64	1.00	3217	205887	474	2302.23	148.5	46.16
	Pref. Laterale	100	99	0.99	7854	777544	1858	2389.57	591.1	75.26
C4	Pref. Centrale	93	96	1.03	6793	652119	1539	2360.00	516.3	76.01
	Ripresa di getto	93	96	1.03	6793	652119	1505	2307.86	182	26.79

Table 9:Summary of Compression Test Results on H/D=1 samples

Test for determining Elastic Modulus

The tests were conducted on samples with an H/D ratio of 2 using the BRT Universal Machine in force-controlled mode. Metal plates were placed on the machine grips to provide horizontal support surfaces and a 1000 kN load cell, equipped with a spherical joint, was installed in series with the machine. An additional metal plate was positioned on top of the specimen to create a second contact surface, ensuring uniform stress distribution across the samples.

To measure deformation during the test, on the lateral face of each specimen three strain gauges spaced 120° apart were attached. These measurements were used to calibrate the non-contact measurement system (Digital Image Correlation) used to measure all the deformations until failure using three video cameras 120° apart. The complete setup is shown in Figure 109. The testing procedure followed the UNI EN 12390-13 standard and is illustrated in the Figure 110.





Figure 109: Test setup

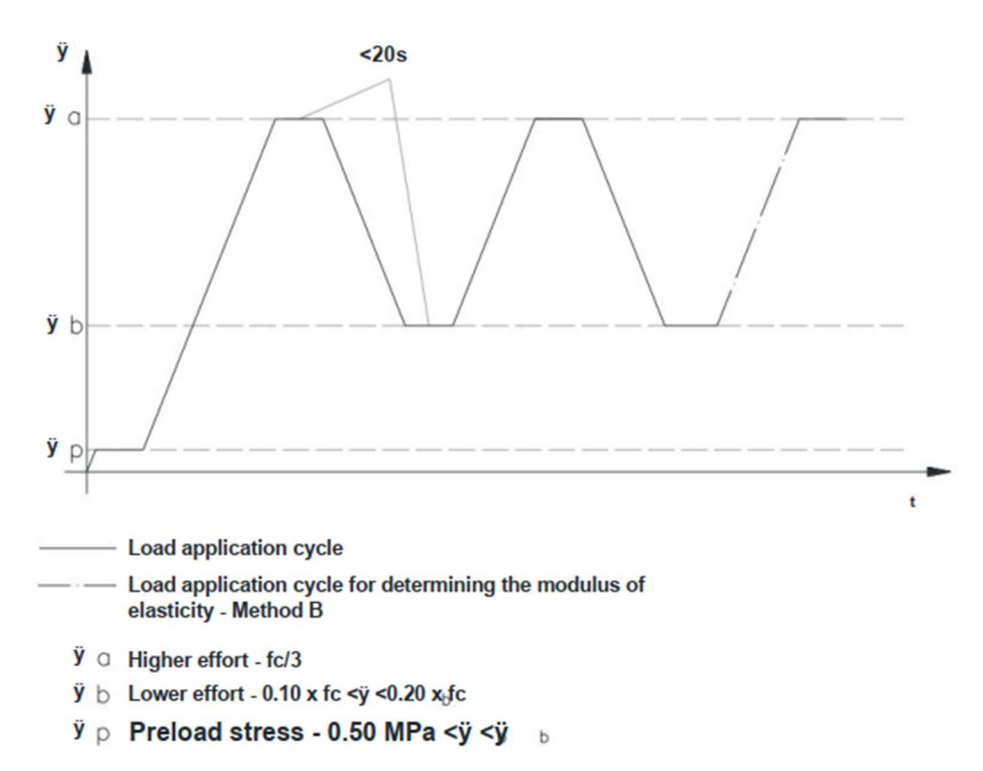


Figure 110: Load history for test

The average values obtained from the compression tests were used. Due to uncertainties in the material strengths, these values were calibrated below those specified in the standard. For each sample, an initial elastic test was performed and then the specimen was completely unloaded. A second test was carried out to reach failure to obtain the

stress-strain curves. Tables 10,11 report the values of elastic modulus and compressive strength of all samples.

C	Localizzazione	Diametro	Altezza	H/D	Δε1	Δσ1	E1	Δε2	Δσ2	E2	E
Camp.	Localizzazione	[mm]	[mm]	[#]	[µm/m]	[MPa]	[GPa]	[µm/m]	[MPa]	[GPa]	[GPa]
	¥.	20		OF						.00	i
C1	Pref. Laterale	93	185	1.99	340.81	14.44	42.370	327.29	14.46	44.18	43.275
	Pref. Centrale	93	188	2.02	409.71	14.42	35.196	407.76	14.46	35.462	35.329
	Ripresa di getto	64	113	1.77	284.34	7.53	26.482	281.86	7.54	26.751	26.617
	Pref. Laterale	93	187	2.01	352.96	14.42	40.854	360.39	14.49	40.206	40.530
44					449.15	14.42	32.105	450.03	14.46	32.131	
C2	Pref. Centrale	93	188	2.02	448.730	14.460	32.224	447.310	14.460	32.327	32.197
	Ripresa di getto (R)	64	128	2.00	328.81	7.53	22.901	343.20	7.50	21.853	22.377
	Pref. Laterale	93	189	2.03	354.25	14.42	40.706	369.32	14.46	39.153	39,929
C3	Pref. Centrale	93	190	2.04	350.78	14.41	41.080	356.56	14.46	40.554	40.817
	Ripresa di getto	64	132	2.06	239.17	7.49	31.317	241.91	7.50	31.003	31.160
	Pref. Laterale	100	206	2.06	302.89	12.47	41.170	315.73	12.51	39.622	40.396
C4	Pref. Centrale	100	193	1.93	336.95	12.45	36.949	342.77	12.50	36.468	36.708
	Ripresa di getto	93	187	2.01	294.80	6.61	22.422	308.99	6.69	21.651	22.037

 $Table \ 10: Summary \ of \ the \ Modulus \ tests \ results$

C	F	Diametro	Altezza	H/D	Area	Volume	Peso	Densità	Carico	σ
Camp.	Localizzazione	[mm]	[mm]	[#]	[mm²]	[mm³]	[g]	[kg/m³]	[kN]	[MPa]
	3		36		91	3				No.
George :	Pref. Laterale	93	185	1.99	6793	1256688	3103	2469.19	348.95	51.37
C1	Pref. Centrale	93	188	2.02	6793	1277067	3104	2430.57	371.78	54.73
	Ripresa di getto	64	113	1.77	3217	363520	814	2239.22	108.09	33.60
	Pref. Laterale	93	187	2.01	6793	1270274	3096	2437.27	503.49	74.12
C2	Pref. Centrale	93	188	2.02	6793	1277067	3099	2426.65	436.30	64.23
	Ripresa di getto (R)	64	128	2.00	3217	411775	910	2209.95	70.03	21.77
0 01		N	The state of the s	9	5	9				25
	Pref. Laterale	93	189	2.03	6793	1283860	3120	2430.17	415.52	61.17
C3	Pref. Centrale	93	190	2.04	6793	1290653	3127	2422.81	411.10	60.52
	Ripresa di getto	64	132	2.06	3217	424643	948	2232.46	132.22	41.10
	3	7)	70 - 0	3 3		7	a	:	×	578
	Pref. Laterale	100	206	2.06	7854	1617920	3911	2417.30	534.69	68.08
C4	Pref. Centrale	100	193	1.93	7854	1515818	3628	2393.43	487.26	62.04
	Ripresa di getto	93	187	2.01	6793	1270274	2845	2239.67	179.19	26.38

Table 11: Summary of the Compression tests results

3.2.4.2. Steel reinforcement

Six different types of reinforcement bars were identified, and tensile tests were performed on each typ.

Type 1 is a round bar with an approximate diameter of 14 mm (Figure 111).



Figure 111: Detail of the type 1 bar

Type 2 is a shaped (approximately square) bar with equivalent diameter of 15 mm (Figure 112).



Figure 112: Detail of the type 2 bar

Type 3 is a shaped (approximately square) bar with equivalent diameter of 14 mm (Figure 113).



Figure 113: Detail of the type 3 bar

Type 4 is a smooth bar from a mesh with diameter of 10 mm (Figure 114). Type 5 is a smooth bar from a mesh with diameter of 8 mm (Figure 114).



Figure 114: Detail of the type 4 and 5 bars

Type 6 is a shaped (approximately square) bar with equivalent diameter of 8 mm (Figure 115).



Figure 115: Detail of the type 6 bar

To standardize deformation values, the machine stroke was divided by the free length between the grips. This method introduces some uncertainty. Consequently, the elastic modulus cannot be determined directly from the force-displacement graph. An extensometer was mounted during the initial part of the tensile test to measure deformations, and then removed after yielding of the sample. Another source of uncertainty is related to the cross-section of the reinforcing bars, particularly when they are not circular. Samples were measured to calculate equivalent diameter based on a steel density of 7850 kg/m³. Additional uncertainty arises from the effective load-

bearing area, as reinforcement bars can be damaged or corroded, reducing the actual strength.

Table 12 shows a summary of tensile tests.

	ф	eq.	ı		f	y	f	u	Α	gt
Camp.	valore	media	valore	media	valore	media	valore	media	valore	media
	[m	m]	[GI	Pa]	[MPa]		[MPa]		[%]	
1a	14.07	14.12	212.976	210.817	439.39	442.39	641.54	643.21	18.28	18.390
1b	14.18	±	205.648	±	445.52	±	646.00	±	17.87	±
1c	14.12	0.05	213.828	4.497	442.25	3.07	642.09	2.43	19.02	0.583
2a	15.17	15.21	165.162	180.830	341.57	367.54	482.88	540.55	5.35	5.730
2b	15.23	±	205.434	±	345.18	±	535.64	±	6.00	±
2c	15.24	0.04	171.895	21.572	415.87	41.89	603.13	60.28	5.84	0.339
3a	13.89	13.85	-	195.613	411.41	395.31	629.46	609.35	5.09	5.107
3b	13.74	±	204.966	±	382.56	±	583.69	±	6.06	±
3c	13.92	0.10	186.260	13.227	391.98	14.72	614.89	23.38	4.17	0.945
4a	9.83	9.79	211.923	201.044	498.97	536.75	566.52	600.54	4.93	2.435
4b	9.82		213.671		523.46		600.11		1.20	
4c	9.44		216.407	±	585.10		629.80		1.02	±
4d	9.87	±	173.604	ı.	555.35	±	615.33	±	3.61	-
4e	9.89		187.754		536.25		611.55		1.08	
4f	9.91	0.18	202.904	17.011	521.39	30.08	579.94	23.57	2.77	1.617
5a	8.05	8.03	201.902	198.012	525.20	513.59	594.16	577.95	1.45	1.712
5b	8.09		211.762		520.98		606.55		3.56	
5c	7.96	±	182.955	±	452.16	±	483.41		1.18	
5d	8.00	_ <u>_</u>	181.221	ı.	533.79	ı ı	596.27	±	1.23	±
5e	8.07				510.15		581.92		1.81	
5f	8.04	0.05	212.221	15.122	539.28	31.76	605.42	47.17	1.04	0.944
6a	8.11	8.10	136.424	215.206	483.97	493.02	671.14	667.20	10.30	9.610
6b	8.11	±	216.485	±	497.34	±	672.27	±	10.73	±
6c	8.08	0.02	213.928	1.808	497.76	7.84	658.19	7.82	7.80	1.582

Table 12: Summary of Tensile tests on reinforcement

4. Finite Element Model

Evaluation of RC slab was performed with finite element analysis, transforming a physical body into a model with finite number of elements. Finite element model was created in ANSYS WORKBENCH 2025 R2.

4.1. Material models for non-linear analysis

4.1.1. Concrete model

To describe non-linear behaviour of concrete the Menetrey-Willam model was used. The Menetrey-William model realized in ANSYS can represent different concrete properties, such as different tensile and compressive strength, nonlinear hardening, softening and dilatancy. Linear or exponential softening can be modelled using ANSYS software and both meet the requirements of CEB-FIP Model Code (Figures 116, 117) [7,8,9].

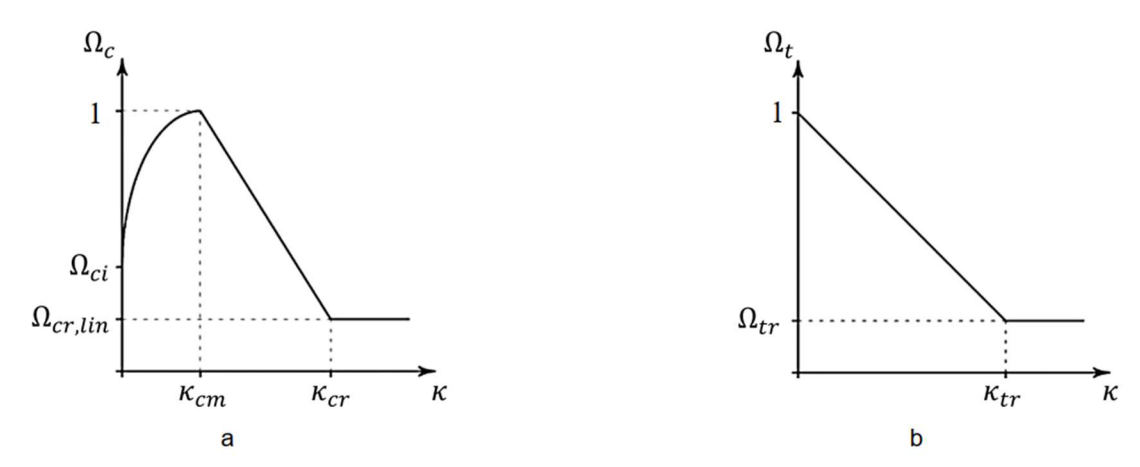


Figure 116: Hardening/softening functions with linear softening: a - in compression; b - in tension

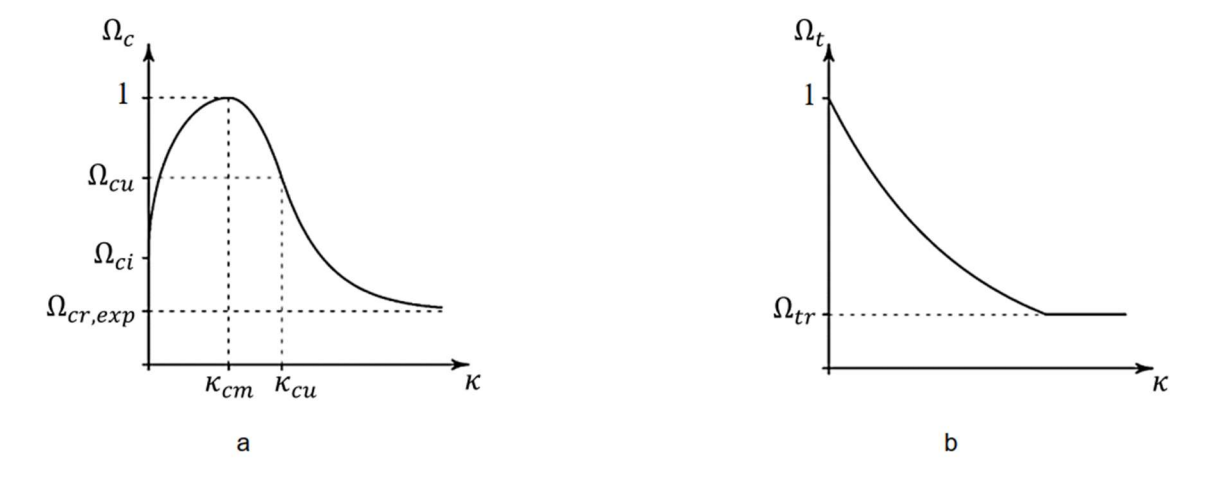


Figure 117: Hardening/softening functions with exponential softening: a-in compression; b-in tension

To obtain input parameters for the model mainly CEB-FIP Model Code [7,8] is used according to the recommendations of [9].

In this study model with linear softening was used. Concrete is considered to behave elastically up to

$$\Omega_{ci} = \frac{\sigma_{co}}{f_c} = \frac{f_c^{1.855}}{60 f_c}.$$

Equation 1: Relative stress at start of nonlinear hardening

The peak strain ε c1 at uniaxial compressive strength is defined as the minimum of two values:

$$\varepsilon_{c1} = \min \begin{cases} -0.0022, \\ -\frac{0.7 f_c^{0.31}}{1000}. \end{cases}$$

Equation 2: Plastic strain at uniaxial compressive strength

Residual compressive relative stress in case with linear softening is equal to 0.2. Ultimate strain in compression ϵ_{ult} depends on the strength grade of concrete and it can be determined by formula:

$$\varepsilon_{ult} = n \cdot \varepsilon_{c1}$$

Equation 3: Ultimate strain in compression

Where n is constant for certain grade of concrete (Table 13)

Concrete grade	C20	C40	C60	C80
n	3	2	1.5	1.2

Table 13: Coefficient n to describe ultimate strain

Tensile strength is found by:

$$f_c \le 50: f_t = 0.3 (f_c)^{\frac{2}{3}};$$

 $f_c > 50: f_t = 2.12 \cdot \ln\left(1 + \frac{(f_c + \Delta f)}{10}\right).$

Equation 4: Tensile strength of concrete

Biaxial compressive strength of concrete:

$$f_{bc} = \left(1.2 - \frac{f_c}{1000}\right) \cdot f_c$$

Equation 5: Biaxial compressive strength of concrete

Dilatancy refers to the nonlinear increase in volume that occurs due to shear deformation. The reason for this is the accumulation of microcracks in the inner structure of the material. To characterize this phenomena dilatancy angle is used. Typical values for concrete are 8°-15°.

By implying the above equations, the results of material testing were used to determine the input values for the concrete constitutive law. Table 14 presents a summary of the data for the Menetrey-William model for four samples.

Sample	Part	Uniaxial compress ive strength [Mpa]	Young's Modulus E [GPa]	Poisson's Ratio	Uniaxial tensile strength [Mpa]	Biaxial Compressive Strength [MPa]	Dilatancy angle [°]	Plastic strain at uniaxial compressive strength	Ultimate effective plastic strain in compression	Relative stress at start of nonlinear hardening	Residual Compressive Relative stress	Plastic strain limit in tension	Residual tensile relative stress
	Lateral	51.37	43.275	0.2	4.11	59.01	15	0.00237	0.00415	0.48362	0.2	0.01	0.2
C1	Central	54.73	35.329	0.2	4.21	62.68	15	0.00242	0.00424	0.51054	0.2	0.01	0.2
	Cast in-situ	33.60	26.617	0.2	3.12	39.19	15	0.00220	0.00550	0.33641	0.2	0.01	0.2
	Lateral	74.12	40.530	0.2	4.71	83.45	15	0.00266	0.00339	0.66167	0.2	0.01	0.2
C2	Central	64.23	32.197	0.2	4.47	72.95	15	0.00254	0.00363	0.58542	0.2	0.01	0.2
	Cast in-situ	21.77	22.377	0.2	2.34	25.65	15	0.00220	0.00660	0.23212	0.2	0.01	0.2
	Lateral	61.17	39.929	0.2	4.39	69.66	15	0.00251	0.00376	0.56149	0.2	0.01	0.2
C3	Central	60.52	40.817	0.2	4.37	68.96	15	0.00250	0.00375	0.55638	0.2	0.01	0.2
	Cast in-situ	41.10	31.160	0.2	3.57	47.63	15	0.00222	0.00443	0.39965	0.2	0.01	0.2
	Lateral	68.08	40.396	0.2	4.56	77.06	15	0.00259	0.00389	0.61529	0.2	0.01	0.2
C4	Central	62.04	36.708	0.2	4.41	70.60	15	0.00252	0.00378	0.56831	0.2	0.01	0.2
	Cast in-situ	26.38	22.037	0.2	2.66	30.96	15	0.00220	0.00605	0.27355	0.2	0.01	0.2

Table 14: Input values for concrete properties

4.1.2. Steel reinforcement model

Steel reinforcement behaviour is modelled using bilinear isotropic hardening model. However, the plastic portion of the curve is modelled as a straight horizontal line, thereby excluding the hardening effect.

Table 15 summarizes the data used for steel modelling, obtained from laboratory tests.

	Туре	· mm		Young's Modulus E [GPa]	fy [MPa]	fu [MPa]	Poisson's Ratio
Steel	1	14	round	210.817	442.309	643.21	0.3
	2	15	"square"	180.830	367.54	540.55	0.3
	3	14	"square"	195.613	395.31	609.35	0.3
	4	10	round	201.044	536.75	600.54	0.3
	5	8	round	198.012	513.59	577.95	0.3
	6	8	"square"	215.206	493.02	667.20	0.3

Table 15: Input values for steel properties

4.2. Geometry modelling

For modelling of concrete SOLID185 elements were used. It is an eight nodes solid element with three degrees of freedom at each node: translations in the nodal x, y, and z directions. Element properties include plasticity, hyperelasticity, stress stiffening, creep, large deflection, and large strain capabilities. [10]

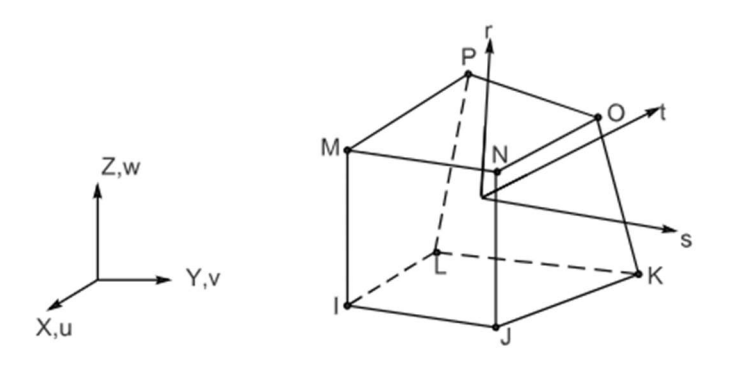
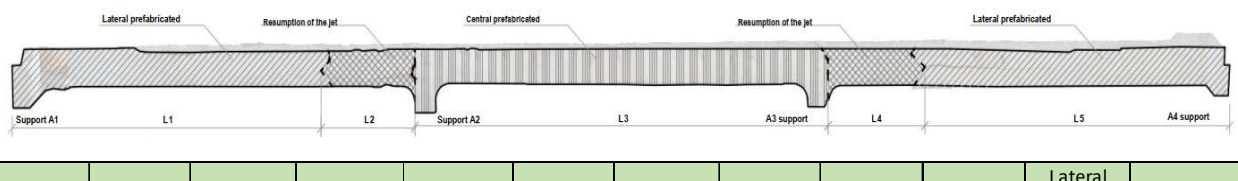


Figure 118: SOLID185 - 3D 8-Node Structural Solid

The slab section generally consists of two lateral parts and one central precast part, connected by two cast-in-situ joints. In the model, each segment was represented as a separate solid with its own assigned material properties. Several simplifications were introduced to reduce the complexity of computation. The interface between the precast and cast in situ parts was assumed to follow a vertical alignment. The top surface of the slabs was modelled as a perfectly flat plane, disregarding the irregularities and unevenness present in real samples. In addition, vertical segments of the partitions were excluded from the model, as their contribution to the global structural response was considered negligible.

Table 16 presents the summary of the geometry dimensions.



Sample	Lateral Precast Left L1 [mm]	l Precast	Cast-in-situ joint Left L2 [mm]	ioint Left	Central Precast L3 [mm]	Central Precast Height [mm]	Cast-in- situ joint Right L4 [mm]	Cast-in-situ joint Right Height [mm]	Lateral Precast Right L5 [mm]	Lateral Precast Right Height [mm]	Length in longitudinal direction [mm]
C1	2182	228	681	228	2927	215	700	225	2154	221	2500
C2	2170	214	701	214	2952	210	671	222	2135	218	2500
C3	2158	194	692	211	2935	202	659	220	2176	221	2480
C4	2194	216	668	211	2933	212	688	218	2165	220	2440

Table 16: Concrete geometry dimensions in model

Reinforcement was modelled as discrete using REINF264 elements. This element is suitable for simulating reinforcing fibres with arbitrary orientations. Each fibre is modelled separately as a spar that has only uniaxial stiffness (default) or conductivity. The nodal locations, degrees of freedom, and connectivity of the REINF264 element are identical to those of the base element [11].

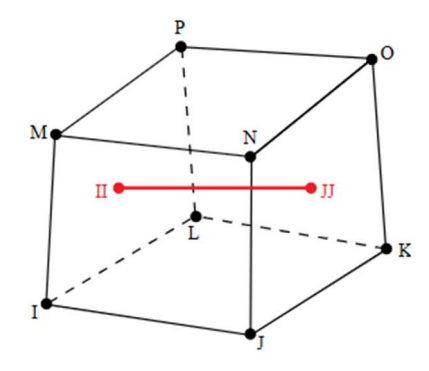


Figure 119: 3D 8-Node Solid with REIN264 element

The reinforcement patterns were modelled to fully reflect the investigated samples, except for type E bars located in the vertical partition segments. Table 17 presents a summary of reinforcement amount in each model in both directions.

	Longitud	dinal direction		
Sample	Part	Top mesh	Bottom mesh	Additional bars
	Lateral Left	11ø8	11ø8	
	Cast in-situ Left	49	1 8	
C1	Central	17ø8	17ø8	1ø18
	Cast in-situ Right	69	8	
	Lateral Right	10ø8	10ø8	
	Lateral Left	11ø8	10ø8	
	Cast in-situ Left	70	8	
C2	Central	17ø8	17ø8	2ø8
	Cast in-situ Right	40	8	
	Lateral Right	10ø8	10ø8	
	Lateral Left	11ø8	11ø8	
	Cast in-situ Left	59	8	
C3	Central	17ø8	17ø8	2ø18
	Cast in-situ Right	69	18	
	Lateral Right	11ø8	11ø8	
	Lateral Left	9ø8	11ø8	
	Cast in-situ Left	50	18	
C4	Central	17ø8	17ø8	2ø18
	Cast in-situ Right	50	18	
	Lateral Right	11ø8	11ø8	

	Tranverse direction												
Sample	Part	Top mesh type A	Bottom mesh type A	Туре В	Type C	Type D from lateral to cast-in- situ	Type D from central to cast-in- situ	Type F					
	Lateral	12ø10	25ø10										
C1	Central	12ø10	25ø10	16ø10	14ø14	16ø15	9ø15	12ø14					
	Cast in-situ	-	=										
	Lateral	13ø10	25ø10										
C2	Central	12ø10	25ø10	16ø10	14ø14	17ø15	9ø15	12ø14					
	Cast in-situ	-	-										
	Lateral	12ø10	25ø10										
C3	Central	13ø10	25ø10	16ø10	14ø14	15ø15	9ø15	12ø14					
	Cast in-situ	-	-										
	Lateral	12ø10	24ø10										
C4	Central	12ø10	24ø10	16ø10	12ø14	15ø15	9ø15	12ø14					
	Cast in-situ	-	-										

Table 17: Reinforcement in longitudinal and transverse directions

4.3. Model setup

Interaction of model segments in contact is characterized by the forces they exert on each other. Distribution of this forces is the main objective of contact formulation. Contact is not automatically accounted for in the equation of motion, so it needs to be included in the modelling system. [12]

Forces at the contact point are decomposed into normal F_n and tangential components F_t (Figure 120).

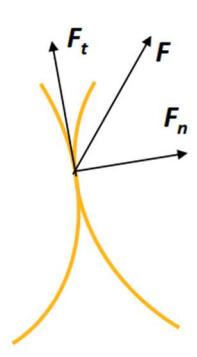


Figure 120: Decomposition of force vector

Normal component resists the interpenetration of bodies, while tangential component resists sliding of bodies along each other. Based on the transfer of these components there are three main types of contacts: bonded, frictionless, and frictional. [12]

To model the interaction between the concrete segments, a bonded contact was implemented to ensure continuity of the deck. In this type of contact, during surface interaction no separation or sliding occurs, meaning that both components are considered infinitely large. [12]

Load was applied through wooden and steel elements to reproduce the required footprint. The contact between the concrete surface and loading plates was defined as frictional.

In frictional contact, in normal direction separation is allowed, whereas interpenetration is restricted. In the tangential direction, the resisting force is a function of the normal force, typically described through a friction law. [12]

According to the data reported in [13] and [14], the static friction coefficient was assumed to be $\mu = 0.62$ for the interaction between wood elements and the concrete surface, and $\mu = 0.57$ for the interaction between steel plates and concrete surface.

REINF264 element assumes perfect bond with the host solid element. The reinforcement strain is taken directly from the strain field of the host solid element and there is no slip between concrete and reinforcement.

Boundary conditions are defined as displacement constraints in the UX, UY and UZ directions for the solid bodies, applied along the lateral edges and at the edges of the connection between the central prefabricated part and the cast-in-situ joints.

The calculation used program-controlled auto time stepping, a direct solver (Sparse Direct Solver), the Newton-Raphson method, with large deflections enabled.

5. Results comparison and model updating

After modelling the samples, four loadings were applied to each model. The results were recorded as vertical deformation measured by probes positioned at locations corresponding to the transducers used in laboratory tests under the load application point. The results of the finite element analysis are presented alongside the laboratory test results to directly compare the maximum deflections.

5.1. Sample C1

First trial of loadings was carried out on the model described in the previous chapter. Loading scheme 2 is applied on the sample C1 in span 1 and span 2.

The following graphs (Figure 121, 122) show the force – displacement curves for span 1 and span 2.

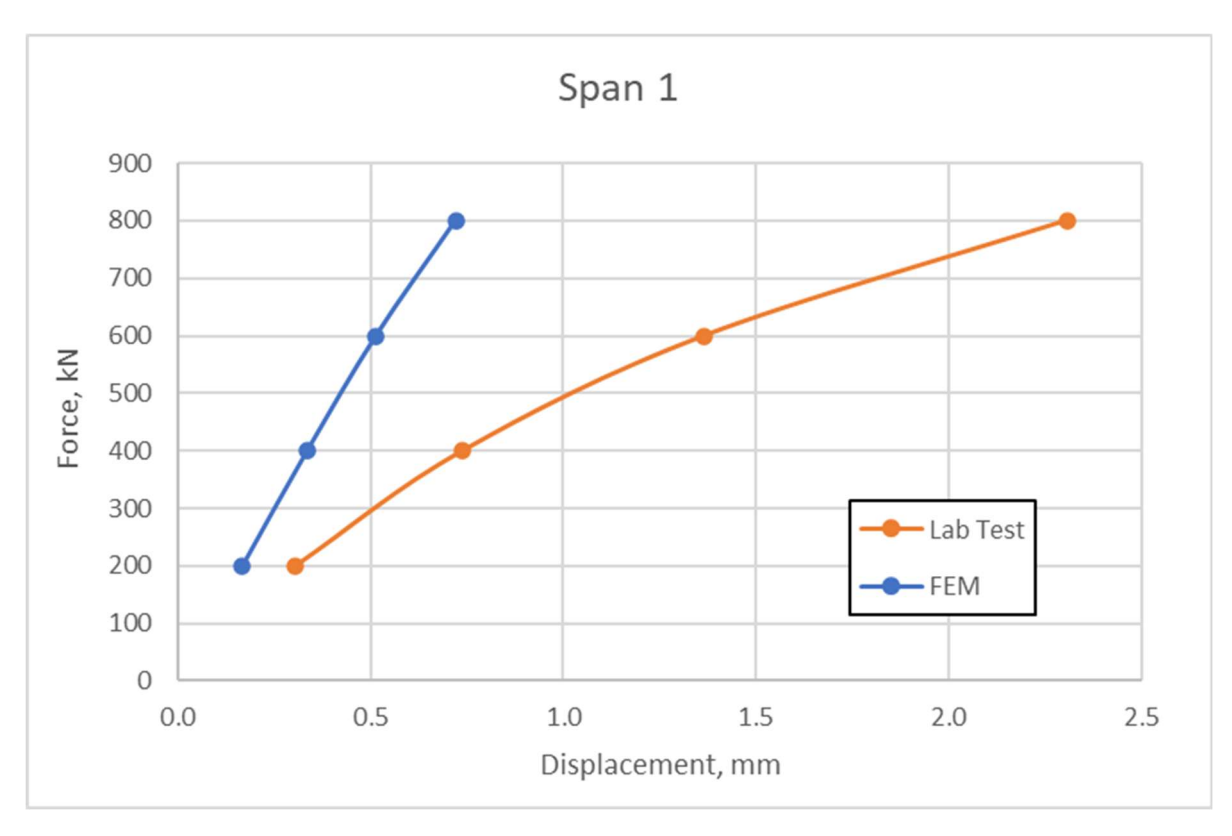


Figure 121: Model C1. Force-displacement curve for span 1



Figure 122: Model C1. Force-displacement curve for span 2

The results of span 1 show significant difference in deflection. The finite element model shows higher rigidity than the real-life situation. To reduce the difference between results several trials were performed. The closest performance was achieved under the assumption of medium continuity provided by joints. The contact surface between the central prefabricated part and cast in situ-joints modelled as bonded, while the contact surface between lateral prefabricated parts and joints to be modelled as frictional with the friction coefficient μ =0.42. Frictional contact means that two contacting geometries can carry shear stresses up to a certain magnitude before they start sliding relative to each other. The model defines an equivalent shear stress at which sliding begins as a fraction of contact pressure. Comparison of results under these assumptions is presented below.

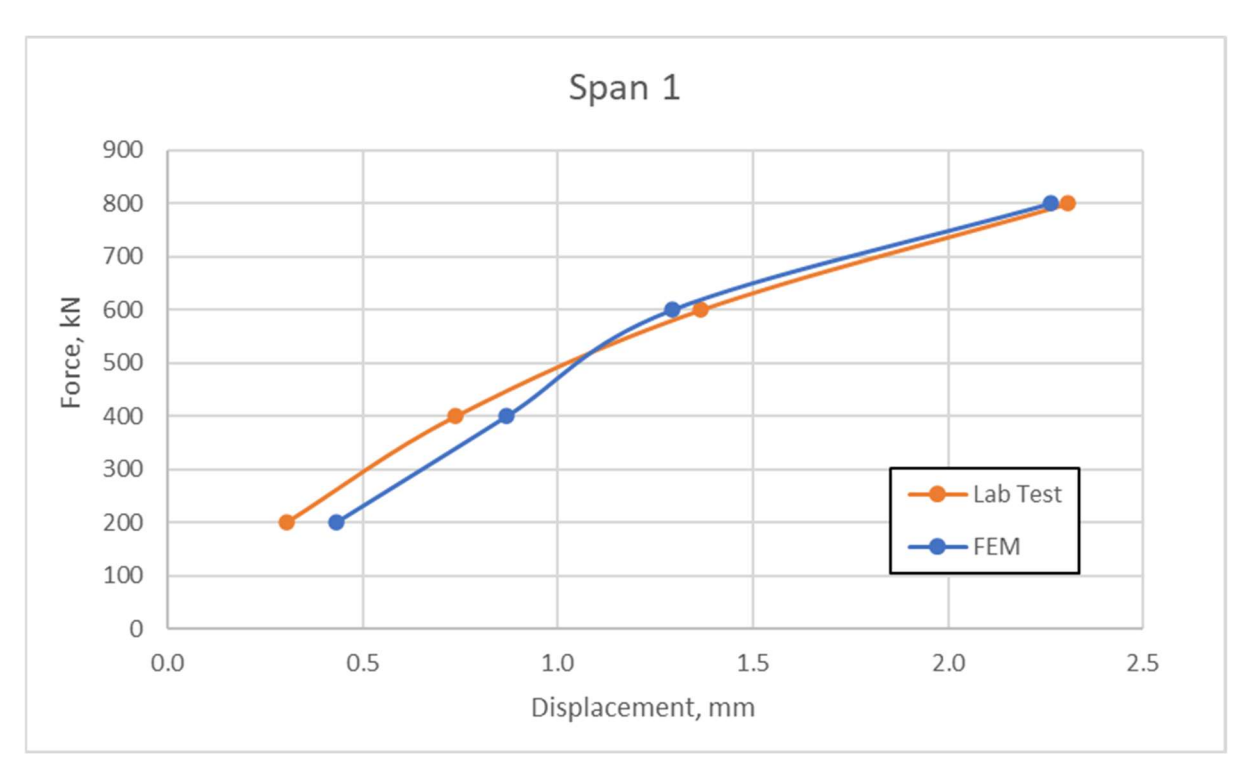


Figure 123: Model C1. Force-displacement curve for span 1, assuming μ =0.42

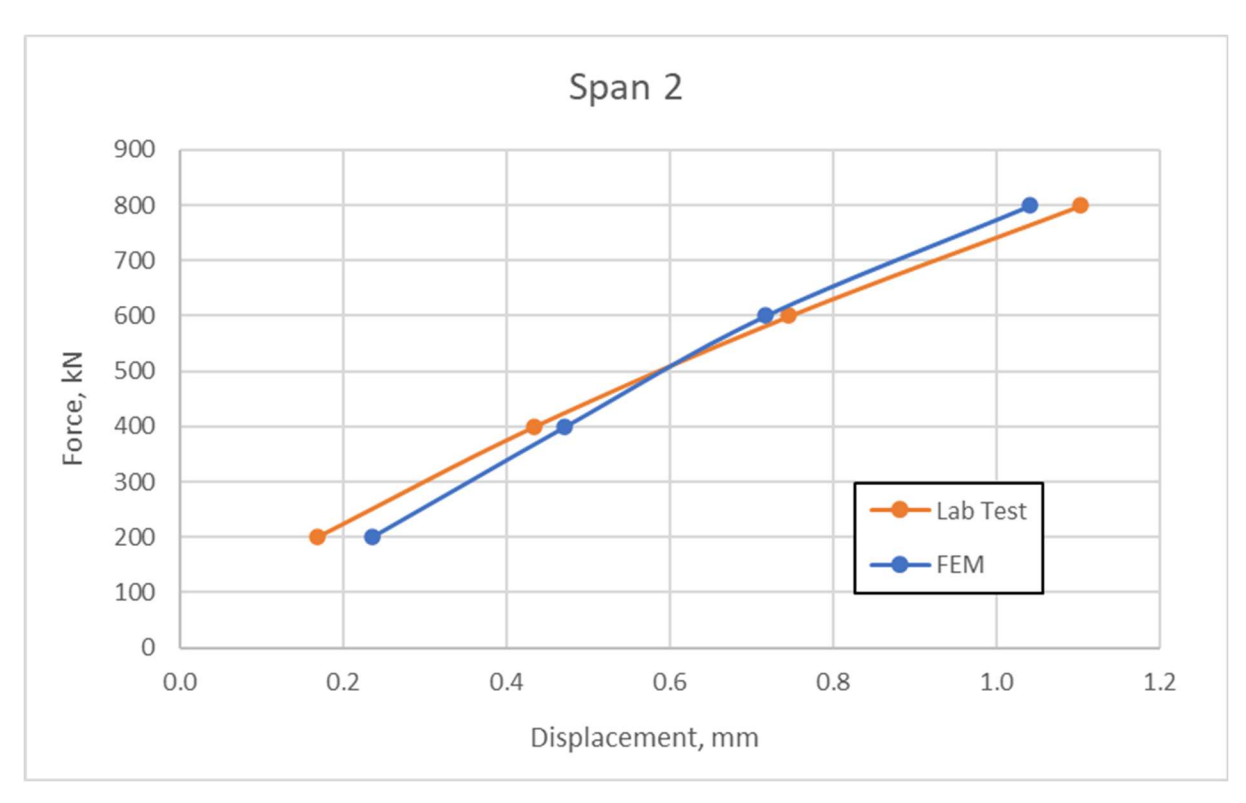
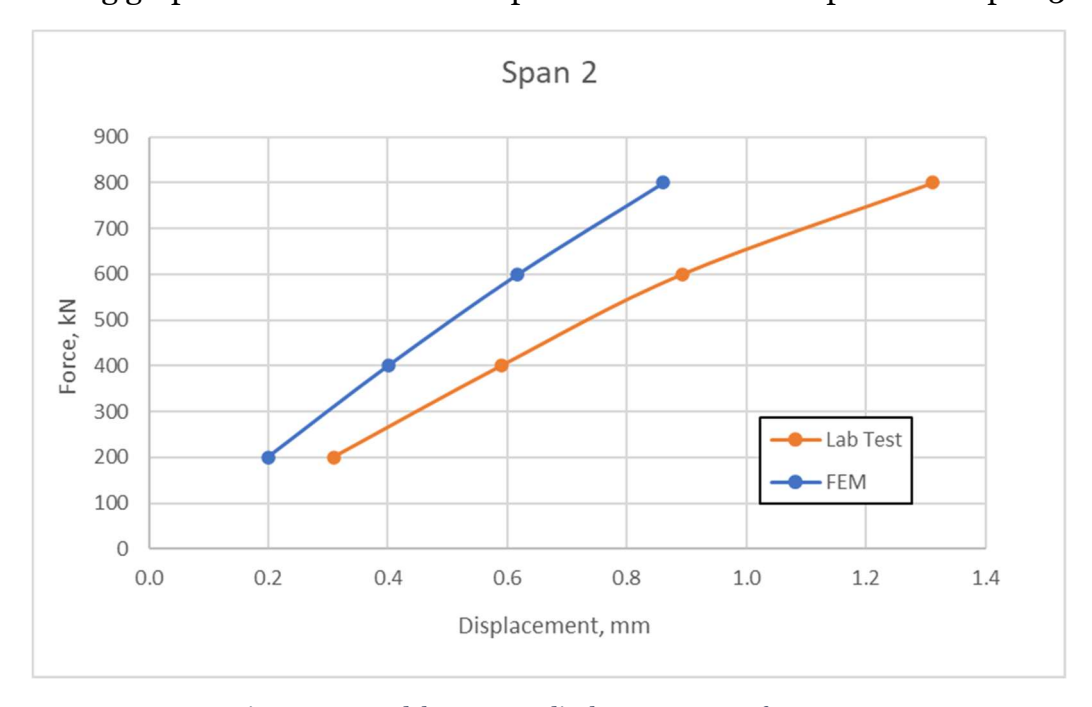


Figure 124: Model C1. Force-displacement curve for span 2, assuming μ =0.42

5.2. Sample C2

First trial of loadings was carried out on the model described in the previous chapter. Loading scheme 2 is applied on the sample C2 in span 2 and span 3.

The following graphs show the force – displacement curves for span 2 and span 3.



Figure~125:~Model~C2.~Force-displacement~curve~for~span~2

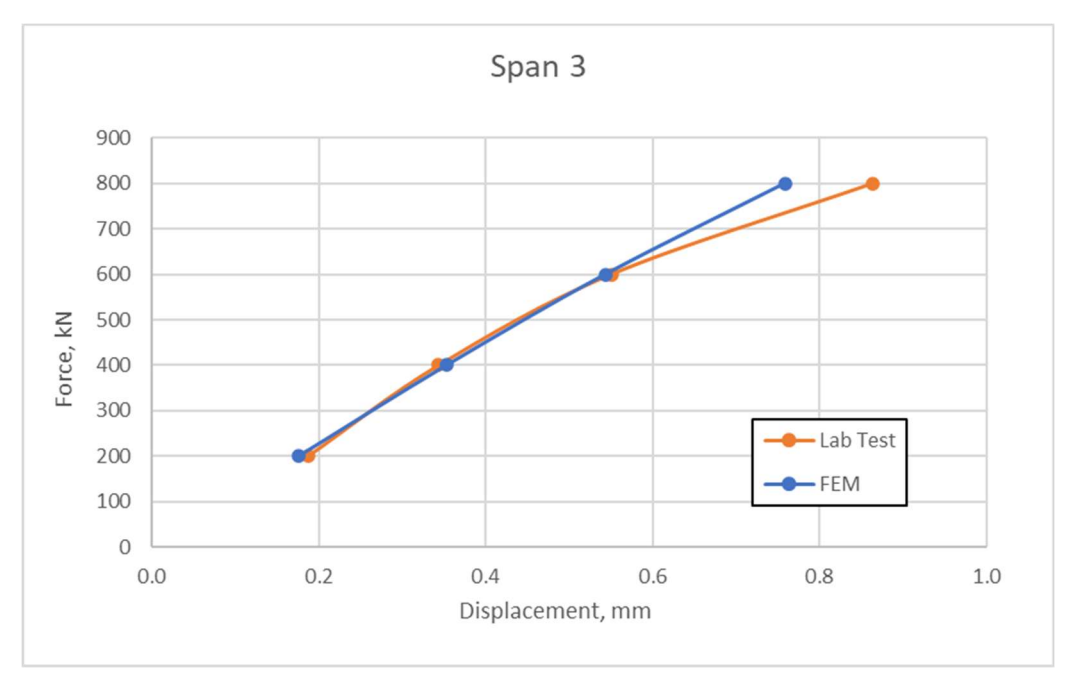


Figure 126: Model C2. Force-displacement curve for span 3

For span 3, the results of the numerical simulation matched the laboratory test results with good accuracy. This agreement indicates that full integrity of the deck is present in at least one of the samples. In this case, the assumptions used in the model provide a reliable representation of real structural response. When a medium continuity is assumed, following the assumptions made in sample C1, a reduction in stiffness and an increase in deflections are observed, which reflects the partial interaction at the joint.



Figure 127: Model C2. Force-displacement curve for span 2, assuming μ =0.42

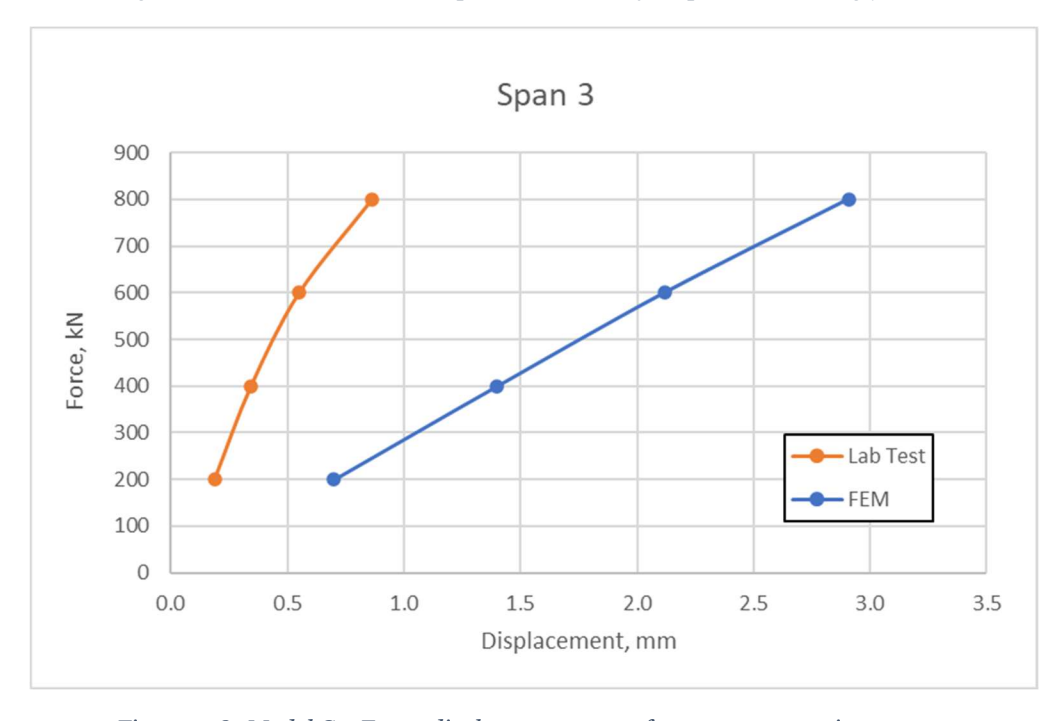


Figure 128: Model C2. Force-displacement curve for span 3, assuming μ =0.42

5.3. Sample C3

First trial of loadings was carried out on the model described in the previous chapter. Loading scheme 3 is applied on the sample C3 in span 1.

The following graph shows the force – displacement curves for span 1.

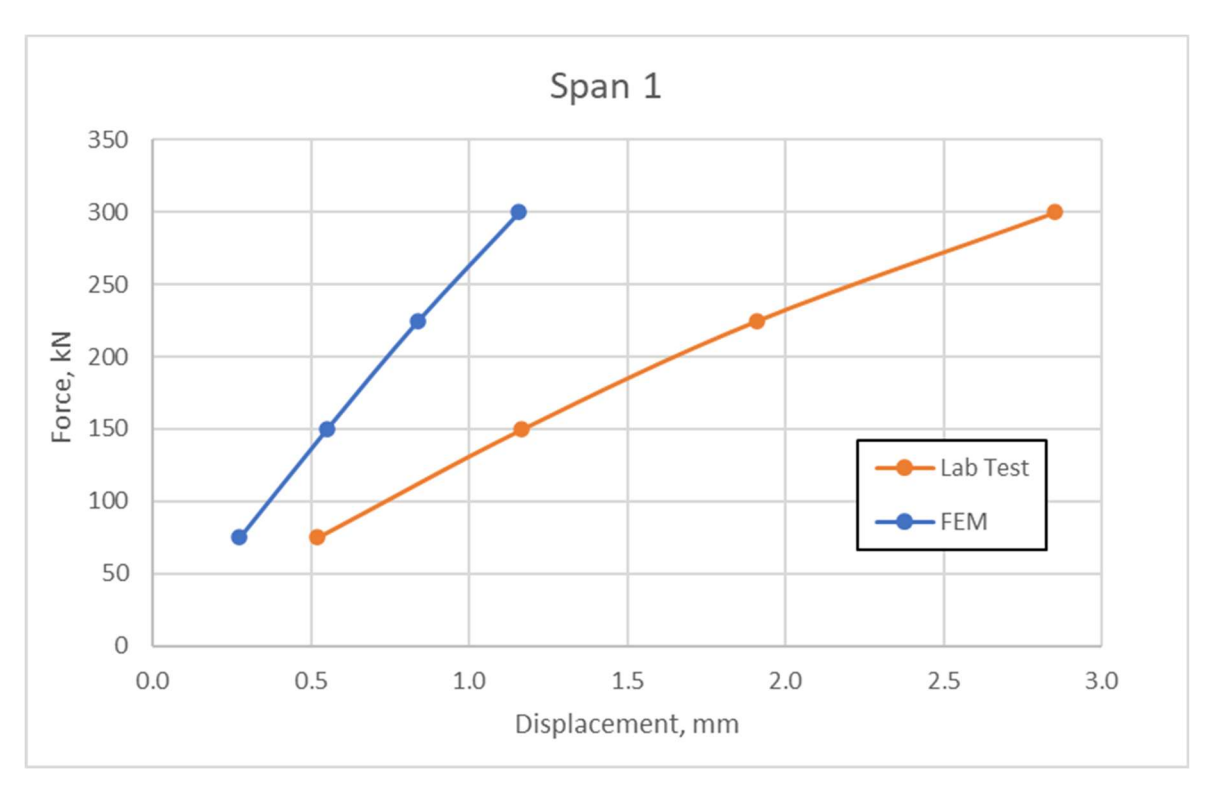


Figure 129: Model C3. Force-displacement curve for span 1

The results obtained in the sample C3 are similar with those of sample C1. The finite element model shows higher stiffness than observed in the laboratory test. To account for this difference, the assumption of medium continuity was introduced, as in the case of sample C1, with a friction coefficient of μ =0.42. Figure 130 presents the results of these simulations.

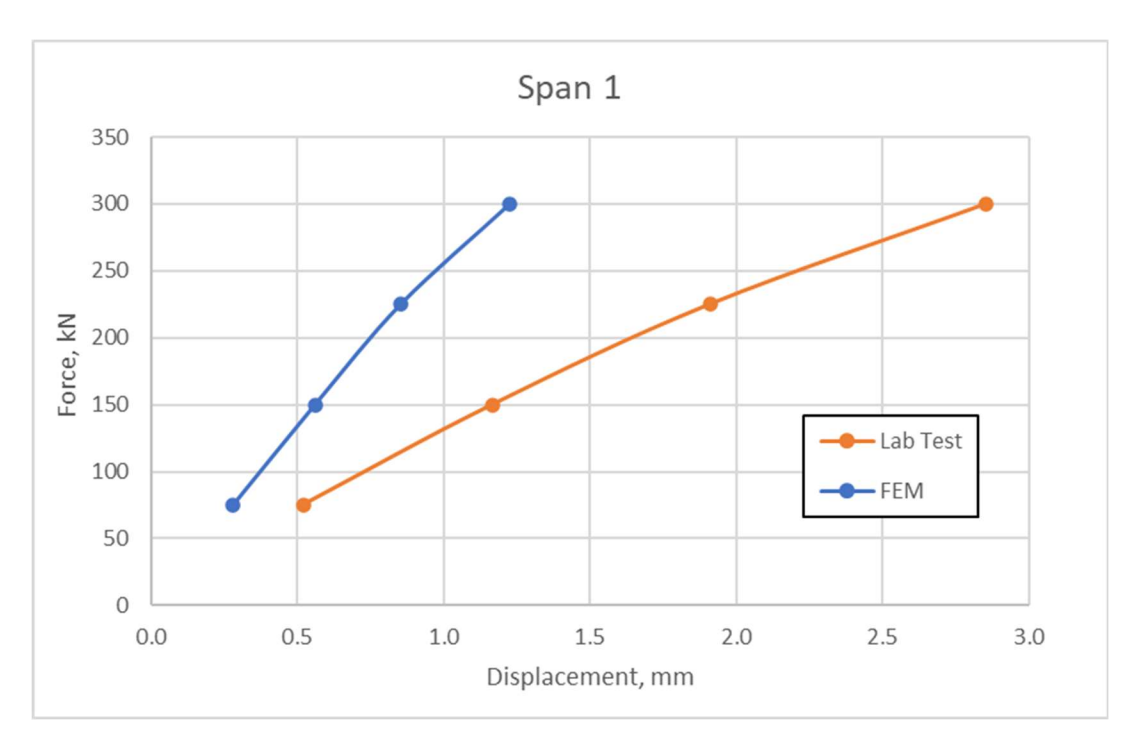


Figure 130: Model C3. Force-displacement curve for span 1, assuming μ =0.42

Since the assumption of μ =0.42 did not provide sufficient results, additional trials were performed. To further reduce the stiffness of the model, a low continuity of the deck was assumed. With μ =0.18, the simulation results closely match the laboratory tests.

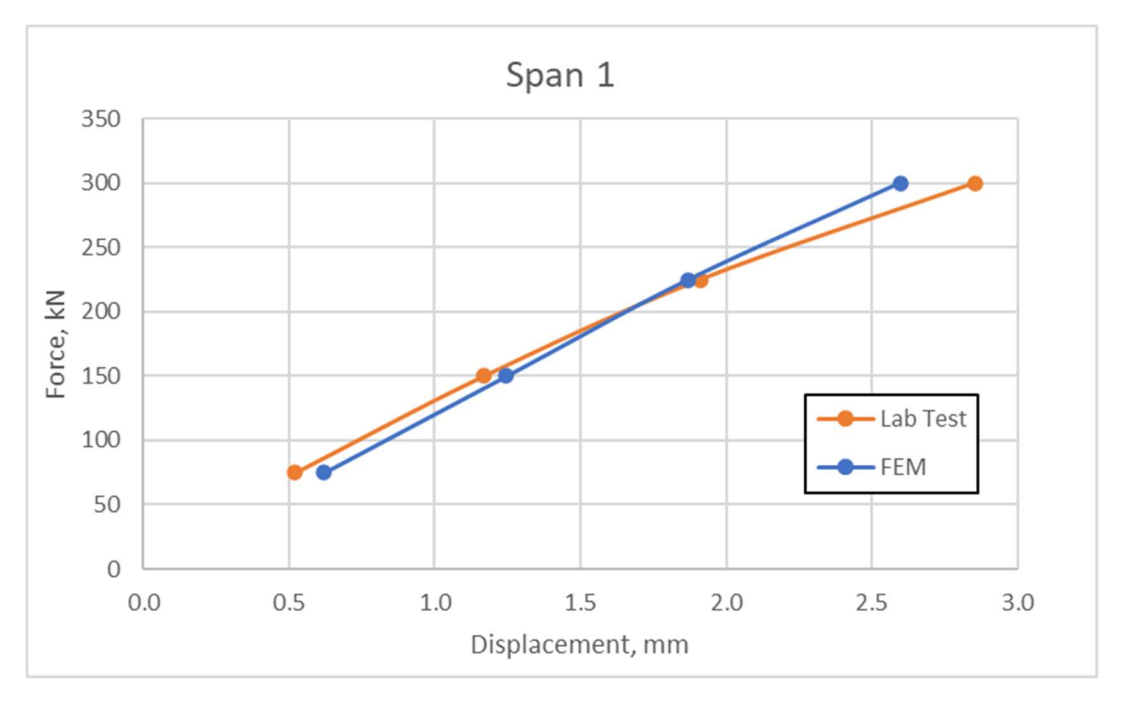


Figure 131: Model C3. Force-displacement curve for span 1, assuming μ =0.18

5.4. Sample C4

First trial of loadings was carried out on the model described in the previous chapter. Loading scheme 3 is applied on the sample C3 in span 1.

The following graph shows the force – displacement curves for span 2.

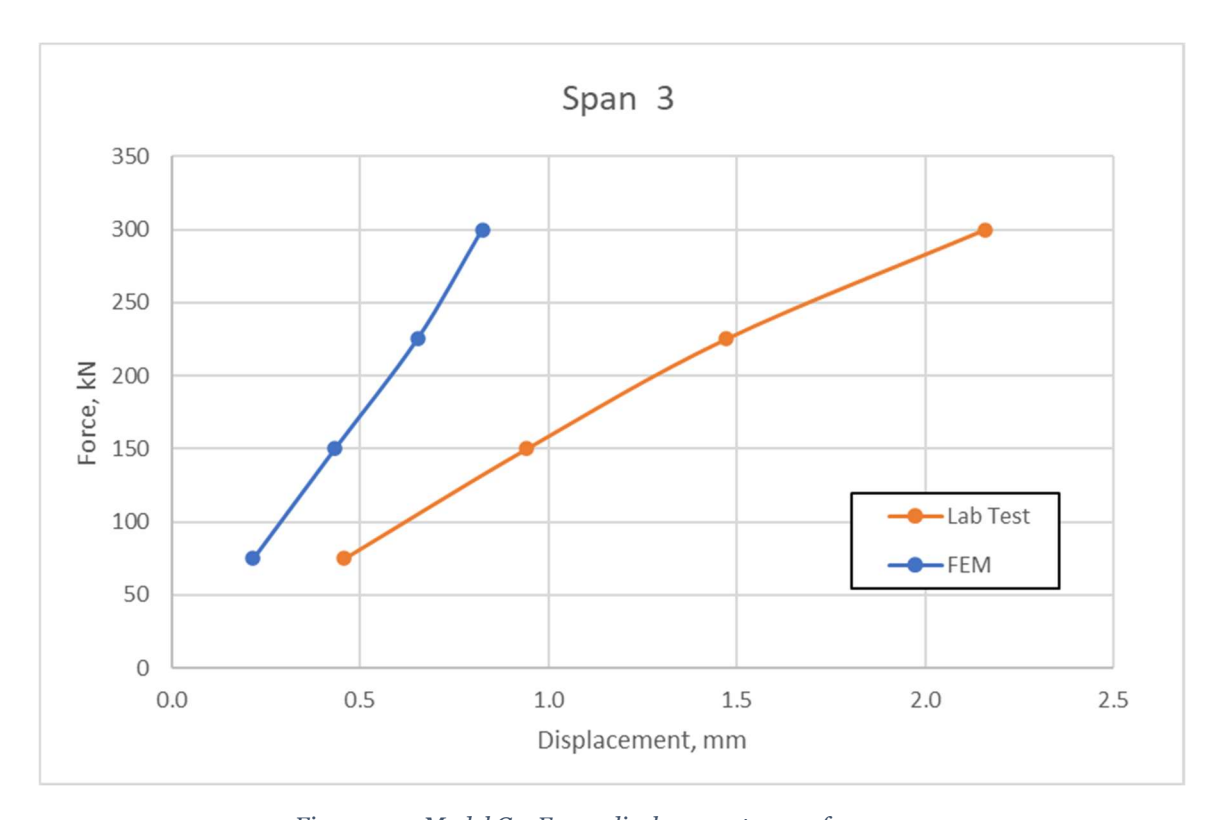


Figure 132: Model C4. Force-displacement curve for span 3

The results obtained in the sample C4 are similar with those of sample C1. The finite element model shows higher stiffness than observed in the laboratory test. To account for this difference, the assumption of medium continuity was introduced, as in the case of sample C1, with a friction coefficient of μ =0.42. Figure 133 presents the results of these simulations.

Since the assumption of μ =0.42 did not provide sufficient results, additional trials were performed. To further reduce the stiffness of the model, a low continuity of the deck was assumed. With μ =0.2, the simulation results closely match the laboratory tests. Figure 134 presents the results of these simulations.

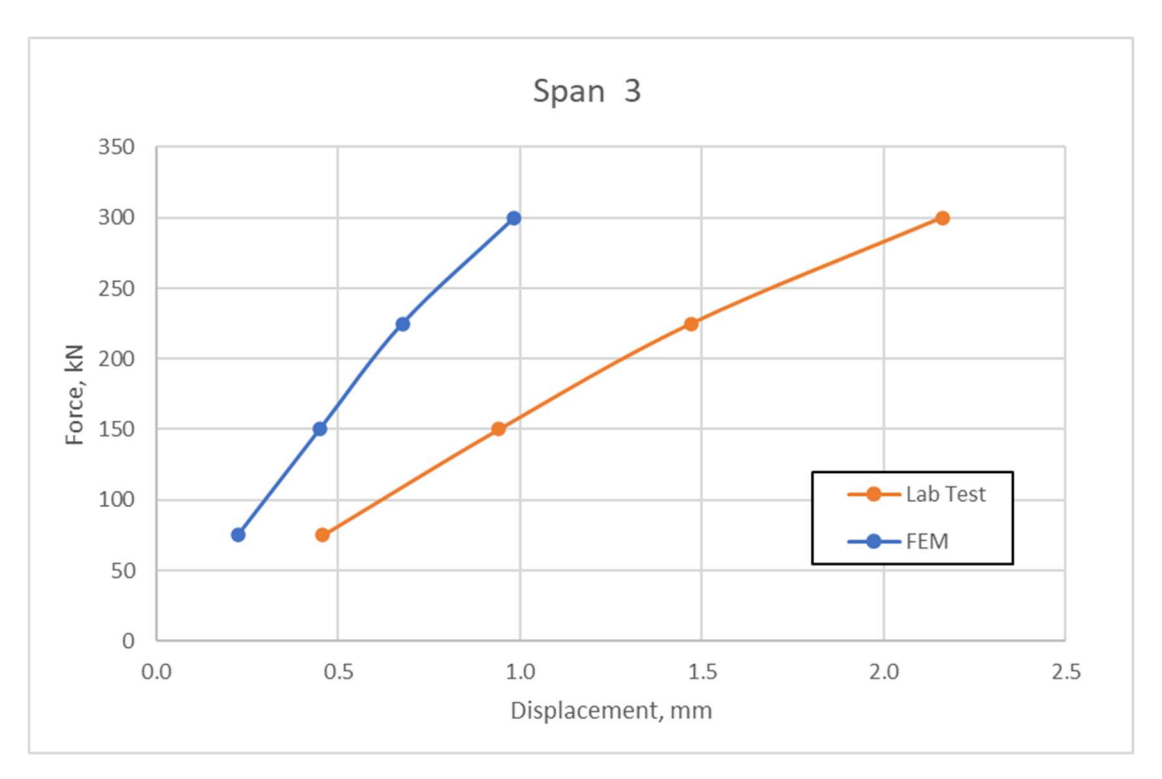


Figure 133: Model C4. Force-displacement curve for span 3, assuming μ =0.42

For this sample optimal $\boldsymbol{\mu}$ was found to be 0.2

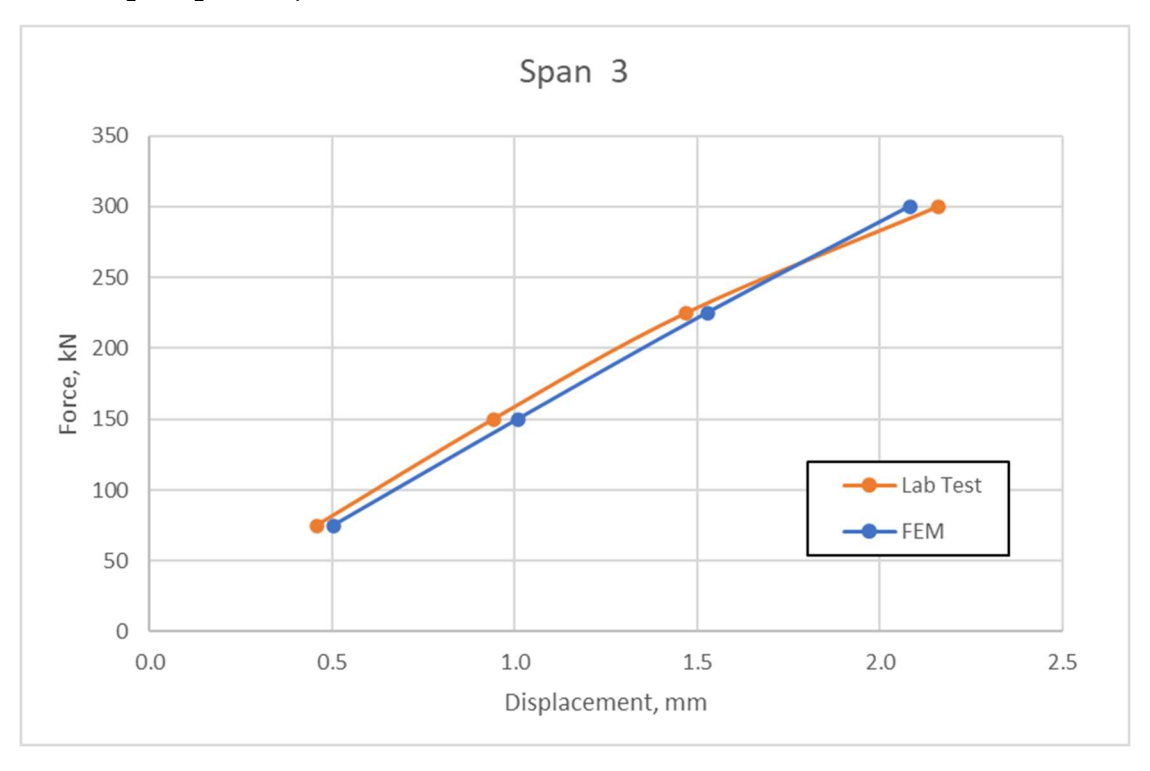


Figure 134: Model C4. Force-displacement curve for span 3, assuming μ =0.2

To summarize the results, the friction coefficient μ represents the continuity factor. The relationship between μ and damage is assumed to be linear to interpret the variability of structural response. A value of μ =1 corresponds to full continuity of the slab, while μ =0 represents compromised continuity, meaning severe damage. A value of μ =0.42 indicates a damage level of 0.58, representing medium continuity. Similarly, μ =0.2 reflects a high level of damage and low continuity.

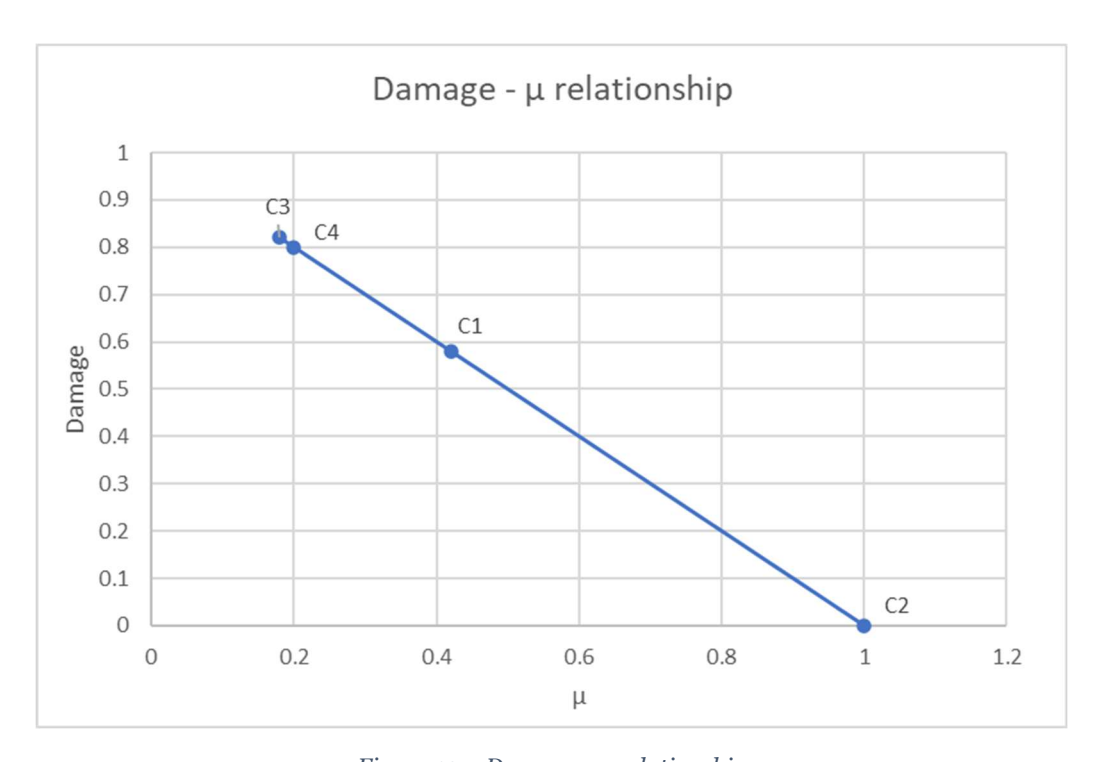


Figure 135: Damage - μ relationship

6. Conclusions

The comparison of laboratory test deformations with finite element model simulations showed significant difference in behaviour. This is due to the influence of the bond between precast and cast-in situ segments in the investigated slabs. Out of four tested samples, one showed a fully bonded response, one showed medium continuity, and two showed low continuity between two concrete types. These results indicate that the interaction between prefabricated and cast-in situ elements is not consistent and strongly influences the overall deck behaviour.

The quality of joints is found to be the main reason for the differences in performance. Possible reasons for weaker behaviour include construction imperfections, loss of bond due to microcracking, reinforcement corrosion, and handling effects during extraction and transportation. These factors reduce the effectiveness of load transfer and cause variation from the ideal monolithic behaviour.

The finite element model generally captured the behaviour of the slabs, particularly in case of full continuity. The divergence occurs in samples with medium or low continuity, indicating that accurate modelling of the interface and local imperfections is critical for a reliable model.

To fully represent the behaviour of the slab with limited deck integrity, detailed information of the joint is necessary. Further targeted investigations could include more extensive data of degradation state and parameters for advanced bond law modelling. This comprehensive data will increase the reliability of finite element models for existing slabs.

7. Bibliography

- [1] European Commission (2015)" New European technical rules for the assessment and retrofitting of existing structures" Joint Research Centre
- [2] Ministero delle Infrastrutture e dei Trasporti, Consiglio Superiore dei Lavori Pubblici (2020) "Linee Guida per la Classificazione e Gestione del Rischio la Valutazione della sicurezza ed il Monitoraggio dei Ponti esistenti".
- [3] Fabio Di Trappani "Safety Assessment and Retrofitting of Existing Structures and Infrastructures"
- [4] Ministero Infrastrutture e Trasporti (2018) "Normativa Tecnica Italiana per le Costruzioni (NTC2018)"
- [5] Agenzia Nazionale per la Sicurezza delle Ferrovie e delle Infrastrutture Stradali e Autostradali (2022) "Istruzioni operative per l'applicazione delle Linee Guida per la Classificazione e Gestione del Rischio la Valutazione della sicurezza ed il Monitoraggio dei Ponti esistenti".
- [6] Santarsiero, G., Masi, A., Picciano, V., Digrisolo, A. (2021) "The Italian Guidelines on Risk Classification and Management of Bridges: Applications and Remarks on Large Scale Risk Assessments", Infrastructures 2021, 6, 111. https://doi.org/10.3390/infrastructures6080111
- [7] CEB-FIP Model Code 90 (1993) CEB Bulletin 213/214. Thomas Telford Ltd. ISBN: 978-0-7277-1696-5, London.
- [8] fib. Model Code for Concrete Structures 2010 (2013) International Federation for Structural Concrete. ISBN: 978-3-433-03061-5.
- [9] A. Dmitriev, Y. Novozhilov, D. Mikhalyuk, and V. Lalin. (2020). "Calibration and validation of the Menetrey-Willam constitutive model for concrete," Construction of Unique Buildings and Structures; Volume 88 Article No 8804. doi:10.18720/CUBS.88.4
- [10] Ansys Mechanical APDL Element Reference. Release 2024R2. https://ansyshelp.ansys.com/public/account/secured?returnurl=////Views/Secured/corp/v242/en/ans_elem/Hlp_E_SOLID185.html
- [11] Ansys Mechanical APDL Element Reference. Release 2024R2. https://ansyshelp.ansys.com/public/account/secured?returnurl=///Views/Secured/corp/v242/en/ans_elem/Hlp_E_REINF264.html
- [12] Ansys. Introduction to contact. https://innovationspace.ansys.com/courses/wp-content/uploads/sites/5/2019/05/2.5.1-Introduction-on-contact_New_Template_Master.pdf

- [13] J.R. Aira, F. Arriaga, G. Íñiguez-González, J. Crespo. (2014) "Static and kinetic friction coefficients of Scots pine (Pinus sylvestris L.), parallel and perpendicular to grain direction". Materiales de ConstruCCión Vol. 64, Issue 315, July—September 2014, e030. ISSN-L: 0465-2746. http://dx.doi.org/10.3989/mc.2014.03913, Table 1
- [14] B. G. Rabbat, M. ASCE, H. G. Russell. (1985) "Friction Coefficient of Steel on Concrete or Grout". Journal of Structural Engineering Volume 111, Issue 3. https://ascelibrary.org/doi/10.1061/%28ASCE%290733-9445%281985%29111%3A3%28505%29